Aortic Dendritic Cell Subsets in Healthy and Atherosclerotic Mice

and

The Role of the miR-17~92 Cluster in Dendritic Cells

Subsets dendritischer Zellen in der Aorta gesunder und atherosklerotischer Mäuse und die Rolle des miR-17~92 Clusters in dendritischen Zellen

Doctoral thesis for a doctoral degree
at the Graduate School of Life Sciences,
Julius-Maximilians-Universität Würzburg,
Section Biomedicine

submitted by

Martin Busch

from

Saarbrücken

Würzburg 2013

Submitted on: ……..……..

Members of the *Promotionskomitee*:

Chairperson: **Prof. Dr. Alexander Buchberger**

Primary Supervisor: **Prof. Dr. Alma Zernecke**

Supervisor (Second): **Prof. Dr. Manfred Lutz**

Supervisor (Third): **PD Dr. Heike Hermanns**

Date of Public Defence: **…….**

Date of Receipt of Certificates: **…….**

For my parents.

“To live is the rarest thing in the world. Most people exist, that is all.”

Oscar Wilde

Table of Contents

Index of Abbreviations

°C	Degree Celsius
AA	Amino acid
APC	Antigen presenting cell / Allophycocyanin
APOE	Apolipoprotein E
BIM	B cell leukemia/lymphoma 2-like factor 11
bp	Base pair
BSA	Bovine serum albumin
$CaCl_2$	Calcium chloride
CCL17	Chemokine (C-C motif) ligand 17
CD	Cluster of differentiation
cDC	Conventional dendritic cell
CDP	Common dendritic cell progenitor
CFSE	Carboxyfluorescein succinimidyl ester
CLP	Common lymphocyte progenitor
CO_2	Carbon dioxide
Cre	Cre recombinase
CTLA4	Cytotoxic T-lymphocyte-associated protein 4
CX3CR1	Chemokine (C-X3-C) receptor 1
Cy3	Cyanine 3
Cy5.5	Cyanine 5.5
Cy7	Cyanine 7
d	Day
DAPI	4,6-Diamidino-2-phenylindole
DC	Dendritic cell
DNA	Deoxyribonucleic acid
dNTP	Deoxyribonucleotide triphosphate
DTR	Diphteria toxin receptor
EDTA	Ethylenediaminetetraacetic acid
EtBr	Ethidium bromide
EYFP	Enhanced yellow fluorescent protein
FACS	Fluorescence activated cell sorting
FCS	Fetal calf serum
FITC	Fluorescein isothiocyanate
FLT3	Fms-like tyrosine kinase 3
FLT3L	Fms-like tyrosine kinase 3 ligand
FOXP3	Forkhead box P3
g	Gravitational force/gramm
gDNA	genomic deoxyribonucleic acid
GM-CSF	Granulocyte-macrophage colony stimulating factor
HBSS	Hank’s balanced salt solution
HEK293F	Human embryonic kidney 293 F (name of a cell line)
hi	High

HLA-DR	Human leukocyte antigen
HPRT	Hypoxanthine-guanine phosphoribosyltransferase
HSC	Hematopoietic stem cell
ICOS	Inducible costimulatory molecule
IDO	Indoleamine 2,3-dioxygenase (protein)
IFNα	Interferon alpha
IFNγ	Interferon gamma
IL	Interleukin
Indo	Indoleamine 2,3-dioxygenase (gene)
INOS	inducible nitric oxide synthase
int	intermediate
IRF8	Interferon regulatory factor 8
l	Liter
KCl	Potassium chloride
kDa	Kilo Dalton
KH_2PO_4	Monopotassium phosphate
KYN	L-Kynurenine
LB medium	Lysogeny broth
LDL	Low-density lipoprotein
Ldlr	Low-density lipoprotein receptor
lo	low
loxP	Site of recombination in the Cre-lox System
LPS	Lipopolysaccharide
Ly6c	Lymphocyte antigen 6 complex
M	Molarity
mac	Macrophage
MAPK	Mitogen-activated protein kinases
M-CSF	Macrophage colony-stimulating factor
MDP	Macrophage and DC progenitor
MFI	Mean fluorescence intensity
mg	Milligramm
$MgCl_2$	Magnesium chloride
MHCII	Major histocompatibility complex
migDC	Migratory dendritic cell
mm	Millimeter
mM	Millimolar
miRISC	Micro ribonucleic acid-induced silencing complexes
miRNA	Micro ribonucleic acid
mRNA	Transfer ribonucleic acid
mTor	Mechanistic (also: mammalian) target of rapamycin
µg	Microgramm
µl	Microliter
µm	Micrometer
Na_2HPO_4	Disodium phosphate
NaCl	Sodium chloride

NF-KB	Nuclear factor kappa-light-chain-enhancer of activated B cells
NK cells	Natural killer cells
nt	Nucleotide
oligo(dT)	Oligo desoxythymidin
OVA	Ovalbumin
oxLDL	Oxidised low-density lipoprotein
PAMP	Pathogen associated molecular pattern
PBS	Phosphate buffered saline
PE	Phycoerythrin
PerCP	Peridinin chlorophyll
PFA	Paraformaldehyde
PIPES	Piperazine-N,N′-bis(2-ethanesulfonic acid)
PMA	Phorbol-12-myristat-13-acetat
pre-miR	Precursors of microRNA
pri-miRNA	primary microRNA
PRR	Pattern recognition receptor
PTEN	Phosphatase and tensin homolog
PU.1	Spleen focus forming virus proviral integration oncogene spi1
RA	Retinoic acid
resDC	Resident dendritic cells
RNA	Ribonucleic acid
rpm	Rotations per minute
RPMI-1640	Roswell Park Memorial Institute (medium)
RT-qPCR	Reverse transcription quantitative polymerase chain reaction
SDS	Sodium dodecyl sulfate
SEM	Standard error of mean
SIRPα	Signal-regulatory protein alpha
SMA	Smooth muscle cell actin
SMC	Smooth muscle cell
TGFβ	Transforming growth factor beta
Th1	T helper Type 1 cell
Th17	T helper Type 17 cell
Th2	T helper Type 2 cell
Tip-DC	TNF-iNOS-producing dendritic cell
TLR	Toll-like receptor
TNFα	Tumor necrosis factor alpha
Treg	regulatory T cells
TRIS	2-Amino-2-(hydroxymethyl)-propan-1,3-diol
tRNA	transfer ribonucleic acid
TRP	L-Tryptophan
UTR	Untranslated region
VCAM-1	Vascular cell adhesion molecule 1

1 Abstract/Zusammenfassung

1.1 Abstract

Atherosclerosis is accepted to be a chronic inflammatory disease of the arterial vessel wall. Several cellular subsets of the immune system are involved in its initiation and progression, such as monocytes, macrophages, T and B cells. Recent research has demonstrated that dendritic cells (DCs) contribute to atherosclerosis, too. DCs are defined by their ability to sense and phagocyte antigens, to migrate and to prime other immune cells, such as T cells. Although all DCs share these functional characteristics, they are heterogeneous with respect to phenotype and origin. Several markers have been used to describe DCs in different lymphoid and non-lymphoid organs; however, none of them has proven to be unambiguous. The expression of surface molecules is highly variable depending on the state of activation and the surrounding tissue. Furthermore, DCs in the aorta or the atherosclerotic plaque can be derived from designated precursor cells or from monocytes. In addition, DCs share both their marker expression and their functional characteristics with other myeloid cells like monocytes and macrophages.

The repertoire of aortic DCs in healthy and atherosclerotic mice has just recently started to be explored, but yet there is no systemic study available, which describes the aortic DC compartment. Because it is conceivable that distinct aortic DC subsets exert dedicated functions, a detailed description of vascular DCs is required. The first part of this thesis characterizes DC subsets in healthy and atherosclerotic mice. It describes a previously unrecognized DC subset and also sheds light on the origin of vascular DCs.

In recent years, microRNAs (miRNAs) have been demonstrated to regulate several cellular functions, such as apoptosis, differentiation, development or proliferation. Although several cell types have been characterized extensively with regard to the miRNAs involved in their regulation, only few studies are available that focus on the role of miRNAs in DCs. Because an improved

understanding of the regulation of DC functions would allow for new therapeutic options, research on miRNAs in DCs is required.

The second part of this thesis focuses on the role of the miRNA cluster *miR-17~92* in DCs by exploring its functions in healthy and atherosclerotic mice. This thesis clearly demonstrates for the first time an anti-inflammatory and atheroprotective role for the *miR17-92* cluster. A model for its mechanism is suggested.

1.2 Zusammenfassung

Atherosklerose ist eine chronisch-entzündliche Erkrankung der arteriellen Gefäßwand und zahlreiche Zellen des Immunsystems, wie zum Beispiel Monozyten, Makrophagen, T und B Zellen sind an der Entstehung und Entwicklung beteiligt. Aktuelle Forschungsergebnisse haben gezeigt, dass auch dendritische Zellen (DCs) zur Atherosklerose beitragen. DCs sind durch ihre Fähigkeit gekennzeichnet, Antigene zu erkennen, aufzunehmen, zu migrieren und andere Immunzellen, wie zum Beispiel T Zellen, zu aktivieren. Auch wenn alle DCs diese funktionellen Merkmale teilen, so sind sie in Bezug auf ihren Phänotyp oder Ursprung eine eher heterogene Gruppe. Zahlreiche Oberflächenmoleküle wurden in der Vergangenheit genutzt, um DCs in lymphatischen und nicht-lymphatischen Geweben zu beschreiben. Allerdings hat sich keines dieser Moleküle als spezifisch und unverwechselbar erwiesen. Die Expression von Oberflächenmolekülen ist sehr variabel und hängt nicht nur vom Aktivierungszustand der DCs, sondern auch vom umliegenden Gewebe ab. Dazu kommt, dass DCs in der Aorta, beziehungsweise im atherosklerotischen Plaque, von designierten Vorläuferzellen, aber auch von Monozyten abstammen können und DCs das Profil ihrer Oberflächenmoleküle, sowie ihre funktionellen Eigenschaften, mit anderen myeloiden Zellen wie Monozyten und Makrophagen teilen.

Neuere Arbeiten haben damit begonnen das Repertoire an DCs in der Aorta von gesunden und atherosklerotischen Mäusen zu untersuchen. Da es naheliegt, dass verschiedene DC Untergruppen ganz bestimmte Funktionen ausüben, wird eine detaillierte Beschreibung vaskulärer DCs in der Forschung benötigt. Weil es hierzu allerdings bislang kaum Studien gibt, untersucht der erste Teil dieser Arbeit zum ersten Mal systematisch die in gesunden und atherosklerotischen Mäusen vorkommenden Gruppen an DCs. Sie beschreibt außerdem eine zuvor nicht beachtete DC-Untergruppe und gibt Aufschluss über den Ursprung vaskulärer DCs.

In den letzten Jahren wurde gezeigt, dass microRNAs (mirRNAs) zahlreiche zelluläre Vorgänge wie Apoptose, Differenzierung, Entwicklung und Proliferation regulieren können. Obwohl viele Zelltypen in Bezug auf die in ihrer Regulation

eingebundenen mirRNAs charakterisiert wurden, gibt es nur wenige Studien, die sich mit der Rolle von mirRNAs in DCs beschäftigen.

Der zweite Teil dieser Arbeit konzentriert sich auf die Rolle der miRNA Gruppe *miR-17~92* in DCs und untersucht deren Rolle in gesunden und atherosklerotischen Mäusen. Diese Arbeit zeigt erstmals eine deutliche anti-inflammatorische und protektive Rolle dieser miRNA und schlägt ein Modell für die entdeckten Mechanismen vor.

2 Introduction

2.1 A General View on Atherosclerosis

Today atherosclerosis is established to be a chronic inflammatory disease of the arterial vessel wall (Hansson and Hermansson, 2011; Libby, 2002; Ross, 1999) and represents the most frequent cause of death and morbidity in industrialized countries. One of the earliest documented cases of atherosclerosis is about 5300 years old (Gostner et al., 2011; Murphy et al., 2003), nonetheless, atherosclerosis is responsible for more than 16 million deaths per year, today (Dahlof, 2010; Lloyd-Jones, 2010). The progressing narrowing of the vascular lumen and the risk for rupture and thrombus formation can give rise to cerebrovascular disease and coronary artery disease, such as acute coronary syndrome, myocardial infarction or stroke (Weber and Noels, 2011). Therefore, atherosclerosis has been studied since the beginning of the twentieth century and the knowledge has evolved accordingly. Due to strong clinical and experimental evidence its association with hyperlipidemia, atherosclerosis has been considered to be a mainly lipid-driven disease of a merely passive accumulation of cholesterol in the vessel wall in the early years of research (Ross and Harker, 1976). However, the picture is more complex and today we know that several factors play a role in the initiation and progression of atherosclerosis: Besides hyperlipidemia, other factors such as dysfunctions of the endothelium, chronic inflammation of the vessel wall, alterations in smooth muscle cell growth, uptake and deposition of lipids and cholesterol or infections contribute to the initiation and development of the disease (Hansson and Hermansson, 2011; Libby, 2002; Ross, 1999; Weber et al., 2008).

Nowadays, the initiation of atherosclerosis is accepted to be caused by endothelial activation and dysfunction. Several factors seem to play a role: Signs of systemic inflammation as well as disturbances of the laminar blood flow can trigger endothelial activation and cause endothelial dysfunctions, leading to the focal development of lesions (Moore and Tabas, 2011). The

earliest types of lesions, so-called fatty streaks, can already be found in infants (Napoli et al., 1997).

It is known from experimental, clinical and epidemiological data that high blood lipid and cholesterol levels promote atherosclerosis. Low-density lipoproteins (LDL) carrying cholesterol in the blood system are important for initiation of atherosclerosis. These carriers consist of esterified or unmodified cholesterol, triglycerides, phospholipids and apolipoprotein B100 (ApoB100), enabling them to accumulate in the intima, for example by binding to proteoglycans of the extracellular matrix (Hansson and Hermansson, 2011; Skalen et al., 2002; Tabas et al., 2007; Weber and Noels, 2011). Upon retention and accumulation of LDL particles, diverse modifications, such as aggregation, lipolysis, and oxidation can ultimately lead to the activation of endothelial cells or resident macrophages. Importantly, the degree of modification is not uniform and LDL for example can either be comparatively low or even highly oxidized. Oxidized LDL (oxLDL) is therefore rather a term for a heterogeneous group of modifications than for a distinct level of oxidation (Hansson and Hermansson, 2011). Nevertheless, LDL and oxLDL can contribute to activation of the endothelium, subsequently triggering the expression of adhesion molecules, thereafter enabling leukocytes to migrate from the blood stream into the nascent plaque (Weber and Noels, 2011). A vicious circle finally promotes plaque growth: Lipid accumulation drives leukocyte migration into the nascent plaque, conversely, these inflammatory cells contribute to lipid accumulation as well. Fatty streaks, consisting of T cells and monocyte derived macrophage-like lipid-loaded foam cells, slowly progress to early plaques.

The progression of atherosclerosis is characterized by leukocyte migration, along with accumulating apoptotic cells, debris and cholesterol crystals that form a necrotic core while a fibrous cap of collagen and smooth muscle cells covers fibroatheromatous plaques. Infiltrating cells like T cells and mast cells release enzymes, metalloproteinases and other pro-inflammatory mediators, leading to a thinning of the fibrous cap that prevents contact of pro-thrombotic plaque material with the blood (Hansson and Hermansson, 2011; Weber and Noels, 2011; Weber et al., 2008). Ultimately, unstable plaques can rupture and

the release of plaque material activates the coagulation cascade, leading to thrombus formation and a high risk for vascular occlusion.

Research on atherosclerosis is based on clinical but also on experimental data and the most frequent model organism for studies on atherosclerosis is the mouse. There are differences in atherosclerosis between mice and men, for example in lesion distribution, and not all stages of atherosclerosis, such as plaque rupture and thrombosis, can be analyzed in mice (Bentzon and Falk, 2010). But numerous critical processes are shared (Getz and Reardon, 2012) and in total there are more similarities than differences. The two most important murine atherosclerosis models currently in use are mice deficient in low-density lipoprotein receptor (LDLR) or apolipoprotein E (APOE). Even on normal low-fat rodent chow, *Apoe*-deficient mice develop complex vascular plaques over time, that resemble human lesions. This lesion formation can be accelerated when mice are fed a high fat diet. Interestingly, differences in diet can result in different plaque morphologies, for example cellularity and foam cell formation, and not all immunological effects can be observed on every diet (Bentzon and Falk, 2010; Getz and Reardon, 2012). Although the *Apoe*-deficient mouse is a widely used model, it has disadvantages, too. For example it is not suitable for the generation of bone marrow chimeras. In contrast, *Ldlr*-deficient mice allow such experiments, since LDLR is involved in lipoprotein uptake and clearance. Loss of *Ldlr* leads to increased plasma lipid levels. In contrast to APOE, LDLR is not expressed on bone marrow cells or macrophages but exerts its function on hepatocytes (Schiller et al., 2001) and therefore allows the generation of bone marrow chimeras (Maganto-Garcia et al., 2012). Since atherosclerosis is a complex disease, *in vivo* mouse models are crucial for research. These model organisms have helped to uncover the complex network of immune cells that play a crucial role in the development of atherosclerosis.

2.2.1 Atherosclerosis – A Disease Involving the Immune System

Despite its complexity involving many different cell types that are not part of the immune system, such as smooth muscle cells, endothelial cells or platelets, the concept of atherosclerosis being a chronic inflammatory disease has been accepted in the field of cardiovascular research, today (Weber et al., 2008). In the past years, research has focused on different immune cells to elucidate their contribution to atherosclerosis and to understand in which state of this slowly progressing disease different cell types play a role.

One of the early events is the recruitment of blood-derived monocytes following endothelial activation (Moore and Tabas, 2011). Chemokines released by the endothelium are recognized by cognate chemokine receptors on monocytes and promote their migration into the forming lesion. This migration can be blocked by antagonizing either the chemokine or the receptors and results in prevention or reduction of atherogenesis (Mestas and Ley, 2008). Monocytes are part of the innate immune system and since they can migrate very quickly to sites of inflammation they contribute to the initiation of immune responses. They migrate from a splenic reservoir to the site of infection where they can give rise to macrophages or dendritic cells upon tissue entry (Swirski et al., 2009). In atherosclerosis, the lymphocyte antigen 6 complex (LY6C) expressing subset of monocytes is increased dramatically and within lesions they can convert to macrophages under the influence of macrophage colony-stimulating factor (M-CSF) (Smith et al., 1995; Swirski et al., 2007).

Macrophages constitute the predominant cell type in atherosclerotic plaques (Hansson and Hermansson, 2011) and not only their differentiation from monocytes, but also their local proliferation, apoptosis is now accepted to contribute to lesion development (Andres et al., 2012). Within the lesion they can uptake oxLDL or LDL using scavenger receptors, such as type A scavenger receptor and CD36. However, several additional mechanisms for uptake must play a role, such as macropinocytosis, because deletion of these receptors does not mitigate disease (Kruth et al., 2005; Moore et al., 2005). The

cholesteryl esters of ApoB100 containing particles that are taken up are hydrolyzed into free cholesterol and free cholesterol is subsequently re-esterified by acyl CoA:cholesterol acyltransferase (Chang et al., 1997). These processes lead to intracellular droplet formation and the resulting change in cell morphology is termed foam cell formation. Therefore, the accumulation of lipids into the vessel does not only trigger monocytes to migrate into the vessel wall and differentiate to activated macrophages, but it is also amplified by these cells in a positive feedback loop.

While macrophages contribute to plaque growth, T lymphocytes are also recruited to lesions at the same time and by similar mechanisms, although to a lesser frequency compared to macrophages. They become activated *in situ* and the release of pro-atherogenic factors accelerates lesion development. T cells play an important role in atherosclerosis, since it is a T helper Type 1 (Th1) driven disease (Benagiano et al., 2003; Hansson et al., 2006; Tedgui and Mallat, 2006). Several lines of evidence underline the role of this particular T cell subset in lesion progression: Interferon gamma (IFNγ), the signature cytokine of Th1 cells, is released by T lymphocytes in atherosclerotic plaques (Stemme et al., 1995) and also the Th1-stimulating interleukins IL-12 and IL-18 have been identified within plaques (Benagiano et al., 2003; Uyemura et al., 1996). Inhibition of Th1 cells or the use of genetically engineered knockout mice for either *Il12*, *Il18*, *Ifng*, the *Ifng* receptor (*Ifngr*) or the Th1 lymphocyte specific transcription factor (*Tbx21*) result in reduced atherosclerosis, highlighting the importance of Th1 cells (Buono et al., 2005; Buono et al., 2003; Davenport and Tipping, 2003; Elhage et al., 2003; Gupta et al., 1997; Laurat et al., 2001). Data on T helper Type 2 (Th2) or IL-17 producing T (Th17) cells is in part contradictory and needs further research (Hansson and Hermansson, 2011; Hansson et al., 2006).

There is no doubt on the impact of Th1 lymphocytes on atherosclerosis, however, another subset of T cells has gained attraction in the past decade: Regulatory T cells (Treg) can prevent the expansion of self-reactive lymphocytes and T cell responses, thereby limiting and controlling immune response. Several studies have identified a crucial role of Treg functions in

autoimmune diseases and it is widely accepted that these cells are required to balance immune reactions. It is not known in detail how Treg exert their ability to limit effector responses *in vivo*, but several studies have demonstrated that they act through various mechanisms that involve the secretion of anti-inflammatory cytokines like transforming growth factor beta (TGFβ) or IL-10, or the direct interaction with antigen presenting cells (APC) (Belkaid, 2007). These interactions involve, for example, the co-stimulatory molecules CD80/CD86 or CD28 (Greenwald et al., 2005) and a deficiency in these interactions leading to a loss of Treg is associated with a significant increase in atherosclerotic lesions (Ait-Oufella et al., 2006). Accordingly, the adoptive transfer of Treg also reduces lesion development (Mor et al., 2007). Although these studies provide only indirect evidence for Treg effects on atherosclerosis and future research needs to address unresolved questions (Sasaki et al., 2012), further evidence comes from studies on inducible costimulatory molecule (*Icos*)-deficient mice. ICOS is expressed on activated T cells (Dong et al., 2001) and it is required for Treg function (Herman et al., 2004; Kohyama et al., 2004). Studies with *Icos*-deficient mice suggest that Treg are capable of limiting plaque development (Gotsman et al., 2006; Mallat et al., 2007; Sasaki et al., 2012), underlining their powerful potential to balance and control immune reactions. As mentioned earlier, Treg do not only act on T lymphocytes to limit effector responses. There is data supporting that Treg can also exert their functions through APC. The group of APC is rather heterogeneous and includes monocytes, macrophages but also DCs. Direct interactions of Treg with DCs have been suggested to be important for Treg functions (Tang et al., 2006) and Treg have been demonstrated to induce, for example, downregulation of co-stimulatory molecules (Cederbom et al., 2000) or IL-12 secretion in DCs (Sato et al., 2005). Interestingly, DCs are also capable of directly influencing Treg behavior and functions (Sato et al., 2003; Yamazaki et al., 2003; Yamazaki et al., 2006).

Among the various mechanisms DCs use to influence T cell polarization, research has identified the L-tryptophan (TRP) metabolism to be crucial. TRP catabolism mediated by indoleamine 2,3-dioxygenase (IDO) activity in DCs is important for the induction of peripheral tolerance (Mellor and Munn, 2004). IDO is a monomeric enzyme of approximately 41 – 45 kDa (Katz et al., 2008; Mellor

and Munn, 2004) and is involved in the conversion of L-tryptophan to L-kynurenine (KYN) (Adams et al., 2012). Interestingly, a second important TRP converting enzyme termed IDO2 has been described. Although IDO and IDO2 do not show a high level of homology, they both display similar mechanisms for TRP degradation. Interestingly, albeit IDO2 levels are higher than IDO levels, up to 50 % of the common population lack functionally active Ido2 alleles, due to single nucleotide polymorphisms (SNP). This suggests a more critical role for IDO than for IDO2 (Katz et al., 2008). IDO is induced upon inflammatory stimuli, such as IFNγ and lipopolysaccharide (LPS) (Katz et al., 2008), and several studies have demonstrated that IDO expression can inhibit priming of T cell antigens (Fallarino et al., 2003; Grohmann et al., 2000; Mellor and Munn, 2004), induce tolerance to pancreatic islet-cells (Grohmann et al., 2002), lung (Swanson et al., 2004) or liver (Miki et al., 2001) allografts and ameliorate autoinflammatory diseases, such as experimental autoimmune encephalomyelitis (EAE) (Sakurai et al., 2002) or colitis (Gurtner et al., 2003). Although several mechanisms for IDO-mediated induction of peripheral tolerance have been proposed, the detailed mechanisms remain elusive and data suggests that several pathways exist in parallel (Mellor and Munn, 2004): The depletion of TRP could increase uncharged tryptophanyl-transferRNA, resulting in stress responses within the T cell. Furthermore, a mechanistic (mammalian) target of rapamycin (mTor)-mediated block of the translational machinery has been proposed. Not only the depletion of TRP, but also the increase of downstream metabolites, such as KYN, has been implied in mediating IDO effects. They have been shown to induce proliferation arrest of selective apoptosis (Mellor and Munn, 2004). Interestingly, a feedback loop between IDO-expressing DCs and tolerogenic T cells has also been suggested: cytotoxic T-lymphocyte-associated protein 4 (CTLA4) expressing Tregs can signal to IDO-competent DCs and induce IDO expression. This outside-in signaling could also influence the production of other factors involved in the induction of Tregs, such as cytokines (Mellor and Munn, 2004). In summary, IDO is crucial in the induction or peripheral tolerance, although the detailed mechanisms are not well described.

With the development of atherosclerosis involving several different cell types of the immune system, such as monocytes, macrophages, DCs and T lymphocytes, it becomes obvious that this disease is more than merely a passive accumulation of lipids in the vessel wall. Atherosclerosis is a complex disease characterized by the involvement of both innate and adaptive immunity. Therefore, it is crucial to investigate the role of immune cells to improve our understanding of the processes that drive disease progression. In the past decades research had focused on monocytes, macrophages and T cells, but as already indicated in the interaction of DCs with Treg, there are other types of cells worth looking at. In recent years DCs drew attention in the field and also this thesis focuses on DCs.

2.2 Dendritic Cells

In 1973, Steinman and colleagues described DCs for the first time as a new type of cell that they had discovered in the spleen. Using light microscopy they found a previously unrecognized cell type amongst splenic cells that could adhere to glass slides. They observed a mono-nuclear and stellate or dendritic morphology and termed these cells dendritic cells (Steinman and Cohn, 1973). Subsequently, they characterized them (Steinman and Cohn, 1974; Steinman et al., 1979; Steinman et al., 1974) and the importance of DCs to our understanding of the immune system has been highlighted by awarding the Nobel Prize in Physiology or Medicine 2011 to Ralph M. Steinman for discovering the dendritic cell (Lanzavecchia and Sallusto, 2011). Being part of the innate immune system but capable of instructing adaptive immunity, DCs bridge the two worlds of our immunity (Paul, 2011).

Research on DCs has become highly complex and controversial, mainly for two reasons: On the one hand, DCs do not represent a homogenous cell type and their features and functions can vary tremendously. DCs can be divided in different subsets; they can activate or suppress the immune system, migrate to distinct sites, interact with various cell types and secrete different cytokines. On the other hand, they can mature and change their properties and they are also able to change the surface marker expression. Up to now there are no unambiguous and unique markers available to distinguish DC subsets and to

segregate them from other myeloid cells like macrophages or monocytes in all tissues and activation states (Satpathy et al., 2012b). This is the second hurdle that complicates DC research. Markers vary depending on tissue and *in vivo* occurring and *in vitro* generated DCs cannot be compared directly. Furthermore, myeloid cells, such as monocytes and macrophages, share surface markers. There will always be room for discrepancies and controversies in the description of DCs until unique markers have been identified. This present work is based on currently accepted definitions on DCs, however, the scientific debate is still ongoing and defining DCs subsets remains a controversial issue.

2.2.2 Origin of Dendritic Cells

Four major groups of DCs have been proposed: conventional DC (cDC), Langerhans cells, plasmacytoid DCs and monocyte-derived DCs (Belz and Nutt, 2012; Satpathy et al., 2012b). This work will mainly focus on cDCs.

Conventional DCs, sometimes also termed classical DCs, originate from the bone marrow where a specific cytokine milieu is required for DC development from hematopoietic progenitors. Although the detailed downstream mechanisms induced by these cytokines remain to be elucidated, it is demonstrated that FMS-related tyrosine kinase 3 (FLT3) ligand (FLT3L), macrophage colony-stimulating factor (M-CSF) and granulocyte-macrophage colony stimulating factor (GM-CSF) are crucial for DC differentiation. Briefly, hematopoietic stem cells (HSC) in the bone marrow give rise to common myeloid progenitors (CMP) and a $FLT3^+$ CMP subset that can progress to macrophage and DC progenitor (MDP) cells. Early experiments suggested that DCs can also differentiate from common lymphoid precursor (CLP) cells, however, since CMP are 10-fold more abundant than CLP it is now widely accepted that DCs originate from CMP (Liu and Nussenzweig, 2010). Therefore, the discrimination between myeloid and lymphoid DCs is not appropriate any longer (Ardavin, 2003). MDP can either develop into common DC progenitor (CDP) cells or leave the bone marrow and become monocytes (Belz and Nutt, 2012).

As mentioned earlier, under inflammatory conditions DCs can also arise from monocytes (Belz and Nutt, 2012; Swirski et al., 2007; Swirski et al., 2009). However, detailed experiments on whether or not monocytes are direct precursors of DCs in steady state have led to a complex picture: Monocytes can lose the expression of typical monocyte markers such as CD14 and CD64 and phagocytosis can lead to the expression and upregulation of typical DC markers like CD80, CD86 or HLA-DR (Randolph et al., 1998). These cells are capable of typical DC functions such as mixed leukocyte reactions, however, these markers are not necessarily unique to DCs and several cell types expressing co-stimulatory molecules can induce mixed leukocyte reactions (Liu and Nussenzweig, 2010). Furthermore, monocytes that become activated during infection with *Listeria monocytogenes* for example also acquire a DC-like phenotype. Their characteristic ability to produce tumor necrosis factor alpha (TNFα) and inducible nitric oxide synthase (iNOS) led to the term of TNF-iNOS-producing DCs (Tip-DC) (Serbina et al., 2003). Although monocyte-derived DC-like cells showed several similarities to DCs in these studies, they functionally differed. Taking these experiments together, monocytes can differentiate into DC-like cells with unique properties and features that overlap with those of DC, but these monocyte-derived cells remain at the intersection between DCs and monocytes and do not represent the origin of DCs in steady state (Liu and Nussenzweig, 2010).

Like MDP that leave the bone marrow and turn into monocytes, CDP can egress the bone marrow as well. They exit the bone marrow as precursor DCs (preDC) or plasmacytoid DCs (pDC) (Belz and Nutt, 2012). Adoptive transfer experiments suggest that CDP are downstream of either CMP or MDP, because both of these two precursor cell subsets give rise to CDP and monocytes. DCs and monocyte lineage diverge at this step: CDP cannot differentiate into monocytes (Liu et al., 2009). PreDCs that emerge from DCP differentiate under steady-state conditions into various conventional DC (cDC) subsets within the spleen or lymphoid tissue (Belz and Nutt, 2012). In conclusion, DCs and monocytes share progenitors but they diverge at the stage of CDP. DCs can be further divided in subsets; however, this will be discussed later.

Among the earlier mentioned cytokines relevant to DC development, FLT3L is probably the best studied growth factor. Because $FLT3^+$ CMP are amongst one of the earliest stages in differentiation, FLT3L is of crucial importance. Mice deficient in FLT3 have significantly reduced DCs numbers and the same is true for *Flt3l*-deficient mice, although to a lesser extend (McKenna et al., 2000; Waskow et al., 2008). However, not all cDC subsets depend on FLT3L (Ginhoux et al., 2009), underlining the complexity of the DCs lineage and also leaving room to speculate about other ligands for FLT3. FLT3L can also be used for *in vitro* cultures of bone marrow-derived DC, yielding several cDC subsets and also pDCs (Brasel et al., 2000; Naik et al., 2005). Adoptive transfer experiments have underscored the role of FLT3/FLT3L and in principle all DCs can be generated from any $FLT3^+$ precursor cell *in vivo* or *in vitro* (Belz and Nutt, 2012; D'Amico and Wu, 2003; Ginhoux et al., 2009; Karsunky et al., 2003; Onai et al., 2007). In line with these results, administration of FLT3L leads to an expansion of DC numbers *in vivo* (Waskow et al., 2008).

In addition to FLT3L-supplemented cultures of bone marrow-derived DC, GM-CSF is also frequently used for *in vitro* generation of DCs and plays an important role in DC development. While GM-CSF receptor deficient mice have only modestly reduced DC numbers in lymphoid organs (Vremec et al., 1997), the loss of DCs in *Csf2 Flt3l* double deficient mice is more pronounced compared to *Flt3l*-deficiency alone (Kingston et al., 2009) and *Csf2* or *Csf2* receptor (*Csf2ra*)-deficient mice have reduced numbers of migratory DCs in skin and gut (Bogunovic et al., 2009; Kingston et al., 2009). In line with these findings, the administration or overexpression of GM-CSF leads to increased DC numbers (Daro et al., 2000; Vremec et al., 1997). Circulating GM-CSF levels are very low under steady-state conditions, but since they increase under inflammatory conditions (Hamilton, 2008), GM-CSF is considered to play a more pronounced role for DCs in inflammation or infection (van de Laar et al., 2012).

2.2.3 Dendritic Cell Subsets

The classification of DCs into subsets is controversial and complex. Both ambiguous markers for subset definition and complicated differentiation from precursor cells shared with other myeloid cells with similar functions contribute. Various overlapping groups of DCs have been proposed and DCs were grouped, for example by origin (lymphoid DC, myeloid DC, monocyte-derived DC), function (steady-state DC, inflammatory DC) or location (circulating DC, resident DC, migratory DC, Langerhans cells, dermal DC, lamina propria DC, splenic DC, vascular DC) (Naik, 2008; Shortman and Naik, 2007). This work focuses on DCs as they occur in secondary lymphoid organs (spleen and lymph nodes), as well in the non-lymphoid tissue of the aorta.

The majority of DCs in steady-state conditions is represented by preDC-derived cDCs. They are highly phagocytic, specialized in antigen-processing and presentation and in contrast to for example macrophages they are profoundly stimulatory to naïve T cells. Once DCs are differentiated from their designated precursor cell, they possess a high phagocytic capacity and low levels of major histocompatibility complex (MHC) class I and II levels. In this state they are referred to as immature DCs. However, once they have encountered antigens, DCs show reduced phagocytic capacity, but high expression of MHC class I and II molecules (Satpathy et al., 2012b).

The group of cDC can be further subdivided based on tissue and marker expression. Markers such as E-cadherin-ligand CD103, CD11b, CD4 and CD8α (called CD8 in the following) have been used to discriminate DCs subsets within spleen and lymphatic tissue. The spleen, for example, comprises three typical DCs subsets: $CD4^+$ DC, $CD8^+$ DCs and $CD4^-CD8^-$ DCs (Belz and Nutt, 2012). In the lymph node, DCs are not only categorized by CD4 and CD8 surface expression, but they are in parallel distinguished based on MHCII expression. DCs are considered to be lymphoid tissue resident DCs (resDC, $MHCII^{low}$) or migratory DCs (migDC, $MHCII^{high}$) (Idoyaga et al., 2013). While CD4 and CD8 are used to discriminate DC subsets in lymphoid organs, CD103 and CD11b are commonly used in non-lymphoid organs. $CD103^+$ DCs can be considered the counterpart of lymphoid $CD8^+$ DCs and $CD11b^+$ DCs resemble lymphoid

$CD4^+$ DCs. However, there are also studies demonstrating differences, depending on the organ-specific milieu (Satpathy et al., 2012b).

While in the past decades numerous studies have investigated the ontogeny and subset differentiation of DCs in various lymphoid and non-lymphoid organs (Belz and Nutt, 2012), in recent years research focused on the intestinal DCs repertoire of the lamina propria and mesenteric lymph nodes (Persson et al., 2010). However, there are only few studies that investigated the role of aortic DCs in atherosclerosis (Doring and Zernecke, 2012; Manthey and Zernecke, 2011; Weber et al., 2008).

2.2.4 Dendritic Cells in Atherosclerosis

Several different types of immune cells can be found in atherosclerotic lesions, such as T cells, B cells, monocytes, macrophages and also DCs (Bobryshev, 2010; Hansson, 2005; Manthey and Zernecke, 2011; Moore and Tabas, 2011; Weber et al., 2008). DCs can already be found in the arterial intima of healthy young individuals (Millonig et al., 2001) and such a network of vascular DCs can be observed in healthy mice as well, with a localization different to that of vascular macrophages (Jongstra-Bilen et al., 2006). In human carotid plaques, symptomatic patients have higher DCs frequencies than asymptomatic patients (Kawahara et al., 2007) and DCs have also been observed in rupture-prone regions of the plaque (Yilmaz et al., 2004). In *Cd11c-EYFP* reporter mice, 0.25 – 0.5 % of all aortic cells express EYFP and these cells were also mainly localized to the intima. The same study showed that these cells can also be found in regions prone to atherosclerosis – the aortic root, cardiac valves and in the lesser curvature of the aortic arch (Choi et al., 2009).

The localization of DCs to the arterial vessel wall depends at least in part on vascular cell adhesion molecule 1 (VCAM-1) and chemokine (C-X3-C) receptor 1 (CX3CR1), since DCs numbers in knockout mice for *Vcam1* and *Cx3cr1* are reduced (Jongstra-Bilen et al., 2006; Liu et al., 2008). In contrast to macrophages that primarily arise from $LY6C^{hi}$ monocytes under inflammatory conditions (Swirski et al., 2007), DCs are considered to be rather differentiated from $LY6C^{lo}$ monocytes (Tacke et al., 2007). However, this picture is not

ambiguous *in vivo*, since DCs can arise from both types of circulating monocytes (Geissmann et al., 2003). Furthermore, DCs cannot only be recruited to plaque lesions, but they can also proliferate *in situ* as suggested by data with *Cfs2*-deficient mice or GM-CSF administration (Shaposhnik et al., 2007; Zhu et al., 2009). Interestingly, the influence of GM-CSF is dependent on the model for atherosclerosis (Ditiatkovski et al., 2006). The presence of DCs in atherosclerotic plaques and their increase with plaque growth indicates a role for lesional DCs. In fact, these DCs have been demonstrated to affect plaque development by various mechanisms that include secretion of pro- or anti-inflammatory cytokines, uptake and modification of lipoproteins and cholesterol or recruitment, stimulation and polarization of T cells (Manthey and Zernecke, 2011; Niessner and Weyand, 2010).

As mentioned in the beginning, progression of atherosclerosis is Th1 driven and therefore the ability of lesional DCs to interact with T cells is of critical importance. *In vitro*, DCs sorted from the aorta are capable to induce T cell proliferation and it has been demonstrated that plaque DCs can sample antigens from the circulation *in vivo* and present them to induce T cell proliferation *in vitro* (Choi et al., 2009; Weber et al., 2011). The local influence of DCs towards T cells is underscored by the abundance of lesional T cells that display high specificity for lipoproteins and their modifications (Stemme et al., 1995). Clonally expanded T cells also point to an interaction between DCs and T cells directly within atherosclerotic plaques (Paulsson et al., 2000).

Increasing blood lipid levels lead to rapid lipid depositions in regions prone to atherosclerosis, where lipid-loaded $CD11c^+$ DCs can be found within days of onset. Depletion of these $CD11c^+$ DCs reveals their critical role in the accumulation of lipids in the early phase of lesion formation, since it significantly reduces lipid accumulation (Paulson et al., 2010). Furthermore, DCs play a role in the control of cholesterol homeostasis after the initiation phase: Depletion of $CD11c^+$ DCs for a short time, two weeks after the onset of high fat diet feeding, leads to increased levels of cholesterol. Conversely, an increase in DC life-span results in decreased cholesterol levels and reduced plaque burden, despite an increased pro-atherogenic signature (Gautier et al., 2009). But DCs do not only

regulate lipoprotein and cholesterol homeostasis, they are also affected by dyslipidemia, hypercholesterolemia and the accumulation of modified or naïve lipoproteins. Both LDL and oxLDL, for example, can upregulate co-stimulatory molecules while oxLDL is also capable to induce IL-6 secretion, T cell proliferation and upregulation of scavenger receptors (Manthey and Zernecke, 2011; Niessner and Weyand, 2010).

Accumulated lipoproteins undergo several chemical modifications and it is not surprising that this variety of modified lipoproteins has different and in part contradictory consequences for DCs activation. Low to moderate levels of dyslipidemia, for example, induce disease aggravation and enhance local inflammatory responses (Angeli et al., 2004) while severe levels of dyslipidemia inhibit DCs activation (Shamshiev et al., 2007). This study also demonstrates that different DCs subsets (namely $CD8^+$ and $CD8^-$) respond differently to dyslipidemia, explaining at least in part why severe hypercholesterolemia results in a shift of T helper cell responses from Th1 to Th2 (Zhou et al., 1998). However, other studies demonstrate that DCs maintain their capacity for priming T cells under conditions of dyslipidemia (Packard et al., 2008). In conclusion, the effect of modified lipoproteins on DCs is complex and due to the various modifications and the increasing levels during disease progression non-uniform.

While the above mentioned studies have tried to explore functions of aortic DCs and their role in atherogenesis, fewer studies have attempted to classify the heterogeneous aortic DC compartment. Recently, Choi et al. prepared the basis for detailed subset analysis of aortic DCs (Choi et al., 2011) and this work will be the foundation of the first part of this thesis. Based on functional criteria, they successfully segregated $CD11c^+MHCII^+$ DCs from $CD11c^-MHCII^+$ macrophages in the aorta. While macrophages showed poor immune stimulatory capacity but high phagocytic activity, the opposite was true for DCs. They also underlined their results using M-CSF-deficient mice in which they saw a significant reduction in macrophages. Furthermore, they distinguished DCs based on the expression of E-cadherin-ligand CD103. Choi and colleagues demonstrated that $CD103^+$ DCs do not express CD11b or F4/80 and used $CD103^+$ and $CD11b^-$

F4/80$^-$ synonymously. Using *Flt3*-deficient mice they showed that CD103$^+$ DCs are FLT3 dependent and found a systemic reduction in regulatory T cells. This is in line with an increase in plaque burden when these mice were fed a high-fat diet. In contrast, CD11b$^+$F4/80$^+$ DCs were M-CSF dependent and they were not affected by deletion of *Flt3*. This is one of the first studies to demonstrate distinct DC subsets with individual functions in the aorta of healthy and atherosclerotic mice.

The first part of this presented thesis extents and to refines the work of Choi et al. and to tries to resolve the origin of aortic DCs. Therefore, aortic DC subsets of healthy as well as of mice fed a high-fat diet for six or twelve weeks were analyzed. As macrophages, cDCs and monocyte-derived DCs share functions and also classical markers, such as CD11b and F4/80, novel markers for DCs, such as SIRPα and CD64, were tested in this thesis to allow improved discrimination. Since aortic DCs actively participate in shaping atherosclerosis, they represent an attractive target for therapeutic approaches. However, to exploit their central role, the current understanding of lesional DCs needs to be improved. Starting from the healthy aorta, DC subsets need to be described side by side with lesion development. Therefore, the characterization of DC subsets at different stages of atherosclerosis within this study allows improvement of our knowledge and provides a basis for the investigation of future DC-specific therapies.
The first part of this thesis is also being prepared for publication while writing this thesis. Parts of this thesis will under the title “Dendritic cell subset distributions in the aorta in healthy and atherosclerotic mice”.

2.3 A General View on MicroRNAs

Recent studies have started to explore the general role of microRNAs in DCs and the introduction to microRNAs and their impact on DCs has been published (Busch and Zernecke, 2012).

MicroRNA (miRNAs) have emerged as key players in the regulation of various critical cellular functions, such as development, apoptosis, differentiation or

proliferation (He et al., 2011; Jiang et al., 2011a; Salaun et al., 2011; Thomas et al., 2012; Wu et al., 2011), and represent a class of approximately 21 nucleotide (nt) long RNAs. They are processed from precursor molecules that are transcribed from either independent miRNA genes, or small parts of protein-coding transcripts. In brief, a long primary transcript (pri-miRNA) containing several hairpins is catalyzed by a complex containing the RNase III-type endonuclease DROSHA into short miRNA precursors (pre-miRNAs) with a length of approximately 70 nt. These pre-miRNAs are exported into the cytosol where they are further processed, until finally mature miRNAs of approximately 21 nucleotides are assembled into the miRNA-induced silencing complexes (miRISC) (Bushati and Cohen, 2007; Du and Zamore, 2005; Filipowicz et al., 2008; Rana, 2007). These complexes localize to miRNA-binding sites that are present in the 3′-untranslated region of targeted messenger RNAs (mRNAs).

MRNAs frequently possess multiple miRNA binding sites, both for one particular as well as for different miRNAs, each consisting of seven to eight nucleotides (Nielsen et al., 2007). Upon binding to their targets, miRISCs facilitate either degradation or translational repression of target mRNAs (Filipowicz et al., 2008). Although these modes of miRISC-mediated silencing are well accepted, the exact mechanisms are yet to be elucidated. For miRNA-mediated degradation of mRNA, both deadenylation of the 3′-poly(A) tail and decapping play a role. Translational repression, however, seems to require independent and alternative mechanisms (Behm-Ansmant et al., 2006; Giraldez et al., 2006). In addition, the initiation of translation may be targeted by miRNAs by yet again different modes of action (James et al., 2010). However, there is an ongoing discussion about the detailed mechanisms of miRNA-mediated target repression, and the development of a unifying model is still in progress (Djuranovic et al., 2011; Huntzinger and Izaurralde, 2011).

Single miRNAs can target several mRNAs (Bushati and Cohen, 2007). In addition, certain families of miRNAs can be transcribed in an orchestrated manner and are believed to target complex functions by acting in concert on different mRNA targets. For example, the *miR-17~92* cluster members (consisting of *miR-17*, *miR-18a*, *miR-19a*, *miR-19b-1*, *miR-20a* and *miR-92a-1*)

and their paralogues in the *miR-106b~25* cluster (comprising *miR-106b*, *miR-93*, and *miR-25*) can promote hematopoietic cell expansion in mice, with *miR-17*, *miR-20*, *miR-93* and *miR-106b* sharing an AAAGUGC motif in their seed region, enabling them to act on similar mRNA targets. *MiR-17/20/93/106* promote hematopoietic cell expansion by targeting sequestosome 1-regulated pathways in mice (Meenhuis et al., 2011). These concerted effects are crucial to miRNA-mediated regulation, as single miRNAs exert only modest effects on protein levels (Baek et al., 2008). In general, it is now well accepted that miRNAs act as fine-tuning elements, rather than major post-transcriptional regulators.

Interestingly, miRNA can also cross cell borders and participate in regulating cellular functions across the cell membrane, thereby playing a role in signaling. Free miRNAs have been discovered in the blood (Vasilescu et al., 2009). Bound to high-density lipoproteins (HDL) they can be delivered to recipient hepatocytes where they contribute to target downregulation (Vickers et al., 2011). Moreover, microvesicles released from cells can contain and transfer miRNAs to recipient cells. For example, monocyte-secreted microvesicles carry functional *miR-150* and target endothelial migration (Zhang et al., 2010). Endothelial-derived apoptotic bodies can transfer *miR-126* to confer paracrine CXCL12-dependent vascular protection (Zernecke et al., 2009). In addition, exosomes generated from T cells, B cells, and DCs have distinct miRNA profiles and can transfer these to other cells (Mittelbrunn et al., 2011; Thery et al., 2009). Only recently, the exosome-mediated transfer of functional miRNAs has been demonstrated to occur between DCs (Montecalvo et al., 2012).

All these studies demonstrate an important role for miRNAs, however, the knowledge about the mechanism behind is poor and currently we are far from understanding the exact nature of miRNA-mediated functions.

2.3.1 MicroRNA in Dendritic Cells

Only few studies have investigated the role of miRNA in DCs and none of them has focused on DCs in the context of atherosclerosis. Nevertheless, bone marrow-, monocyte-derived DCs or the development and differentiation of DCs have been investigated (El Gazzar and McCall, 2012; Hashimi et al., 2009; Lu et al., 2011; Sun et al., 2011; Turner et al., 2011). The best characterized miRNA in DCs is *miR-155*. It has been shown to be upregulated during DC maturation, in response to TLR ligands, TNFα and IFNα in both mouse and human (Dunand-Sauthier et al., 2011; Lu et al., 2011; Zhou et al., 2010). Moreover, *miR-155* expression levels are increased in bone marrow-derived DCs upon LPS stimulation (Martinez-Nunez et al., 2009; O'Connell et al., 2009; Tili et al., 2007). The expression of *miR-155* in GM-CSF-derived DCs (Masaki et al., 2007; O'Connell et al., 2010) may furthermore denote its function in the context of DC activation, given the predominant expression of the cytokine GM-CSF during inflammation (Hamilton, 2008). Further evidence for a pro-inflammatory role of *miR-155* comes from the fact that *miR-155* upregulation is associated with enhanced translation of pro-inflammatory TNFα, most likely due to increased transcript stability (Tili et al., 2007). Moreover, *miR-155* is capable of downregulating anti-inflammatory factors, such as Src homology-2 domain containing inositol 5-phosphatase 1 (SHIP1) (O'Connell et al., 2009), upregulating pro-inflammatory signaling (Wang et al., 2010) and governs the ability of DCs to efficiently induce T cell proliferation (Rodriguez et al., 2007). As mentioned before, miRNA can target several mRNAs and therefore it is of no surprise that *miR-155* can also exert anti-inflammatory functions, for example by targeting factors that are part of the NF-κB and p38 MAPK pathway (Ceppi et al., 2009), or known to activate the LPS/TNFα pathway (Tili et al., 2007).

Besides *miR-155*, only *miR-146a* has been characterized extensively in DCs. For example, myeloid cell proliferation is influenced by indirect M-CSF receptor regulation (Boldin et al., 2011) and its induction by transcription factor PU.1 links *miR-146a* to myeloid cell differentiation (Ghani et al., 2011) and DCs. While *miR-155* is considered to exert rather pro-inflammatory effects, *miR-146a* confers fairly anti-inflammatory effects. Its induction upon pro-inflammatory signaling aids in silencing of pro-inflammatory factors, such as TNFα and

desensitizes DCs to TLR-dependent signaling (El Gazzar et al., 2011; Jurkin et al., 2010; Nahid et al., 2011; Taganov et al., 2006).

The data on these miRNA show the relevance of miRNA to DCs biology and they clearly demonstrate that miRNA can regulate pro- or anti-inflammatory properties in DCs. Since atherosclerosis is a chronic inflammatory disease, it is crucial to further investigate miRNA-mediated effects in DCs and evaluate their relevance to development and progression of atherosclerosis.

2.3.2 The microRNA Cluster miR-17~92

As mentioned earlier, miRNA can be expressed from individual pri-miRNA precursor transcripts, but several miRNA can also be generated from a single pri-miRNA. The latter is termed miRNA cluster and one of these clusters is the *miR-17~92* cluster. Although little is known about its role in DCs, it has been described very well in tumor biology (Olive et al., 2010). The cluster, localized on chromosome 13, comprises 6 miRNAs, namely *miR-17*, *miR-18a*, *miR-19a*, *miR-19b-1* (*miR-19b* in the remainder), *miR-20a* and *miR-92a-1* (*miR-92a* in the remainder) and is conserved in various species. Three copies can be found in mammals; the clusters *miR-106b~25* on chromosome 7 and *106a-363* on the X chromosome and the *miR-17~92* cluster (Tanzer and Stadler, 2004).

MiRNA that share a common motif in their seed region are called miRNA family. Four such miRNA families can be found within the *miR-17~92* cluster. The biggest family is the *miR-17* family (including *miR-17*, *miR-18a* and *miR-20a*) while each of the remaining miRNAs represents a family of their own. In one of the first functional studies on *miR-17~92*, its enforced expression led to increased myelocytomatosis oncogene (MYC) levels and accelerated tumor development in a mouse B-cell lymphoma model. Mice deficient for *miR-17~92* are not viable due to severe lung hypoplasia and ventricular septum defects. Furthermore, the same study demonstrated that the cluster is necessary for B cell development (Ventura et al., 2008). Overexpression of *miR-17~92* in lymphocytes leads to lymphoproliferative disease, autoimmunity and contributes to lymphoma development. These disorders were attributed to the tumor suppressor phosphatase and tensin homolog (PTEN) and the pro-apoptotic

protein B cell leukemia/lymphoma 2-like factor 11 (BIM), both targets of *miR-17~92* (Xiao et al., 2008).

Moreover, the cluster has also been examined in T cells. It is differentially regulated in CD8 T cells, induced after CD8 T cell activation and downregulated after clonal expansion and during memory development (Salaun et al., 2011; Wu et al., 2012). Overexpression leads to increased effector activity in CD8 T cells and a loss in CD8 memory T cells. In CD4 T cells the cluster promotes Th1 responses, inhibits peripheral Treg induction and is required for antigen response (Jiang et al., 2011b; Lykken and Li, 2011).

Although there are several studies that have investigated the role of *miR-17~92* in cancer, B or T cell biology, no study has tried to characterize the impact of this particular cluster on DCs, so far. However, Kuipers *et al.* profiled miRNAs differentially expressed in pDCs and DCs (Kuipers et al., 2010). Although their work focuses on *miR-221* and *miR-222*, the profiling data reveals high *miR-17~92* expression in FLT3-cultured bone marrow-derived pDCs and comparably low expression in GM-CSF-cultured bone marrow-derived cDC.

The second aim of this thesis is the characterization of mice with a *Cd11c*-specific deficiency for the cluster *miR-17~92*. This cluster has been studied in cancer, T and B cell biology, however, the relevance to DC development and function is not known. Mice with the *miR-17-92* locus flanked by loxP sites were crossed with *Cd11c-cre* deleter mice. These mice with a *Cd11c*-specific *miR-17~92* deficiency were analyzed in non-inflammatory conditions. Furthermore, they were also crossed with *Ldlr*-deficient mice to investigate the role of *miR-17~92*-deficient DCs in atherosclerosis. This thesis characterizes *miR-17~92*-deficient DCs for the first time and focuses on consequences for T cell phenotype and plaque development. Importantly, knowledge gained from this thesis does not only apply to atherosclerosis: Because of the central role in the immune system, the insights from DC biology gained in this thesis can also be translated to other diseases, such as infectious or autoimmune diseases, for example systemic lupus erythematosus, EAE, graft rejection or colitis.

3 Material and Methods

3.1 Material

3.1.1 Consumables and Instrumentation

All plastic consumables, such as 1/1.5/15/50 ml tubes, PCR tubes, 10/15 cm cell culture dishes, 6-/24-/96-well plates, pipette tips and pipettes and related were obtained from Sarstedt (Nümbrecht, Germany). Injection needles, syringes and related were obtained from BD (Heidelberg, Germany).

Table 1 Special consumables and manufacturer.

Consumables	Manufacturer
384-well plates	Life Technologies (Darmstadt, Germany)
70 µm cell strainer	BD (Heidelberg, Germany)
EDTA tubes	Sarstedt (Nümbrecht, Germany)
Serum gel tubes	Sarstedt (Nümbrecht, Germany)
Star Frost glass slides	Waldemar Knittel Glasbearbeitung (Braunschweig, Germany)
White 96-well plates for luciferase assays	Thermo Scientific (St. Leon-Rot, Germany)

Table 2 Main instrumentation.

Machine	Manufacturer
FACSCantoII	BD (Heidelberg, Germany)
1052 tissue floating bath	GFL (Burgwedel, Germany)
Applied Biosystems 7900HT Fast Real-Time PCR System	Life Technologies (Darmstadt, Germany)
Automated vacuum tissue processor ASP 200S	Leica Microsystems (Nussloch, Germany)
C1000/S1000 Thermal PCR Cycler	Bio-Rad (München, Germany)
Cell culture bench SK-12000	BDK Luft- und Reinraumtechnik (Sonnenbühl, Germany)
cell culture incubators	Binder (Tuebingen, Germany)
centrifuge 5430R	Eppendorf (Hamburg, Germany)
EG 1160 tissue embedding station	Leica Microsystems (Nussloch, Germany)
FLUOstarOPTIMA	BMG Labtech (Ortenberg, Germany)
freezers/refrigerators	Liebherr (Bulle, Switzerland)
Heraeus dry-air oven	Thermo Scientific (St. Leon-Rot, Germany)
Heraeus Fresco 17 centrifuge	Thermo Scientific (St. Leon-Rot, Germany)
Heraeus HERAfreeze -80 °C freezer	Thermo Scientific (St. Leon-Rot, Germany)
HS 1220 stretching table	Leica Microsystems (Nussloch, Germany)
Multipette Xstream	Eppendorf (Hamburg, Germany)
Nanodrop 2000c	Thermo Scientific (St. Leon-Rot, Germany)
pipettes for 0.5 – 10/10 – 100/20 – 200/100 – 100 µl volumina	VWR (Darmstadt, Germany) Eppendorf (Hamburg, Germany)
Pipetus electronic pipette controller	Hirschmann Laborgeraete (Eberstadt, Germany)
PowerPac basic power supply for electrophoresis	Bio-Rad (Muenchen, Germany)

Rainin 8/12x multichannel pipettes	Mettler-Toledo (Giessen, Germany)
RM 2255 S rotary microtome	Leica Microsystems (Nussloch, Germany)
Scissors and forceps for animal preparation	Fine Science Tools (Heidelberg, Germany)
Stereomicrosope SZX10	Olympus (Hamburg, Germany)
Sub-cell GT electrophoresis chamber	Bio-Rad (Muenchen, Germany)
TE3102S/CD225D balance	Sartorius (Goettingen, Germany)
Thermomixer Comfort/Standard	Eppendorf (Hamburg, Germany)

3.1.2 Chemicals

3.1.2.1 Cell Culture and Flow Cytometry

Table 3 Chemicals required for media and solutions in use for cell culture and flow cytometry experiments.

Media, Solutions and Related	Manufacturer
RPMI-1640	Life Technologies (Darmstadt, Germany)
Absolute ethanol, non-denatured	AppliChem (Darmstadt, Germany)
Bovine serum albumin (BSA)	Sigma-Aldrich (Taufkirchen, Germany)
Brefeldin A	Sigma-Aldrich (Taufkirchen, Germany)
Carboxyfluorescein succinimidyl ester (CFSE)	Sigma-Aldrich (Taufkirchen, Germany)
$CD11c^+$ isolation kit	Miltenyi (Bergisch Gladbach, Germany)
$CD4^+CD62L^+$ T cell isolation kit II	Miltenyi (Bergisch Gladbach, Germany)
Cytofix	BD (Heidelberg, Germany)
Cytofix/cytoperm	BD (Heidelberg, Germany)
Dulbecco's Modified Eagle Medium (DMEM)	Life Technologies (Darmstadt, Germany)

Ethylenediaminetetraacetic acid	Sigma-Aldrich (Taufkirchen, Germany)
Fetal calf serum (FCS)	PAA (Pasching, Austria)
Fixation/permeabilization kit	eBioscience (Frankfurt am Main, Germany)
FluoSpheres (1.0 µm, yellow-green)	Life Technologies (Darmstadt, Germany)
Hank's balanced salt solution (HBSS)	Life Technologies (Darmstadt, Germany)
Ionomycin	Sigma-Aldrich (Taufkirchen, Germany)
Liberase Blendzyme TL	Roche (Mannheim, Germany)
L-tryptophan	AppliChem (Darmstadt, Germany)
Mouse serum	Sigma-Aldrich (Taufkirchen, Germany)
OVA (323 – 339, amino acid sequence in three-letter code: H – Ile – Ser – Gln – Ala – Val – His – Ala – Ala – His – Ala – Glu – Ile – Asn – Glu – Ala – Gly – Arg – OH)	AnaSpec (Seraing, Belgium)
Penicillin/streptomycin	Life Technologies (Darmstadt, Germany)
Perm/wash buffer	BD (Heidelberg, Germany)
Phorbol-12-myristat-13-acetat (PMA)	Sigma-Aldrich (Taufkirchen, Germany)
Phosphate buffered saline (PBS)	Life Technologies (Darmstadt, Germany)
Rabbit serum	Sigma-Aldrich (Taufkirchen, Germany)
Stain buffer	BD (Heidelberg, Germany)
β-mercaptoethanol	Life Technologies (Darmstadt, Germany)

Table 4 Cytokines for cell culture experiments.

Cytokines	Manufacturer
GM-CSF	Peprotech (Hamburg, Germany)

Table 5 Assays for blood serum analysis.

Assays and Related	Manufacturer
Amplex red cholesterol assay kit	Life Technologies (Darmstadt, Germany)
EnzyChrom triglyceride assay kit	Medibena (Wien, Austria)

Table 6 Antibodies used in flow cytometry.

Epitope	Fluorophore	Clone	Manufacturer
B220	FITC	RA3-6B2	eBioscience (Frankfurt am Main, Germany)
B220	Pacific Blue	RA3-6B2	BD (Heidelberg, Germany)
B220	V500	RA3-6B2	BD (Heidelberg, Germany)
CD103	APC	2E7	eBioscience (Frankfurt am Main, Germany)
CD103	PE	2E7	eBioscience (Frankfurt am Main, Germany)
CD115	APC	AFS98	eBioscience (Frankfurt am Main, Germany)
CD115	PE	AFS98	eBioscience (Frankfurt am Main, Germany)
CD11b	FITC	M1/70	eBioscience (Frankfurt am Main, Germany)
CD11b	PerCP-Cy5.5	M1/70	eBioscience (Frankfurt am Main, Germany)
CD11b	V500	M1/70	BD (Heidelberg, Germany)
CD11c	AlexaFluor 488	N418	eBioscience (Frankfurt am Main, Germany)
CD11c	APC	N418	eBioscience (Frankfurt am Main, Germany)

CD11c	FITC	N418	eBioscience (Frankfurt am Main, ermany)
CD11c	PE-Cy7	N418	eBioscience (Frankfurt am Main, Germany)
CD172a	FITC	P84	BD (Heidelberg, Germany)
CD19	APC	eBio1D3	eBioscience (Frankfurt am Main, Germany)
CD19	FITC	1D3	BD (Heidelberg, Germany)
CD19	PerCP-Cy5.5	1D3	BD (Heidelberg, Germany)
CD25	APC	PC61.5	eBioscience (Frankfurt am Main, Germany)
CD3ε	APC	145-2C11	eBioscience (Frankfurt am Main, Germany)
CD3ε	APC-Cy7	145-2C11	BD (Heidelberg, Germany)
CD3ε	FITC	145-2C11	eBioscience (Frankfurt am Main, Germany)
CD3ε	PerCP-Cy5.5	145-2C11	BD (Heidelberg, Germany)
CD3ε	V450	500A2	BD (Heidelberg, Germany)
CD3ε	V500	500A2	BD (Heidelberg, Germany)
CD4	APC	RM4-5	eBioscience (Frankfurt am Main, Germany)
CD4	APC-Cy7	GK1.5	BD (Heidelberg, Germany)
CD4	FITC	GK1.5	eBioscience (Frankfurt am Main, Germany)
CD4	PE	RM4-5	eBioscience (Frankfurt am Main, Germany)
CD4	PE-Cy7	GK1.5	eBioscience (Frankfurt am Main, Germany)
CD40	APC	1C10	eBioscience (Frankfurt am Main, Germany)
CD44	PE	IM7	eBioscience (Frankfurt am Main, Germany)

CD44	PerCP-Cy5.5	IM7	eBioscience (Frankfurt am Main, Germany)
CD45	APC-Cy7	30-F11	BD (Heidelberg, Germany)
CD45.1	V450	A20	BD (Heidelberg, Germany)
CD62L	APC	MEL-14	eBioscience (Frankfurt am Main, Germany)
CD62L	FITC	MEL-14	BD (Heidelberg, Germany)
CD62L	PE-Cy7	MEL-14	eBioscience (Frankfurt am Main, Germany)
CD64	APC	X54-5/7.1	BioLegend (Fell,Germany)
CD80	APC	16-10A1	eBioscience (Frankfurt am Main, Germany)
CD86	PE	GL1	eBioscience (Frankfurt am Main, Germany)
CD86	PE	PO3.1	eBioscience (Frankfurt am Main, Germany)
CD8α	PE	53-6.7	eBioscience (Frankfurt am Main, Germany)
CD8α	PE-Cy7	53-6.7	eBioscience (Frankfurt am Main, Germany)
CD8α	V500	53-6.7	BD (Heidelberg, Germany)
F4/80	APC	BM8	eBioscience (Frankfurt am Main, Germany)
F4/80	PE	BM8	eBioscience (Frankfurt am Main, Germany)
FLT3	PE	A2F10	eBioscience (Frankfurt am Main, Germany)
FOXP3	PE	FJK-16s	eBioscience (Frankfurt am Main, Germany)
MHCII	APC	M5/114.15.2	eBioscience (Frankfurt am Main, Germany)
MHCII	eFlour 450	M5/114.15.2	eBioscience (Frankfurt am Main, Germany)
MHCII	FITC	2G9	BD (Heidelberg, Germany)

TCRβ	PerCP-Cy5.5	H57-597	eBioscience (Frankfurt am Main, Germany)
TCRβ	V450	H57-597	BD (Heidelberg, Germany)
TCRγδ	APC	eBioGL3	eBioscience (Frankfurt am Main, Germany)
TCRγδ	FITC	GL3	eBioscience (Frankfurt am Main, Germany)

3.1.2.2 Molecular Cloning and Quantitative Real Time PCR

All primers were obtained from Eurofins MWG Operon (Ebersberg, Germany) and the sequence listed in Table 7 is given in 5'-3' direction.

Table 7 Primers for molecular cloning and quantitative real time PCR.

Name	Primer Sequence
Socs3_1792_for	TCG CTC GAG GCT TTT TTC TCT CTG TTT TG
Socs3_1792_rev	GCG CGG CCG CAA TGT TTC TTT TCT GAG TAT A
Socs3_ctrl_for	TCG CTC GAG CTT AAA TGC CCT CTG TCC CA
Socs3_ctrl_rev	GCG CGG CCG CAC TGA CCG AGA GAT GAC TAG
Socs3_for	ATT TCG CTT CGG GAC TAG C
Socs3_rev	AAC TTG CTG TGG GTG ACC AT
psiCHECK-2_1429_for	GGT TCT TTT CCA ACG CTA TTG T

Table 8 Reagents and kits used for molecular cloning, quantitative real time PCR and luciferase assays.

RT-qPCR, Molecular Cloning and Luciferase Assays	Manufacturer
First strand cDNA synthesis kit	Thermo Scientific (St. Leon-Rot, Germany)
2-Amino-2-(hydroxymethyl)-propan-1,3-diol (TRIS)	AppliChem (Darmstadt, Germany)
Ampicillin	Sigma-Aldrich (Taufkirchen, Germany)
Buffer O	New England Biolabs (Frankfurt am Main, Germany)
Calcium chloride ($CaCl_2$)	Carl Roth (Karlsruhe, Germany)

dNTP mix	Thermo Scientific (St. Leon-Rot, Germany)
Dual-luciferase reporter assay system	Promega (Mannheim, Germany)
Escherichia coli XL10	a gift from H. Hermanns, RVZ, Würzburg, Germany
Ethanol (EtOH)	AppliChem (Darmstadt, Germany)
Ethidium bromide (EtBr)	AppliChem (Darmstadt, Germany)
Fast alkaline phosphatase	Thermo Scientific (St. Leon-Rot, Germany)
Fast alkaline phosphatase buffer	Thermo Scientific (St. Leon-Rot, Germany)
GeneJET plasmid miniprep kit	Thermo Scientific (St. Leon-Rot, Germany)
GeneRuler 1 kb Plus DNA ladder	Thermo Scientific (St. Leon-Rot, Germany)
Glucose	Carl Roth (Karlsruhe, Germany)
Isopropanol	Carl Roth (Karlsruhe, Germany)
LB medium (Lennox)	Carl Roth (Karlsruhe, Germany)
LE agarose	Biozym (Hessisch Oldendorf, Germany)
Magnesium chloride ($MgCl_2$)	AppliChem (Darmstadt, Germany)
Maxima SYBR green/ROX qPCR master mix	Thermo Scientific (St. Leon-Rot, Germany)
miRNeasy mini kit	Qiagen (Hilden, Germany)
miScript II RT kit	Qiagen (Hilden, Germany)
miScript primer assays	Qiagen (Hilden, Germany)
miScript SYBR green PCR kit	Qiagen (Hilden, Germany)
NotI	New England Biolabs (Frankfurt am Main, Germany)
NucleoBond PC 500	Machery-Nagel (Düren, Germany)
NucleoSpin RNA II	Machery-Nagel (Düren, Germany)
Opti-MEM	Life Technologies (Darmstadt, Germany)

Pfu buffer with magnesium chloride ($MgCl_{2)}$	Thermo Scientific (St. Leon-Rot, Germany)
Pfu DNA polymerase	Thermo Scientific (St. Leon-Rot, Germany)
Phusion CG buffer	Thermo Scientific (St. Leon-Rot, Germany)
Phusion hot start II DNA polymerase	Thermo Scientific (St. Leon-Rot, Germany)
Piperazine-1,4-bis-(2-ethanesulfonic acid) (PIPES)	AppliChem (Darmstadt, Germany)
Pre-miR miRNA precursors	Life Technologies (Darmstadt, Germany)
Proteinase K	Thermo Scientific (St. Leon-Rot, Germany)
psiCHECK-2 dual luciferase reporter vector	Promega (Mannheim, Germany)
QIAquick gel extraction kit	Qiagen (Hilden, Germany)
QIAshredder	Qiagen (Hilden, Germany)
Rneasy micro kit	Qiagen (Hilden, Germany)
RNeasy mini kit	Qiagen (Hilden, Germany)
Sodium acetate (NaOAc)	Carl Roth (Karlsruhe, Germany)
Sodium chloride (NaCl)	Carl Roth (Karlsruhe, Germany)
Sodium dodecyl sulfate (SDS)	Carl Roth (Karlsruhe, Germany)
T4 DNA ligase	Thermo Scientific (St. Leon-Rot, Germany)
T4 DNA ligase buffer	Thermo Scientific (St. Leon-Rot, Germany)
Tryptone	Carl Roth (Karlsruhe, Germany)
Turbofect	Thermo Scientific (St. Leon-Rot, Germany)
XhoI	New England Biolabs (Frankfurt am Main, Germany)
Yeast extract	Carl Roth (Karlsruhe, Germany)

3.1.2.3 Histology and Immunohistochemistry

Table 9 Chemicals required for histology and immunohistochemistry.

Histology and Immunohistochemistry	Manufacturer
Citric acid	Carl Roth (Karlsruhe, Germany)
Acid aldehyde	Sigma-Aldrich (Taufkirchen, Germany)
Basic fuchsin	Sigma-Aldrich (Taufkirchen, Germany)
Bovine serum albumin (BSA)	Carl Roth (Karlsruhe, Germany)
Concentrated hydrochloric acid	AppliChem (Darmstadt, Germany)
Disodium phosphate (Na_2HPO_4)	Carl Roth (Karlsruhe, Germany)
Ethanol	AppliChem (Darmstadt, Germany)
Gelatin	Sigma-Aldrich (Taufkirchen, Germany)
Glycerin	Carl Roth (Karlsruhe, Germany)
Hemalm	Merck (Darmstadt, Germany)
HISTO-COMP paraffin	Vogel (Giessen, Germany)
Horse serum	VectorLaboratories (Burlingame, Canada)
Isopropanol	Sigma-Aldrich (Taufkirchen, Germany)
Monopotassium phosphate (KH_2PO_4)	Carl Roth (Karlsruhe, Germany)
Mouse serum	VectorLaboratories (Burlingame, Canada)
Oil-Red-O	Sigma-Aldrich (Taufkirchen, Germany)
Paraformaldehyde (PFA)	Carl Roth (Karlsruhe, Germany)
Polysine slides	Thermo Scientific (St. Leon-Rot, Germany)
Potassium chloride (KCl)	Carl Roth (Karlsruhe, Germany)
Rabbit serum	VectorLaboratories (Burlingame, Canada)
Saturated aqueous picric acid (pH 2.0)	Sigma-Aldrich (Taufkirchen, Germany)
Sirius red	Sigma-Aldrich (Taufkirchen, Germany)
Sodium chloride (NaCl)	Carl Roth (Karlsruhe, Germany)
Sodium citrate	Carl Roth (Karlsruhe, Germany)
Sucrose	Sigma-Aldrich (Taufkirchen, Germany)

Tissue Tek OCT Compound	Sakura Finetek (Staufen, Germany)
Triton X 100	Carl Roth (Karlsruhe, Germany)
Tween-20	AppliChem (Darmstadt, Germany)
Vectashield	VectorLaboratories (Burlingame, Canada)
Vitro-Clud	R. Langenbrinck (Emmendingen, Germany)
Xyline	Carl Roth (Karlsruhe, Germany)

Table 10 Antibodies used in immunohistochemistry.

Epitope	Fluorophore	Clone	Manufacturer
CD3	-	CD3-12	AbD Serotec (Düsseldorf, Germany)
isotype control for CD3 staining	-	IgG2a	AbD Serotec (Düsseldorf, Germany)
rat IgG	AlexaFluor488	polyclonal goat αRat	Life Technologies (Darmstadt, Germany)

3.1.2.3 Media and Solutions for Cell Culture

DC Medium

RPMI-1640 medium with 2 mM L-glutamine supplemented with 10 % FCS, 100 U/ml penicillin/streptomycin and 50 µM β-mercaptoethanol.

HEK cell medium

HEK293 cells were maintained in Dulbecco's Modified Eagle Medium (DMEM), supplemented with 10 % FCS and 100 U/ml penicillin/streptomycin.

3.1.2.4 Media and Solutions for Flow Cytometry

Hank's Complete

HBSS was supplemented with 0.6 % BSA and 300 µM EDTA.

FACS Staining Buffer

FACS staining buffer was prepared from PBS, supplemented with 2 % mouse serum, 2 % rabbit serum and 2 % BSA.

Red Blood Cell (RBC) Lysis Buffer

RBC lysis buffer contained 155 mM NH_4Cl, 10 mM $KHCO_3$ and 0.1 mM EDTA.

3.1.2.5 Media and Solutions for Molecular Cloning

Tail Lysis Buffer

Tail lysis buffer consisted of 10 mM TRIS (pH 8.0), 10 mM EDTA (pH 8.0), 10 mM NaCl and 0,5 % SDS.

TAE Buffer

TAE buffer for gel analysis of PCR products contained 40 mM TRIS, 20 mM acetic acid, and 1 mM EDTA.

Transformation Buffer

Buffer for generation of chemically competent cells was made of 60 mM $CaCl_2$, 10 mM PIPES (pH 7) and 15 % glycerol. Final pH was adjusted to 7.0. Sterile buffer was obtained by filtration (0.22 µm).

LB medium

LB medium was made of ready to use LB medium powder with 35 g/liter in deionized water. Medium was autoclaved.

SOB medium

SOB medium was obtained from 20 g/l tryptone, 5 g/l yeast extract and 0.5 g/l NaCl. Solutes were dissolved in 950 ml deionized water and 250 mM KCl were added. Final pH was adjusted to 7.0, volume was adjusted to 1 liter. Medium was autoclaved and 5 ml sterile 2 M $MgCl_2$ were added.

SOC medium

SOC medium was prepared from SOB medium. 1 l SOB medium was supplemented with sterile (0.22 µm filtration) 20 ml 1 M glucose.

3.1.2.6 Media and Solutions for Histology and Immunohistochemistry

Phosphate Buffered Saline Solution (PBS)

PBS contained 137 mM NaCl, 2.7 mM KCl, 18.61 mM Na_2HPO_4 and 1.8 mM KH_2PO_4 in deionized water. The pH was adjusted to 7.4.

Oil-Red-O Lipid Staining Solution

Oil-Red-O stock solution was prepared from 1 g Oil-Red-O dissolved in 200 ml isopropanol. 180 ml stock solution were added to 120 ml deionized water and incubated for 1 h at room temperature before solution was filtered.

Blocking/Staining Buffer for T cell Staining

The buffer contained 0.1 % BSA in PBS.

Kaiser's Glycerin Jelly

For stock solution 4 g gelatin were dissolved in 21 ml deionized water and 25 ml glycerin were added. Working solution contained 3 parts stock solution and 7 parts deionized water.

3.2 Methods

3.2.1 Mice and Husbandry

C57BL/6J (B6), mir17-92$^{tm1.1Tyj}$/J (*miR-17~92*), C57BL/6-Tg(TcraTcrb)^{425Cbn}/J (*OTII*), B6.Cg-Tg(Itgax-cre)$^{1-1Reiz}$/J (*CD11c-cre*) and B6.129S7-Ldlr^{tm1Her}/J (*Ldlr*) mice were obtained from The Jackson Laboratory (Maine, USA). All mice were bred and maintained within the Zentrum für Experimentelle Molekulare Medizin (ZEMM), Zinklesweg 10 in 97078 Würzburg (B6, *miR-17~92*, *Ldlr, CD11c-cre*) or in the animal facility of the Rudolf-Virchow-Zentrum (RVZ), Josef-Schneider-Straße 2 in 97080 Würzburg (*OTII*). For the induction of atherosclerosis, age-matched knockout and control mice were fed a diet at a starting age of 7-8 weeks (unless otherwise defined). High-fat western diet food containing 15 % milk fat and 1.25 % cholesterol for mice with *Ldlr*-deficiency was obtained from Altromin (Lage, Germany). All experiments conducted were approved by local authorities.

3.2.2 In vivo Experiments

Preparation of Single Cell Suspensions from Bone Marrow for Flow Cytometry

Tibiae were isolated and excessive tissue was thoroughly removed before bone marrow cavities were flushed with Hank's complete. Cells were passed through a 70 µm cell strainer to obtain single cell suspensions, washed and resuspended in Hank's complete to adjust cell count.

Preparation of Single Cell Suspensions from Spleen for Flow Cytometry

Spleens were dissected and passed through a 70 µm cell strainer. Cell suspensions were washed in Hank's complete and incubated in 3 ml RBC lysis buffer for 5 minutes at room temperature. Lysis was stopped by addition of 7 ml Hank's complete and cells were resuspended after being washed in Hank's complete for further processing.

Preparation of Single Cell Suspensions from Lymph Nodes for Flow Cytometry

Peripheral lymph nodes (axillary, brachial and inguinal) were dissected and passed through a 70 µm cell strainer. Cell suspensions were both washed once and resuspended in Hank's complete.

Preparation of Blood for Flow Cytometry

Peripheral blood was obtained from the retro-orbital plexus and collected in EDTA tubes. 150 µl blood were incubated in 3 ml RBC lysis buffer for 5 minutes at room temperature. Lysis was stopped with 7 ml Hank's complete and cells were resuspended in Hank's complete after being washed.

Enzymatic Digestion of Aortic Tissue for Flow Cytometry

For stock solution, 5 mg liberase TL were dissolved in 400 µl deionized water at stored at -20 °C. Aortae were flushed with PBS, dissected, chopped and placed in 142.5 µl RPMI1640, supplemented with 7.25 µl liberase TL stock solution. Tissue was incubated for 30 minutes at 37 °C in a thermo shaker at 1400 rpm and subsequently passed through a 70 µm cell strainer. Cells were washed in Hank's complete and staining for flow cytometry was applied.

Measuring Blood Cholesterol and Triglyceride Levels

Blood was obtained from the heart and collected in serum gel tubes. Serum was prepared by centrifugation at 10 000 g, 20 °C for 5 minutes. Cholesterol and triglyceride levels were measured with the Amplex red cholesterol assay kit or the EnzyChrom triglyceride assay kit, respectively, according to manufacturer's instructions using a FUOstar OPTIMA plate reader.

Adoptive Transfer of Naïve T cells

Naïve CD4 T cells were isolated from transgenic *Cd45.1* mice using the $CD4^+CD62L^+$ T Cell isolation kit II following manufacturer's instructions and $4 \cdot 10^6$ cells per recipient mouse were resuspended in 200 µl PBS and injected intravenously (tail vein injection). Mice were sacrificed 10 d post injection and spleen and lymph nodes were isolated and prepared for flow cytometry. When atherosclerotic mice were used, they were placed on atherogenic diet for 25 days prior to injection and maintained on atherogenic diet for the time after injection to result in 5 weeks of diet.

3.2.3 Histology and Immunohistochemistry

Preparation of Aortae for *En Face* Plaque Measurements

Mice were sacrificed and the heart was punctured to obtain blood. Subsequently, the mice were reperfused with PBS followed by trans-cardial perfusion with 4 % PFA in PBS. Excessive fat and tissue was removed and the aorta was dissected, removed and mounted on gummed glass slides. Slides were left in 4 % PFA in PBS over night and adventitial tissue was removed before oil-red-o staining was performed.

Oil-Red-O Lipid Staining for Aortae

Samples were watered in PBS for 5 minutes before they were dipped ten times in 60 % isopropanol, followed by 15 minutes incubation in oil-red-o working solution. After additional ten dips in 60 % isopropanol samples were mounted in Kaiser's glycerin jelly and images were recorded with a Leica DMLB microscope.

Preparation of Aortic Roots

Mice were prepared as described and the heart was dissected after fixation by reperfusion with 4 % PFA in PBS. After fixation in 4 % PFA over night, hearts were processed automatically following the protocol in Table 11:

Table 11 Protocol for tissue processing using the fully automated Leica ASP 200S tissue processor.

Reagent	Step	Duration	Temperature
70 % ethanol	1	1 hour	
70 % ethanol	2	1 hour	
96 % ethanol	3	1 hour	
96 % ethanol	4	1 hour	
100 % ethanol	5	1 hour	
100 % ethanol	6	1 hour	
100 % ethanol	7	1 hour	
xylene	8	1 hour	45 °C
xylene	9	1 hour	45 °C
xylene	10	1 hour	45 °C
paraffin	11	1 hour	62 °C
paraffin	12	1 hour	62 °C
paraffin	13	over night	62 °C

Samples were embedded in paraffin and subsequently cut in 5 µm serial sections before incubation at 56 °C over night.

Deparaffinization

Sections were incubated in xylene for three times 15 minutes before they were washed twice in 100 % ethanol for 1 minute. Subsequently, samples were incubated twice in 90 % ethanol for 1 minute before they were treated with 70 % ethanol for 1 minute. After that, samples were placed in 70 % ethanol for 10 minutes, followed by a wash in deionized water for 10 minutes before antigen retrieval was performed.

Antigen Retrieval

1.8 ml 0.1 M citric acid were added to 8.2 ml 0.1 M sodium citrate. Volume was adjusted to 100 ml with deionized water and 50 µl Tween-20 were added. Solution was warmed and slides were placed in pre-warmed antigen retrieval solution. Slides were heated in a microwave for 10 minutes before half of the solution was discarded and replaced with fresh antigen retrieval solution. After additional 10 minutes of heat the samples were allowed to cool for 30 minutes at room temperature. Slides were washed twice in PBS before samples were blocked.

T cell Staining of Aortic Roots

Aortic root sections were deparaffinized. Subsequently, antigen retrieval was performed as described and sections were blocked in 30 – 50 µl blocking buffer for 30 minutes. Buffer was removed and primary αCD3 antibody was diluted 1:50 in staining buffer. Isotype controls were prepared using equivalent concentrations. Sections were stained at 4 °C over night before a 15 minute wash in PBS. Samples were washed for additional 5 minutes and secondary antibody was diluted 1:500 in staining buffer before 1 – 2 hours of incubation at room temperature. Sections were again washed for 15 and 5 minutes in PBS and excessive liquid was removed before slides were mounted and nuclei were counterstained with DAPI. Images were recorded with a Leica DMLB fluorescence microscope. Borders were sealed with nail polish.

3.2.4 In vitro Experiments

Bone Marrow-derived Dendritic Cell Culture

Femurs and tibiae were isolated and excessive tissue was thoroughly removed. The bones were prepared under aseptic conditions. After a wash in 70 % ethanol followed by a wash in PBS, the marrow cavities were flushed with PBS. Bone marrow was passed through a 70 µm cell strainer to obtain single cell suspensions and cells were washed in PBS. Cells were seeded at $2 \cdot 10^6$ cells/ml in DC medium supplemented with 50 ng/ml GM-CSF. Culture medium was changed every second day and cell count was adjusted to $2 \cdot 10^6$ cells/ml. Cells were used on day 7 – 8 after the start of the culture.

Antigen-specific T cell Proliferation and Polarization

For antigen-specific T cell proliferation, naïve CD4 T cells were isolated from transgenic *OTII* mice using the $CD4^+CD62L^+$ T Cell isolation kit II following manufacturer's instructions. Average yield was $10 \cdot 10^6$ – $15 \cdot 10^6$ naïve T cells per isolation. Isolated cells were adjusted to $20 \cdot 10^6$ cells/ml and incubated with 5 µM CFSE in RPMI-1640 for 10 minutes at 37 °C. Cells were washed with DC medium and $1 \cdot 10^5$ naïve T cells were seeded with $1 \cdot 10^5$ DCs in 200 µl DC medium, supplemented with 300 ng/ml OVA 323 – 339. Cultures were incubated for 48 h at 37 °C before staining for flow cytometry. Negative controls were not supplemented with OVA. For *in vitro* T cell polarization, T cells were prepared identical but no CFSE staining was performed.

Regulatory T cell Conversion Assay

To assay for the conversion of naïve T cells to regulatory T cells, in vitro regulatory T cell conversion assays were performed as described previously (Azukizawa et al., 2011). Briefly, naïve T cells from transgenic *OTII* mice were isolated using the $CD4^+CD62L^+$ T Cell isolation kit II following manufacturer's instructions. Using the CD11c isolation kit, $CD11c^+$ DCs were isolated from spleens of $Ldlr^{-/-}$ miR-17~92$^{\Delta/\Delta}$ and $Ldlr^{-/-}$ miR-17~92$^{fl/fl}$ mice that had been on high-fat diet for 5 weeks. 6 000 DCs and 25 000 T cells were co-incubated for 5 days with or without 100 ng/ml OVA 323 – 339 and with or without additional 500 mM L-tryptophan.

Phagocytosis Assay

300 000 DCs were seeded in 200 µl DC medium and incubated with $1 \cdot 10^6$ beads (FluoSpheres) for 45 minutes at 37 °C. Cells were washed once and stained for flow cytometry.

3.2.5 Flow Cytometry

Surface Staining

Single cell suspensions were washed in Hank's complete and resuspended in 25 µl Hank's complete and 25 µl FACS staining buffer. Antibodies were added in a 1:300 ratio and cells were incubated for 30 minutes at 4 °C and protected

from light. After staining, cells were washed twice with 200 µl Hank's complete per sample and measured immediately or fixed using cytofix cell fixation buffer (diluted in 50% PBS).

Surface Staining for Aortae

Single cell suspensions were prepared as described and Fc receptors were blocked with CD16/CD32 antibodies (Frankfurt am Main, Germany) in PBS supplemented with 2 % mouse serum, 2 % rabbit serum and 0.2 % BSA prior to fluorescent labeling. 25 µl Hank's complete with antibodies diluted 1:300 were applied for 30 minutes at 4 °C. After staining, cells were washed twice with 200 µl Hank's complete per sample and measured immediately.

Intracellular Staining for FOXP3

After surface staining, cells were stained for FOXP3 using the eBioscience fixation/permeabilization kit. Briefly, cells were pulse vortexed and fixed in 100 µl fixation buffer for 30 minutes at 4 °C. Subsequently, samples were washed in 200 µl permeabilization buffer twice. FOXP3 antibody was diluted 1:100 in 50 µl permeabilization buffer and samples were incubated at 4 °C for 30 minutes, followed by two washes with 200 µl permeabilization buffer. Supernatants were discarded and cells were resuspended in Hank's complete for measurement.

3.2.6 Reverse Transcription Quantitative Real-Time PCR (RT-qPCR)

Detection of mRNA

Whole RNA was isolated using RNeasy mini, micro (depending on sample size) or NucleoSpin RNA II kits followed by cDNA synthesis with oligo(dT) primers was performed with the first strand cDNA synthesis kit. All steps were performed following manufacturer's instructions. Quantitative PCR (qPCR) was performed in 10 µl scale. 20 ng cDNA per reaction and primers at a final concentration of 500 nM were used in conjunction with the maxima SYBR green/ROX qPCR master mix. CDNA serial dilutions were used to verify primer

efficiencies. The setup of the qPCR included initial activation of 15 minutes at 95 ˚C, followed by 40 cycles of 15 seconds denaturation at 95 ˚C, 30 seconds hybridisation at 60 ˚C and 30 seconds elongation at 72˚C. Additional steps of 15 seconds at 95 ˚C, 15 seconds at 60 ˚C and again 15 seconds at 95 ˚C were performed to allow for melting curve analysis in order to ensure amplicon integrity. Results were analyzed using the ddCt method (Livak and Schmittgen, 2001).

3.2.6 Cloning of *Socs3* 3'-UTR Reporter Constructs

Isolation of Template DNA

Template DNA was isolated from murine B6 tail clip biopsy material. Briefly, biopsy material was lysed in 190 µl tail lysis buffer with 10 µl 1 mg/ml proteinase K at 56 °C over night and subsequently centrifuged for 10 minutes at 20 000 g. Supernatant was recovered. 300 µl tail lysis buffer and 50 µl 3 M NaOAc were added. Tubes were shaken vigorously before addition of 450 µl isopropanol. Supernatant was discarded after a centrifugation for 30 minutes at 20 000 g and DNA pellet was washed with 500 µl 70 % EtOH before an additional centrifugation step of 20 minutes at 20 000 g. Pellet was dried thoroughly and dissolved in 75 µl 10 mM TRIS (pH 8.0). Genomic DNA (gDNA) was quantified using spectrometry.

Amplification *Socs3* of 3'-UTR regions

All primers for cloning of Socs3 3'-UTR were designed based on the murine *Socs3* sequence with the accession number NT_096135.6. The region predicted to contain binding sites for *miR-17~92* stretched from 3049 – 3241 (192 bp) and the control region from 2645 – 2841 (196 bp). Primers for the control construct (forward primer: 2645 – 2664, reverse primer: 2822 – 2841) and *miR-17~92* construct (forward primer: 3049 – 3068, reverse primer: 3221 – 3241) introduced recognition sites for restriction enzymes *XhoI* (forward primer) and *NotI* (reverse primer).

PCR mix for the control construct included 2 µl 10 mM dNTP mix, 10 µl 10X *Pfu* buffer with $MgCl_2$, 10 µl 70 ng/µl B6 gDNA, 1 µl 2,5 U/µl *Pfu* polymerase, 2 µl 10 µM Socs3_ctrl_for, 2 µl 10 µM Socs3_ctrl_rev and 73 µl nuclease free water.

Reaction profile started with 3 minutes at 95 °C for activation, followed by 40 cycles of 30 seconds at 95 °C for denaturation, 30 seconds at 52 °C for annealing and 2 minutes at 72 °C for elongation. Final elongation was performed for 10 minutes at 72 °C.

PCR mix for the *17~92* binding construct included 1 µl 10 mM dNT mix, 10 µl 5X phusion CG buffer, 2,5 µl 10 µM Socs3_1792_for, 2,5 µl 10 µM Socs3_1792_rev, 3 µl 100 ng/µl B6 gDNA, 0,5 µl 2 U/µl Phusion polymerase and 28 µl nuclease free water. The reactions were started with 30 seconds at 98 °C for activation, followed by 40 cycles of 10 seconds at 98 °C for denaturation, 30 seconds at 52 °C for annealing and 30 seconds at 72 °C for elongation. Incubation for final elongation was 10 minutes at 72 °C.

Isolation and Digestion of Amplified *Socs3* 3'-UTR Inserts

PCR products for control and *miR-17~92* binding constructs were subjected to gel separation. 2.5 % agarose gels in TAE buffer were used and products were sized in comparison to a double-stranded DNA ladder before bands were excised from gel. 20 µl 1 % EtBr per 100 ml gel were used for visualization. PCR products were isolated using the QIAquick gel extraction kit according to manufacturer's instructions.

Chemically Competent Cells

Chemically competent *Escherichia coli* XL10 were generated from a 100 ml culture of XL10 cells, incubated at 37 °C in LB medium to obtain an optical density (OD_{600}) between 0.4 – 0.6. Cells were harvested by centrifugation at 2700 g, 4 °C for 5 minutes and resuspended in 50 ml pre-cooled transformation buffer. After 30 minutes in ice, cells were harvested again and resuspended in 4 ml transformation buffer. After a second incubation of 30 minutes on ice, cells were aliquoted (200 µl) and frozen in liquid nitrogen. Cells were stored at -80 °C.

Transformation of Competent Cells

Per transformation, 50 µl chemically competent XL10 cells were incubated with up to 6 µl plasmid for 30 minutes on ice. For vector preparation, 0.5 µl 1 µg/µl

psiCHECK-2 were used, for transformation of ligation products up to 6 µl. Subsequently, cells were incubated at 42 °C for 1.5 minutes, followed by 2 minutes on ice. 800 µl SOC medium were added and cells were incubated for 45 minutes at 37 °C. 50 µl and 500 µl of cell suspensions were plated on sterile LB plates. LB plates were made from LB medium, supplemented with 15 % agar. 50 µg/ml ampicillin were used for selection and transformed cells were incubated at 37 °C over night.

psiCHECK-2 Vector Preparation

Competent cells were transformed with psiCHECK-2 dual luciferase reporter vector and single clones were picked 12 h after transformation. LB medium supplemented with 50 µg/ml ampicillin was inoculated and incubated at 37 °C over night before psiCHECK-2 vector was prepared using the NucleoBond PC 500 kit accoding to the manufacturer's manual. Average yield was 1 – 2 µg/µl.

Digestion of *Socs3* 3'-UTR Inserts and psiCHECK-2 Vector

Up to 1.5 µg psiCHECK-2 and 18.5 µl control and miR-17~92 binding inserts from gel extraction were incubated for 16 h at 37 °C with 2.5 µl buffer O, 2.5 µl *XhoI* and 1.5 µl *NotI* in 25 µl total volume. 5' phosphate groups of the vector were removed by incubation of 18 µl vector with 2 µl 10X fast alkaline phosphatase buffer and 1 µ 1 U/µl fast alkaline phosphatase at 37 °C for 20 minutes. Phosphatase was inactivated at 80 °C for 20 minutes. Inserts and vector were applied to a 2.5 % (inserts) or 1 % (vector) agarose gel and after excision purified with the QIAquick gel extraction kit according to manufacturer's instructions.

Ligation of *Socs3* 3'-UTR Inserts and psiCHECK-2 Vector

Inserts and vectors were adjusted to the vector:insert rations of 1:0, 1:3 and 1:6 in 18 µl volume and 2 µl 10X T4 DNA ligase buffer and 0.5 µl 5 U/µl T4 DNA ligase was added. The mix was incubated for 20 minutes at 22 °C and the reaction was stopped at 70 °C for 5 minutes.

Preparation of *miR-17~92* Binding and Control Constructs

Ligation products were transformed into competent cells (see *Transformation of Competent Cells*) and clones were used to inoculate 3 ml of LB medium for plasmid isolation with the GeneJET plasmid miniprep kit, following manufacturer's instructions. Integrity of the inserts was confirmed by sequencing at Eurofins MWG Operon (Ebersberg, Germany) using the psiCHECK-2_1429_for primer to sequence the insert region.

Luciferase Assays

HEK293 cells were seeded at 50 000 cells/ml in HEK medium on 24-well plates and incubated at 37 °C, 5 % CO_2 for 24 hours. For each transfection, 100 µl Opti-MEM were added 5 µl 30 µM Pre-miR miRNA precursor (or Pre-miR miRNA precursor mix at same concentration), 1 µg *Socs3*-3'-UTR reporter construct and 2 µl turbofect. Transfection cocktail was vortexed vigorously and incubated for 15 minutes at room temperature before it was added to cells. 24 h after transfection, cells were washed with PBS and luciferase assays were performed, according to manufacturer's manual (all components were part of Promega's dual-luciferase reporter assay system). Briefly, 100 µl/well passive lysis buffer were applied and cells were shaken for 15 minutes at room temperature on an orbital shaker. 100 µl luciferase assay reagent II were added 20 µl of cell lysate and samples were measured for firefly luciferase activity. 100 µl stop & glo reagent were added and renilla luciferase activity was measured. For analysis, background noise (non-transfected cells) was subtracted and renilla to firefly ratios were calculated for normalization.

3.2.7 Statistical Data Analysis

Flow cytometry data was analyzed in Treestar FlowJo 10.0.4 (Ashland, USA). RT-qPCR data was analyzed in Life Technologies' Sequence Detection Systems (SDS) 2.4.1 (Darmstadt, Germany). Analysis of immunohistochemical data and plaque quantification was performed in Diskus 4.80 (Koeningswinter, Germany).

Statistical analyses were performed in GraphPad Prism 5.02 (La Jolla, USA). Normality was investigated with the Kolmogorov-Smirnov test and t-test or Mann-Whitney test were applied when appropriate. Data was normalized if appropriate and for multiple comparisons one-way ANOVA or Kruskal-Wallis tests followed by Tukey-Kramer or Dunn's post-hoc tests were performed. Differences with $p<0.05$ were considered to be statistically significant.

Prediction of miRNA targets was performed with mirSVR data available from microRNA.org using the mirSVR algorithm on miRanda-predicted microRNA target sites (Betel et al., 2010).

4 Results

4.1 Aortic Dendritic Cell Subsets in Healthy and Atherosclerotic Mice

Multicolor flow cytometry was applied to enzymatically digested aortae of healthy and atherosclerotic mice. In order to identify DCs and their subsets, respectively, a recently described gating strategy for aortic DCs (Choi et al., 2011) was adapted and optimized (Figure 1). $CD19^+$ B and $TCR\beta^+$ T cells were excluded from analysis and $CD11c^+MHCII^+$ DCs identified amongst $CD45^+$ leukocytes. These DCs were subdivided on basis of E-cadherin-ligand CD103 expression into a small $CD103^+$ and a larger $CD103^-$ DC population.

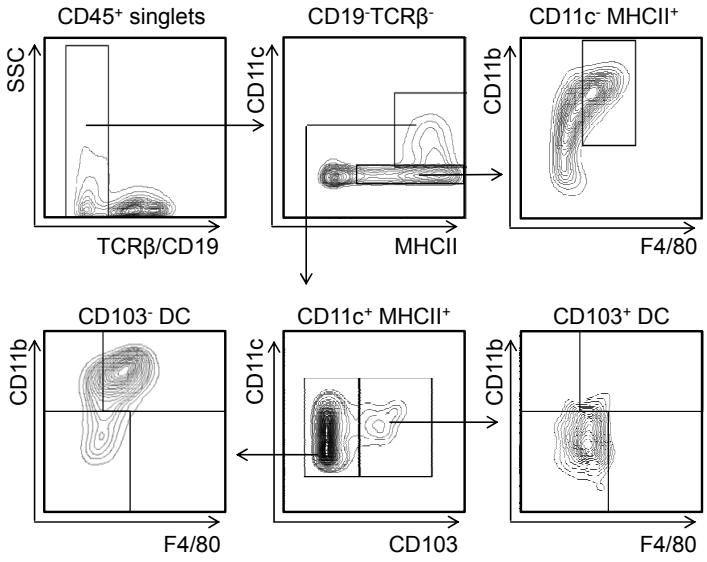

Figure 1 Representative plots for illustration of the gating strategy to identify aortic DC subsets. T and B cells were excluded from analysis on basis of CD19 and TCRβ expression. $CD11c^+MHCII^+$ DCs were subdivided in $CD103^+$ and $CD103^-$ DCs.

The $CD103^+$ DC population did not express CD11b or F4/80, while the $CD103^-$ DC fraction allowed for distinction of three different populations: A large group of $CD11b^+F4/80^+$ DCs and two less abundant subsets of $CD11b^+F4/80^-$ and $CD11b^-F4/80^-$ DCs (Figure 1). Within the subset of $CD11b^-F4/80^-$ cells were sporadic $CD11c^{lo}CD11b^-PDCA^+$ cells (data not shown), indicating the presence

of few pDCs in line with previous reports (Doring et al., 2012; Doring and Zernecke, 2012). However, due to low numbers (125±42 pDCs per aorta, contributing to approximately 1.6 % of $CD11c^+MHCII^+$ DCs) this DC subset was not included into subsequent analyses. All DC subsets were negative for expression of the NK/NKT cell marker NK1.1 (data not shown). In line with previous studies (Choi et al., 2011), $CD11b^+F4/80^+$ macrophages were segregated within the $CD11c^-$ leukocytes (Figure 1).

In order to describe the kinetics of the accumulation of these cell subsets during the development of atherosclerosis, C57BL/6 (B6) mice were compared to low density lipoprotein receptor-deficient *(Ldlr$^{-/-}$)* mice fed normal chow and after 6 and 12 weeks of high-fat diet feeding (Figure 2). In line with previous reports (Galkina et al., 2006; Jongstra-Bilen et al., 2006), DCs and macrophages could be identified in the aortae of healthy B6 mice. Compared to these mice, the numbers of macrophages and DCs in non-atherosclerotic Ldlr mice were slightly increased.

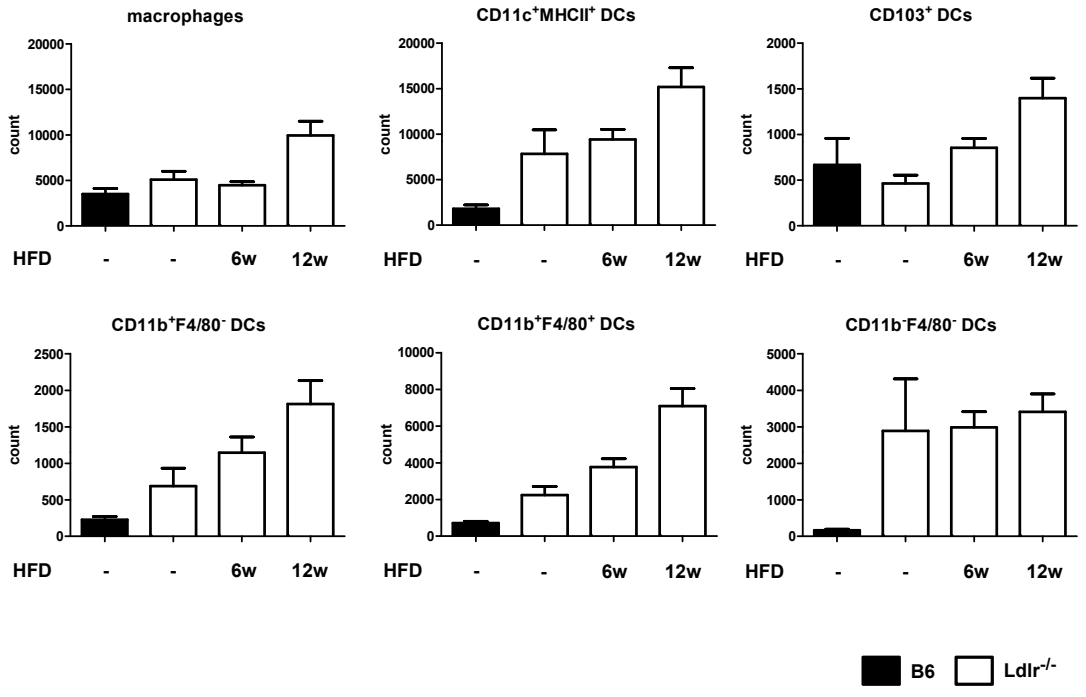

Figure 2 Aortic DC and macrophage numbers of B6 (black bars) and *Ldlr$^{-/-}$* (white bars) mice on normal diet or after 6 or 12 week of high fat diet (HFD). DCs were segregated as described (Figure 1). Bars represent mean ± SEM (n=6-9)

With the duration of diet, DC and macrophage numbers increased in *Ldlr*$^{-/-}$ mice. Mainly CD103^{+} DCs and CD11b^{+}F4/80^{+} DCs contributed to this increase, while CD11b^{+}F4/80^{+} DCs were less elevated. Interestingly, CD11b-F4/80- DC numbers were not altered when Ldlr mice were fed a high-fat diet.

The frequencies of distinct DC subsets within the total DC compartment was analyzed as well (Figure 3) and a slight but non-significant expansion of CD103^{+} DCs was observed, whereas the fraction of CD11b^{+}F4/80^{-} DCs decreased in *Ldlr*$^{-/-}$ mice on high-fat died compared to B6 mice. The fractions of other DC subsets did not display alterations during pro-atherogenic feeding.

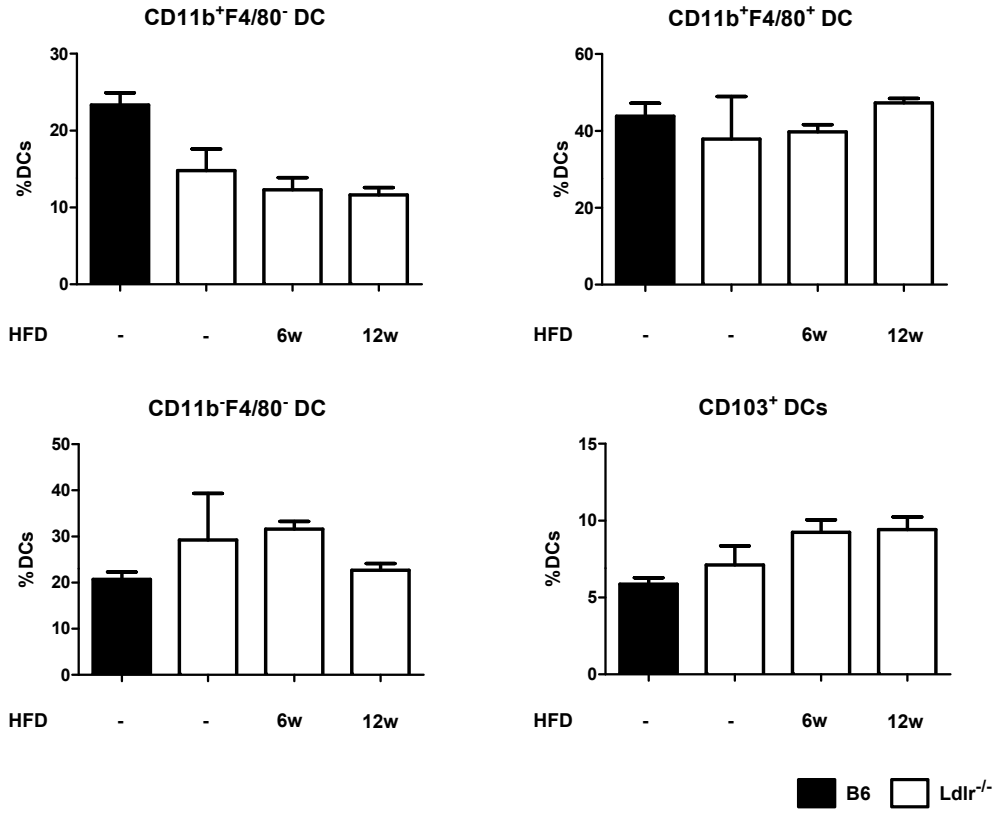

Figure 3 Frequencies of DC subsets within the total DC compartment of healthy and atherosclerotic aortae in B6 mice (black bars) and *Ldlr*$^{-/-}$ mice (white bars) on normal chow and high-fat diet for 6 and 12 weeks. Bars represent mean ± SEM (n=6-9)

Various markers have been used to distinguish DC subsets. One of these markers is the signal-regulatory protein (SIRP)-α that is involved in cell migration and phagocytosis. Recently it has been reported to be expressed on

CD11b$^+$ DCs, monocytes and macrophages (Matozaki et al., 2009a) but its expression on aortic DCs has not been characterized, yet. To address this, the SIRPα expression was investigated for all DC subsets in healthy and atherosclerotic *Ldlr*$^{-/-}$ mice, as well as for macrophages (Figure 4).

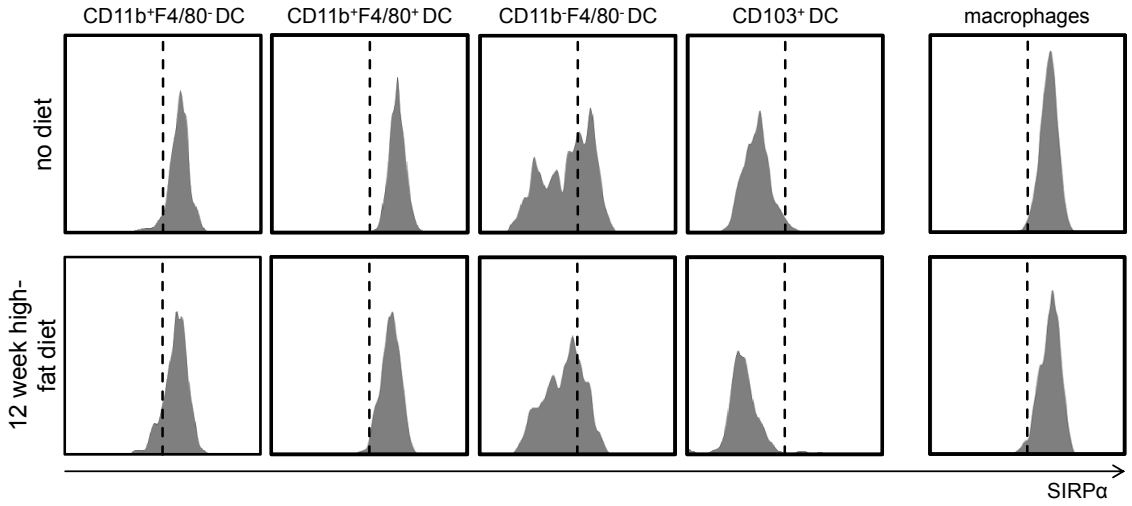

Figure 4 Representative histograms of the SIRPα surface expression on aortic DCs with respect to the distinct subsets described. *Ldlr*$^{-/-}$ mice were fed normal chow (upper panel) or a high-fat diet for 12 weeks (lower panel).

In line with the literature (Matozaki et al., 2009a), macrophages and the CD11b$^+$ DC populations of CD11b$^+$F4/80$^-$ and CD11b$^+$F4/80$^+$ DCs were clearly positive for SIRPα expression. CD11b$^-$F4/80$^-$ DCs did express at intermediate levels, while CD103$^+$ DCs were negative for SIRPα. There was no difference in SIRPα expression between healthy and atherosclerotic *Ldlr*$^{-/-}$ mice.

Although some studies (Choi et al., 2011) tried to shed light on the discrimination of DCs from monocytes/macrophages, this questions remains controversial. To address this, Choi et al. distinguished these cells by functional criteria (Choi et al., 2011). Macrophages for example were demonstrated to display stong phagocytic but poor immune-stimulatory capacity, while this was the other way around for DCs. In addition to this, macrophage development relied on the hematopoietin M-CSF, while DC development was in part M-CSF (CD11b$^+$F4/80$^+$ DCs) and FLT3 (CD103$^+$ DCs) dependent.

To extend this, the DC subset distribution in the aorta was analyzed in *Flt3l*-deficient (*Flt3l*$^{-/-}$) mice (Figure 5). As expected, macrophages were not affected

(Figure 5A) and compared to B6 mice, absolute macrophage numbers were not altered (Figure 5 B, 2929.0±763.1 *vs*. 3517.605.3 macrophages, *Flt3l*$^{-/-}$ *vs*. B6, n.s.).

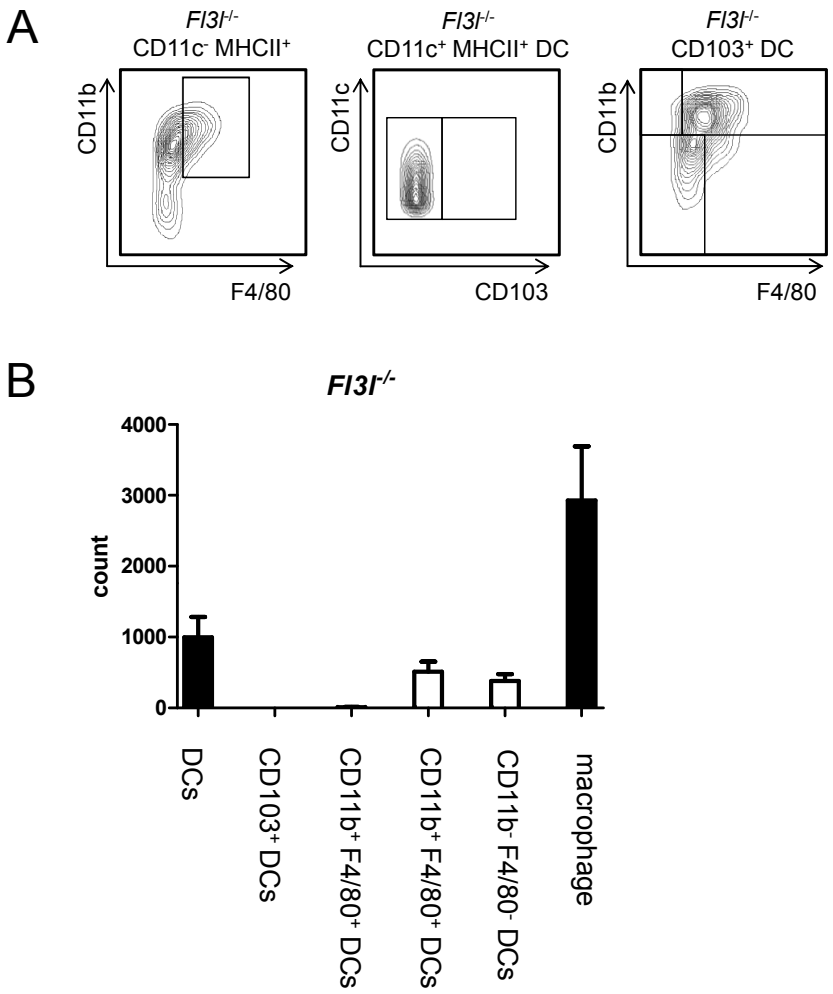

Figure 5 Analysis of the DC compartment in *Flt3l*$^{-/-}$ mice under physiological conditions. Representative FACS plots (A) and absolute numbers (B) of macrophages (mac) and the DC subsets present in the aorta. Bars represent mean ± SEM (n=6)

Similar to Choi et al. (Choi et al., 2011), CD103^{+} DCs were completely absent in *Flt3l*-deficicent mice (Figure 5A) and these mice showed a trend towards reduced total CD11c^{+}MHCII^{+} DC counts (Figure 5 B and not shown, 999.0±287 *vs*. 1827±137 DCs, Flt3l *vs*. B6, n.s.). Analysis of the individual subsets revealed no alterations in CD11b^{+}F4/80^{+} DCs (Figure 5 B, 512.2±143.2 *vs*. 797.2±63.1 DCs, *Flt3l*$^{-/-}$ *vs*. B6, n.s.) and CD11b^{-}F4/80^{-} DCs (Figure 5 B, 382.3±95.9 *vs*. 377.3±36.8 DCs, *Flt3l*$^{-/-}$ *vs*. B6, n.s.). However, the

CD11b^{+}F4/80^{-} DC subset was almost completely absent (Figure 5). These findings clearly confirm the FLT3/FLT3L dependency of CD103^{+} DCs, while they also show that CD11b^{+}F4/80^{+} and CD11b^{-}F4/80^{-} DCs accumulate independent of FLT3L.

Recently, the FCγ receptor 1 CD64 has been described to distinguish macrophages from DCs (Gautier et al., 2012). Furthermore, it was also attributed to be expressed on monocyte derived DCs while cDCs do not express CD64 (Langlet et al., 2012). Therefore, this marker was applied to the newly defined subsets (Figure 6).

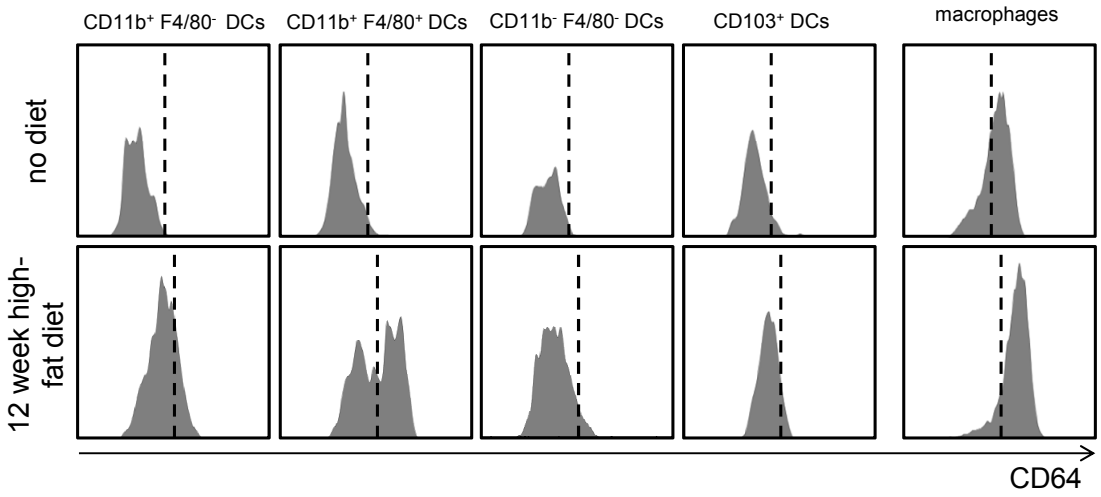

Figure 6 Representative histograms of the CD64 surface expression on aortic DCs with respect to the described subsets. *Ldlr*$^{-/-}$ mice were fed normal chow (upper panel) or a high-fat diet for 12 weeks (lower panel).

As expected, macrophages stained positive for CD64 and none of the DC subsets expressed CD64 in non-inflammatory conditions, indicating that cDCs rather than monocyte-derived DCs resemble the aortic DC compartment under physiological conditions. This is in line with their dependence on FLT3L. However, when atherosclerotic *Ldlr*$^{-/-}$ mice were analyzed, a small fraction of CD11b^{+}F4/80^{-} DCs and about half of the CD11b^{+}F4/80^{+} DCs expressed CD64, while CD11b^{-}F4/80^{-} DCs and CD103^{+} DCs did not. In total, about 21 % of all DCs stained positive for CD64 while all macrophages were positive for the expression of this marker. These data support that CD11b^{+} DCs in the aorta are in part monocyte-derived in atherosclerosis.

4.2 The Role of the miR-17~92 Cluster in Dendritic Cells

To investigate the role of miR-17~92 in DCs commercially available mir17-92$^{tm1.1Tyj}$/J (*miR-17~92*) carrying a *miR-17~92* allele flanked by loxP sites were crossed with *Cd11c*-specific B6.Cg-Tg(Itgax-cre)$^{1-1Reiz}$/J (*CD11c-cre*) deleter mice. Cre recombinase expression under the control of the *Cd11c* promoter causes specific deletion of the *miR-17~92* cluster in CD11c^{+} cells (DCs). These mice will be termed *miR-17~92$^{\Delta/\Delta}$* in the following and were used for experiments in non-inflammatory steady state conditions at an age of 8 – 10 weeks. Control mice did not express cre recombinase and will be termed *miR-17~92$^{fl/fl}$*.

The *miR-17~92$^{\Delta/\Delta}$* and *miR-17~92$^{fl/fl}$* mice were also crossed with B6.129S7-Ldlr^{tm1Her}/J (*Ldlr$^{-/-}$*) mice yielding *Ldlr*-deficient *Ldlr$^{-/-}$ miR-17~92$^{\Delta/\Delta}$* or *Ldlr$^{-/-}$ miR-17~92$^{fl/fl}$* mice, respectively. These mice were used for experiments with diet-induced atherosclerosis as described in materials and methods. Due to limitations within the animal facility *Ldlr$^{-/-}$ miR-17~92$^{\Delta/\Delta}$* or *Ldlr$^{-/-}$ miR-17~92$^{fl/fl}$* were also used for non-diet experiments. If this was the case the mice were fed a normal chow diet and sacrificed at 8 – 10 weeks of age.

4.2.1 Non-Inflammatory Conditions

4.2.1.1 General Characterization

MiR-17~92$^{\Delta/\Delta}$ mice were born in normal Mendelian ratio and did not show any gross abnormalities. They were fertile, bred well, average litter size was comparable to C57BL/6J (B6) mice maintained in the same facility and body weight was not altered compared to *miR-17~92$^{fl/fl}$* controls (Figure 7).

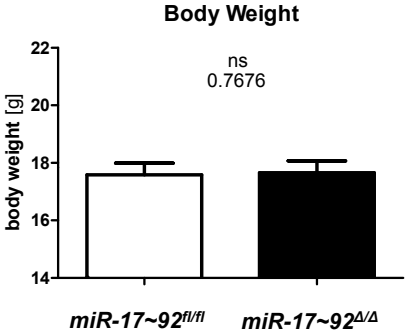

Figure 7 Body weight of *miR-17~92*$^{\Delta/\Delta}$ and *miR-17~92*$^{fl/fl}$ mice. Bars represent mean ± SEM (n=11).

4.2.1.2 Immunological Characterization

To investigate which effect the *Cd11c*-specific deletion exerts on DCs, the immune system of the mice was characterized with respect to DCs and T cells. Since DCs can closely interact with T cells, alterations in the T cell phenotype could give valuable insights in DC functions that are regulated by *miR-17~92*. The following section from Figure 8 to Figure 24 illustrates the findings from *miR-17~92*$^{\Delta/\Delta}$ mice in non-atherogenic conditions, while the next section from Figure 25 to Figure 41 shows data from *Ldlr*$^{-/-}$ *miR-17~92*$^{\Delta/\Delta}$ mice under pro-atherogenic conditions (5 weeks of high-fat diet).

Analysis of peripheral lymph nodes and spleen showed that lymphoid organs in *miR-17~92*$^{\Delta/\Delta}$ mice were not altered in size. While the peripheral lymph nodes displayed a modest but non-significant reduction in cell numbers the spleen did not show any changes in either cell count or organ mass (Figure 8).

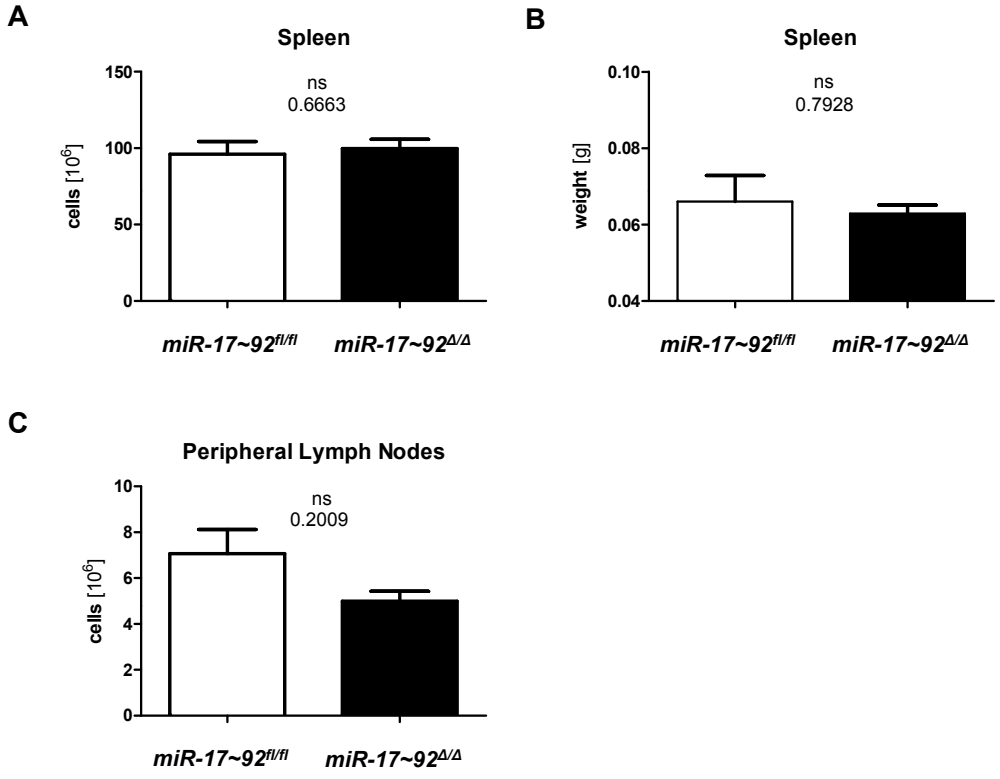

Figure 8 Size of lymphoid organs in *miR-17~92*$^{\Delta/\Delta}$ and *miR-17~92*$^{fl/fl}$ mice. Bars indicate spleen size based on cell counts (A) or organ mass (B) or peripheral lymph node cell counts (C) and represent mean ± SEM (n=11-17).

To investigate the impact of *miR-17~92*-deficiency with respect to DCs, the peripheral lymph nodes, the spleen and the bone marrow were analyzed for cDC and preDC frequencies and phenotype. Conventional DCs were further subdivided into $CD4^+$, $CD8^+$ and $CD4^-CD8^-$ DC subsets to evaluate alterations in DC subset differentiation. PreDCs were identified by surface expression of CD45, CD115, FLT3 and CD11c while they were negative for MHCII (Weigert et al., 2012). Differentiated cDCs were $CD45^+CD11c^+MHCII^+$. Within the bone marrow there was no difference in preDC frequencies, indicating that preDC-dependent development of DCs was not altered (Figure 9).

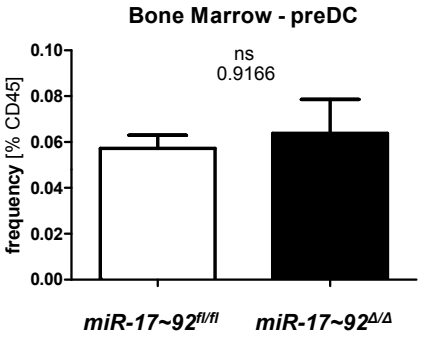

Figure 9 Frequencies of preDCs in the bone marrow compartment. Single cell suspensions from bone marrow of *miR-17~92*$^{\Delta/\Delta}$ or control mice were analyzed for CD11c^{+}CD115^{+}Flt3^{+}MHCII^{-} preDC frequencies using flow cytometry. Bars represent mean ± SEM (n=5).

CDCs within peripheral lymph nodes were not altered (Figure 10). Based on the expression levels of MHCII, cDCs were also subdivided into resDCs (MHCII^{int}) or migDC (MHCII^{hi}). There was no difference for migDCs or resDCs between miR-17~92 CKO and control mice (Figure 10).

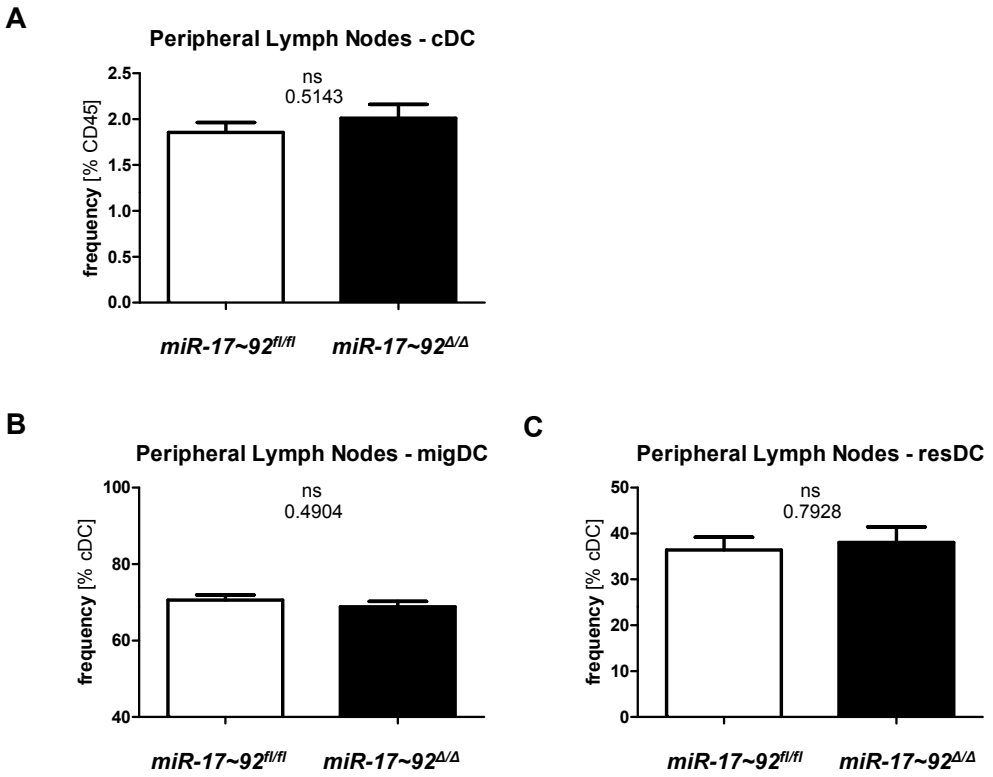

Figure 10 FACS analysis of the DC compartment within peripheral lymph nodes. FACS analysis on single cell suspensions allowed detection of CD11c^{+}MHCII^{+} cDCs (A). Migratory DCs (C) were MHCII^{hi} while resDC (D) were MHCII^{int}. Bars represent mean ± SEM (n=11-16).

To assess whether cDC subsets were altered in *miR-17~92*-deficient mice, the cDCs were subdivided with respect to CD4 and CD8. In line with the previous results, there was no significant difference in DC frequencies when using CD4 and CD8 to subdivide DC subsets (Figure 11).

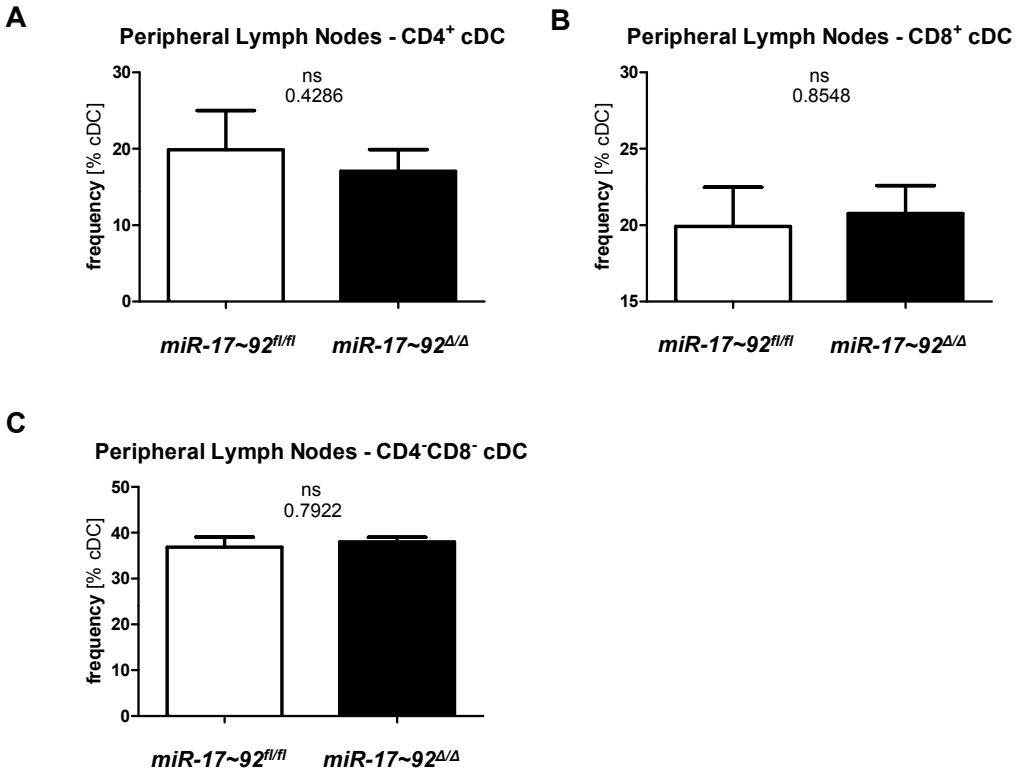

Figure 11 Distribution of DC subsets within peripheral lymph nodes based on the expression of CD4 and CD8 as measured by flow cytometry. Bars indicate distribution of $CD4^+$ (A), $CD8^+$ (B) or $CD4^-CD8^-$ (C) cDCs in peripheral lymph nodes of *miR-17~92*$^{\Delta/\Delta}$ mice and represent mean ± SEM (n=5).

These results indicate that the DC compartment of peripheral lymph nodes was not altered with respect to DC frequencies, phenotype or subset distribution. Analysis of splenic DCs resembles the findings in peripheral lymph nodes. The frequency of cDCs is not changed by *Cd11c*-specific deletion of *miR-17~92*.

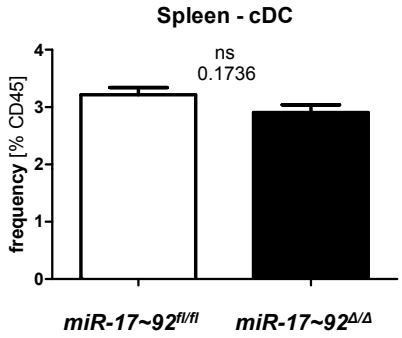

Figure 12 Splenic cDC frequencies measured by FACS. Single cell suspensions of spleen tissue from *miR-17~92*$^{\Delta/\Delta}$ mice and *miR-17~92*$^{fl/fl}$ control animals were subjected to flow cytometry. Bars represent mean ± SEM (n=17-18).

Although it is not possible to divide splenic DC subsets into resDC or migDC, the expression of CD4 and CD8 is widely used do distinguish between different subsets. Based hereupon, no significant difference between *miR-17~92*$^{\Delta/\Delta}$ or *miR-17~92*$^{fl/fl}$ control mice was observed (Figure 13).

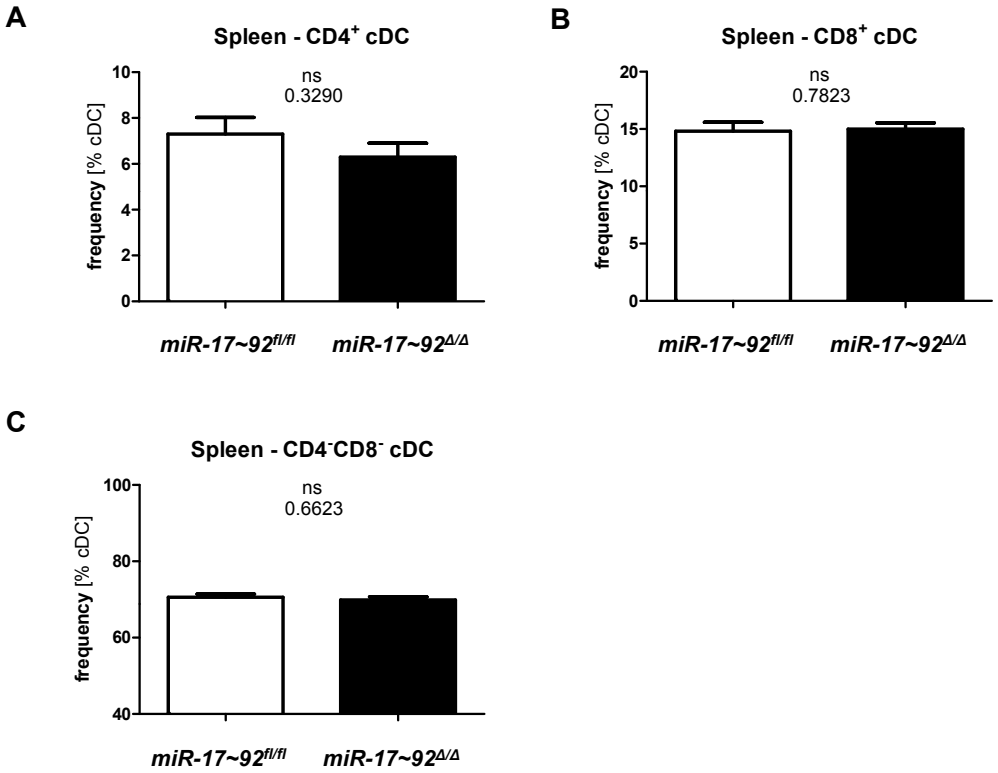

Figure 13 Flow cytometry for DC subsets within spleen based on the expression of CD4 and CD8. Bars indicate CD4$^+$ (A), CD8$^+$ (B) or CD4$^-$CD8$^-$ cDCs in *miR-17~92*$^{\Delta/\Delta}$ and *miR-17~92*$^{fl/fl}$ control mice. They represent mean ± SEM (n=5).

DCs of the aortic root and vessel wall were also investigated in non-inflammatory conditions. As described before, enzymatically digested aortic root and vessels were stained for FACS analysis. Upon exclusion of T and B cells, remaining leukocytes contained $CD11c^{+}MHCII^{+}$ DCs. There was no difference in DC numbers between *miR-17~92*$^{\Delta/\Delta}$ and control mice (Figure 14).

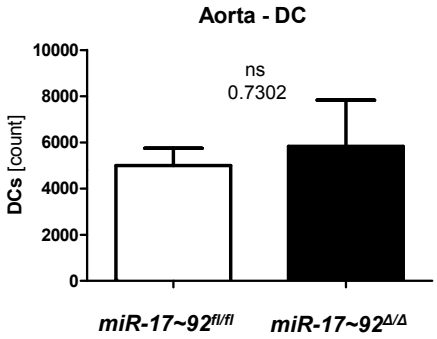

Figure 14 Absolute counts for DCs of single cell suspensions from non-atherosclerotic aortic roots and aortae as measured by flow cytometry in *miR-17~92*$^{\Delta/\Delta}$ and *miR-17~92*$^{fl/fl}$ control mice. Enzymatically digested cell suspensions were analyzed according to the new gating strategy presented in Figure 1. Bars represent mean ± SEM (n=5).

The aortic DC subsets were also analyzed using the new gating strategy. Utilizing CD11b, CD103 and F4/80 there was no difference in subset distribution between *miR-17~92*$^{\Delta/\Delta}$ and *miR-17~92*$^{fl/fl}$ control mice (Figure 15).

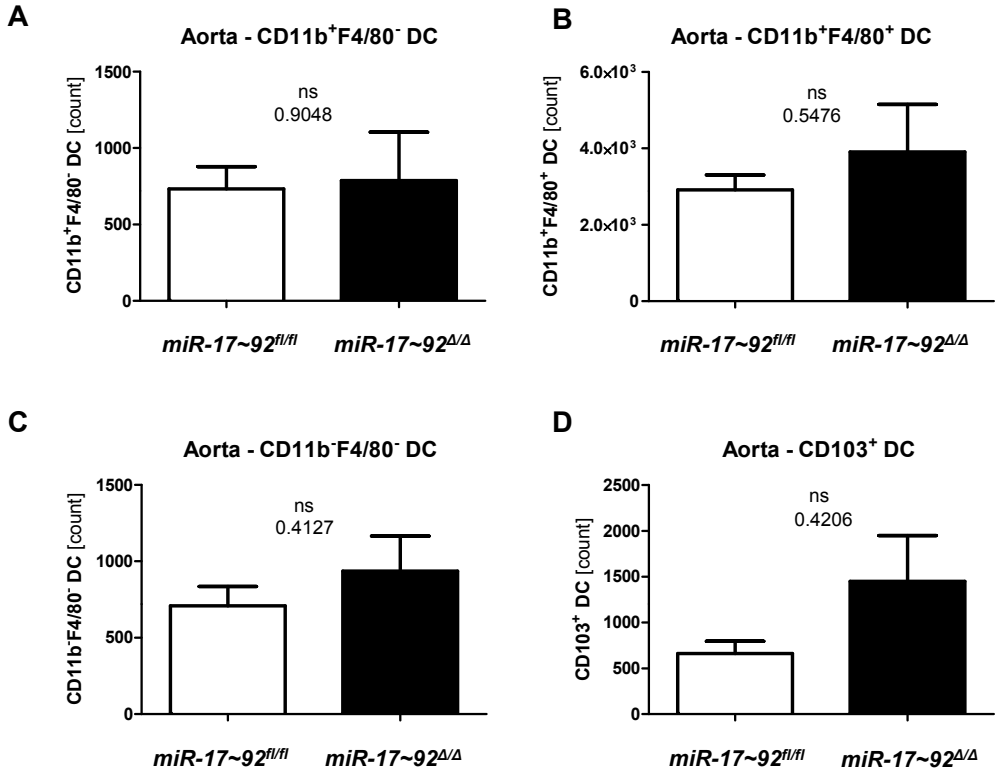

Figure 15 FACS analysis for aortic DC subsets in *miR-17~92*$^{\Delta/\Delta}$ and control mice. DC numbers for CD11b^{+}F4/80^{-} (A), CD11b^{+}F4/80^{+} (B), CD11b^{-}F4/80^{-} (C) and CD103^{+} (D) DCs within the aortic compartment of non-atherosclerotic miR-*miR-17~92*$^{\Delta/\Delta}$ mice compared to *miR-17~92*$^{fl/fl}$ control mice. Bars represent mean ± SEM (n=5).

To extend the characterization of the DC compartment, the surface expression levels of co-stimulatory molecules CD40 and CD86 were analyzed in peripheral lymph nodes (Figure 16 and Figure 17) and spleen (Figure 18). These co-stimulatory molecules can be used as markers for the activation state of DCs. As expected, expression levels on migDCs in peripheral lymph nodes were higher than expression levels on resDC. However, in line with the previous findings concerning the DC phenotype in *miR-17~92*$^{\Delta/\Delta}$ mice, there was no difference between *miR-17~92*-deficient or competent DCs with regard to the expression levels of co-stimulatory molecules CD40 and CD86.

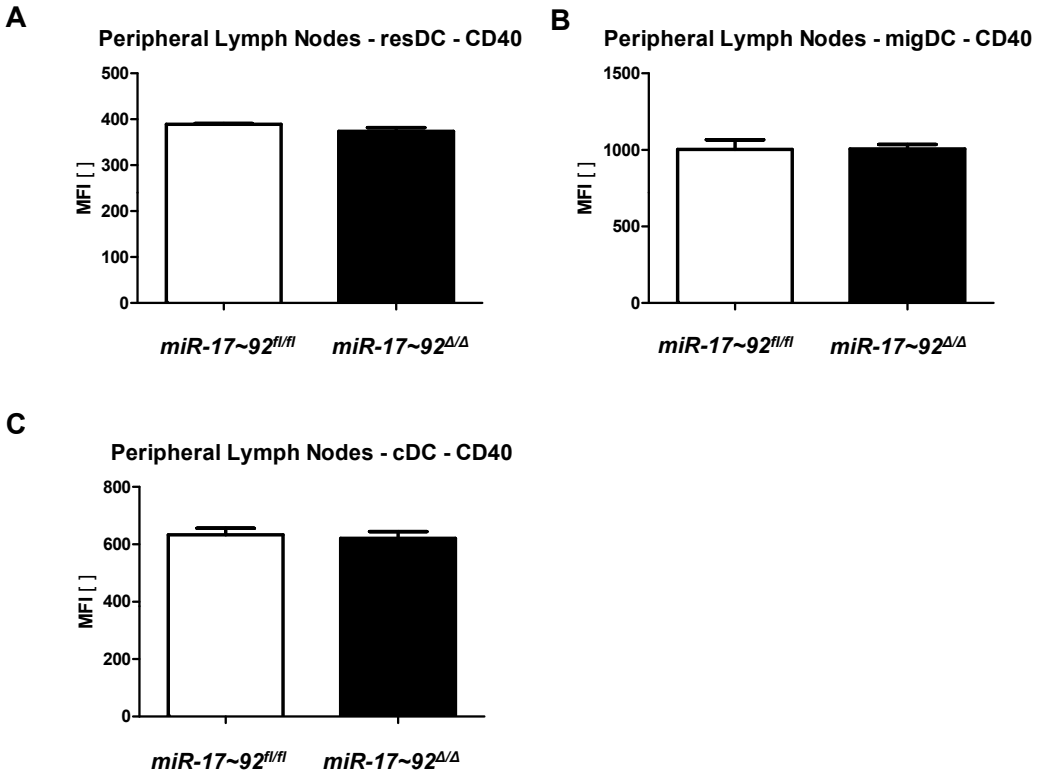

Figure 16 Surface expression of co-stimulatory molecule CD40 on resDC (A), migDC (B) or cDC (C) in peripheral lymph nodes of *miR-17~92*$^{\Delta/\Delta}$ or *miR-17~92*$^{fl/fl}$ control mice measured by flow cytometry. Bars represent mean ± SEM (n=2).

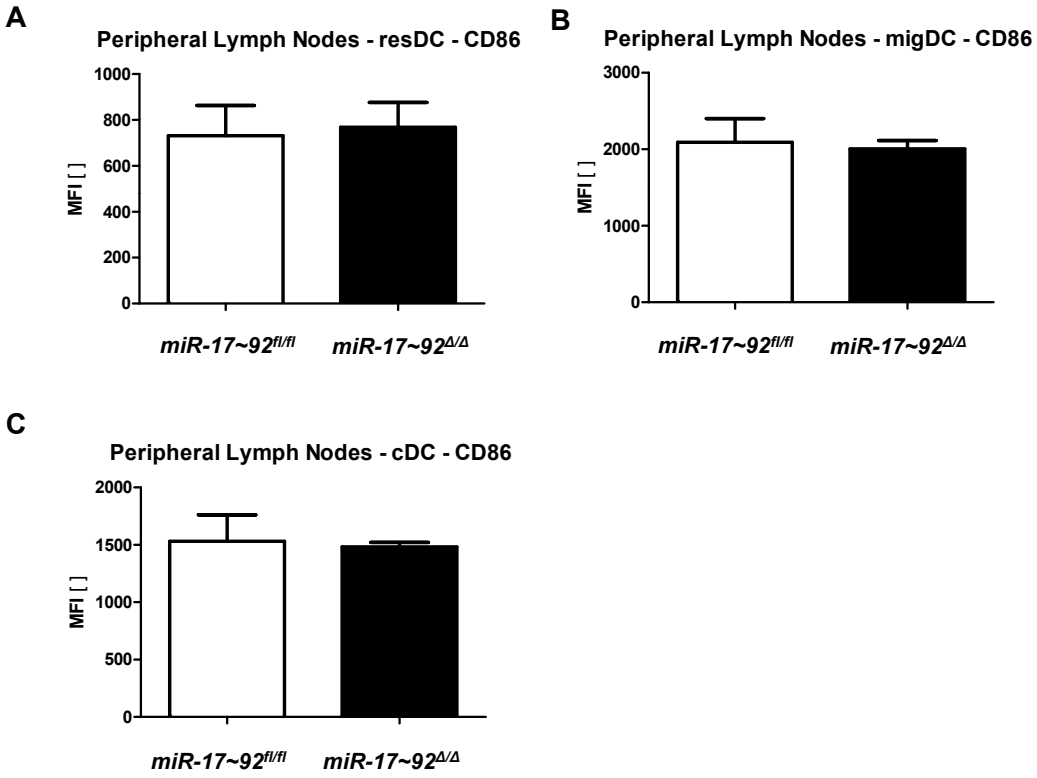

Figure 17 Surface expression of CD86 on resDC (A), migDC (B) or cDC (C) in peripheral lymph nodes of *miR-17~92*$^{\Delta/\Delta}$ or *miR-17~92*$^{fl/fl}$ control mice measured by flow cytometry. Bars represent mean ± SEM (n=2).

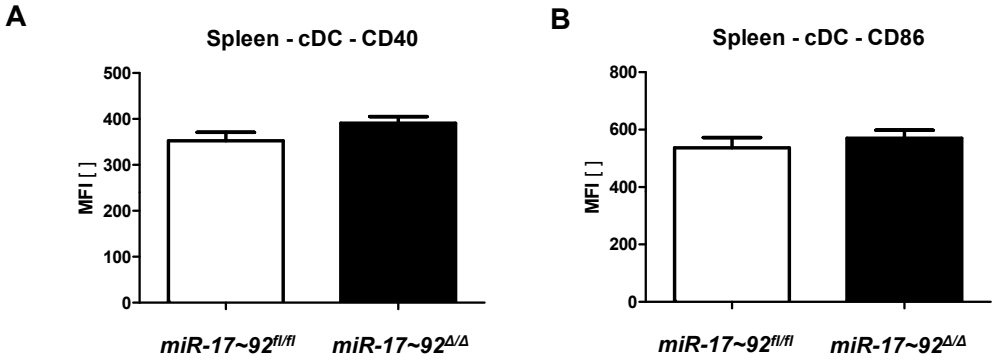

Figure 18 Surface expression of CD40 (A) and CD86 (B) on splenic cDCs of *miR-17~92*$^{\Delta/\Delta}$ or *miR-17~92*$^{fl/fl}$ control mice measured by flow cytometry. Bars represent mean ± SEM (n=2).

The ability of DCs to interact with T cells is a hallmark for DC function. Therefore, the T cell compartment in spleen, lymph nodes and blood of *miR-17~92*$^{\Delta/\Delta}$ mice was analyzed. T cell frequencies in peripheral lymph nodes were unchanged and no difference within the CD4 or CD8 T cell compartment was observed (Figure 19).

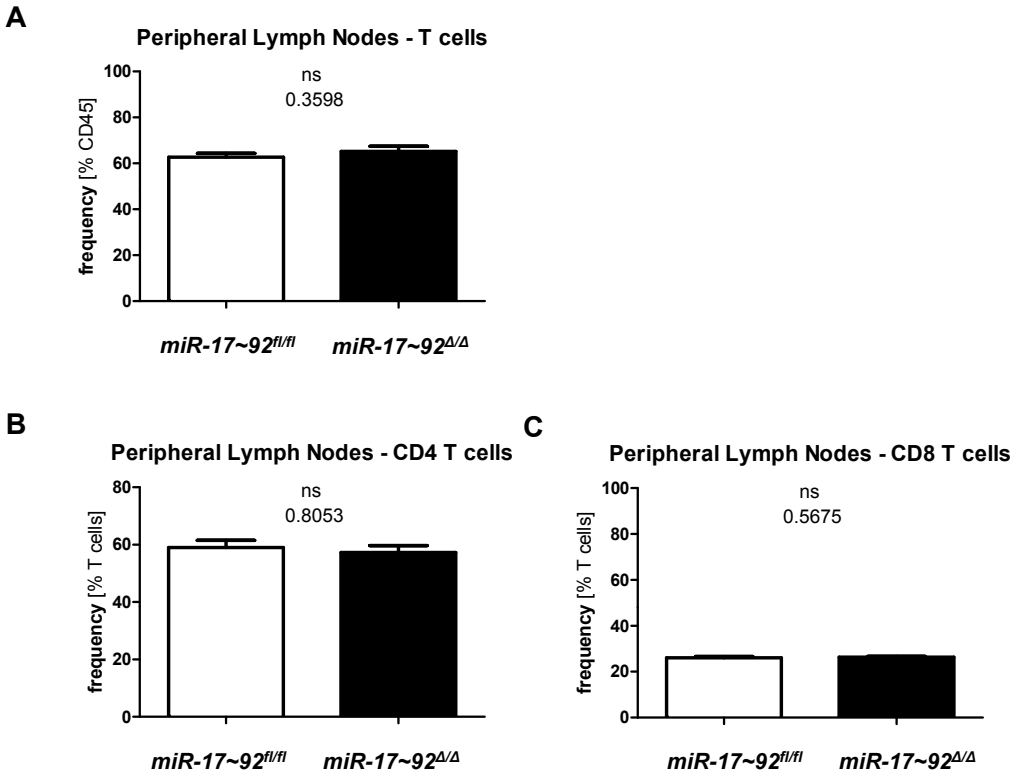

Figure 19 FACS analysis of the T cell compartment within peripheral lymph nodes of *miR-17~92*$^{\Delta/\Delta}$ and control mice. Total T cell frequencies (A), as well as fractions of CD4 (B) and CD8 (C) T cells are depicted. Bars represent mean ± SEM (n=10-11).

T cell activation and polarization characterize the influence of DCs on T cells. Therefore the T cell status was analyzed based on the expression of CD62L and CD44 (Figure 20). Interestingly, the memory CD4 T cell frequency was decreased in *miR-17~92*$^{\Delta/\Delta}$ mice and naïve CD4 T cell frequency was increased. However, the induction of regulatory CD4 T cells remained unaltered in non-atherogenic conditions. To identify regulatory T cells, intracellular stainings for transcription factor FOXP3 were performed and FOXP3^{+}CD25^{+}CD4^{+} T cells were identified as regulatory T cells.

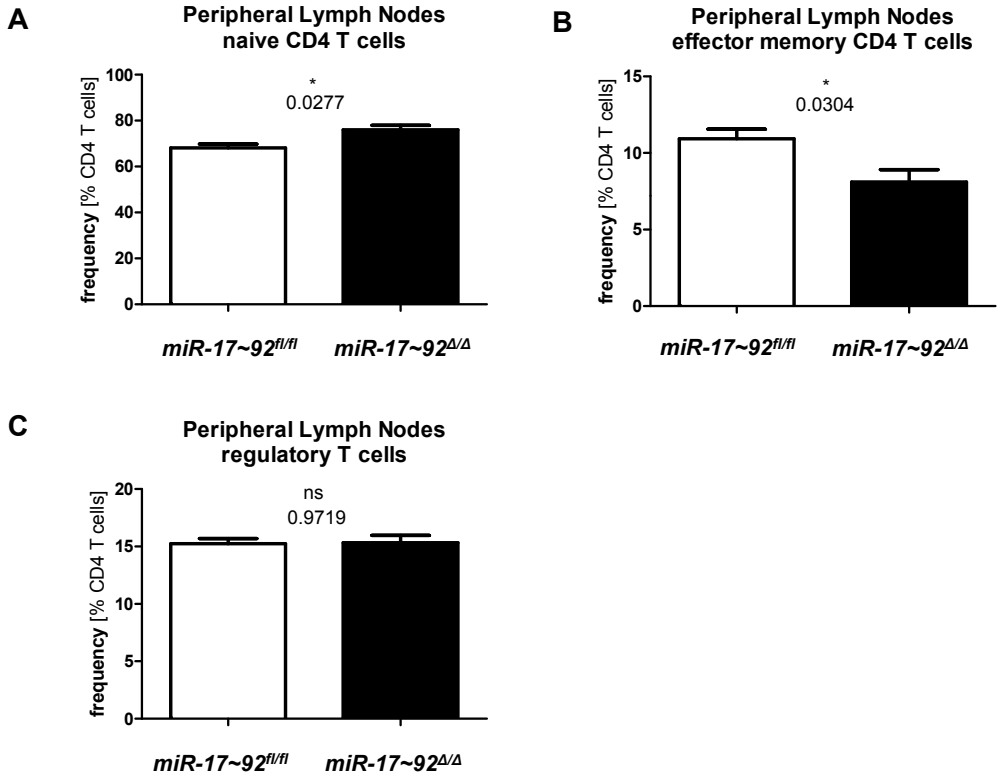

Figure 20 FACS analysis of T cell status in peripheral lymph nodes of *miR-17~92*$^{\Delta/\Delta}$ or *miR-17~92*$^{fl/fl}$ control mice. Naïve CD4 T cells (A) were CD62L^{+} and effector memory CD4 T cells (B) stained positive for CD44 while regulatory T cells (C) were identified with intracellular staining for FOXP3. Bars represent mean ± SEM (n=10-11; *p≤0.05).

The splenic T cell compartment was analyzed accordingly and similar results were obtained. Overall T cell, CD4 T cell and CD8 T cell frequencies were not altered in non-inflammatory conditions (Figure 21).

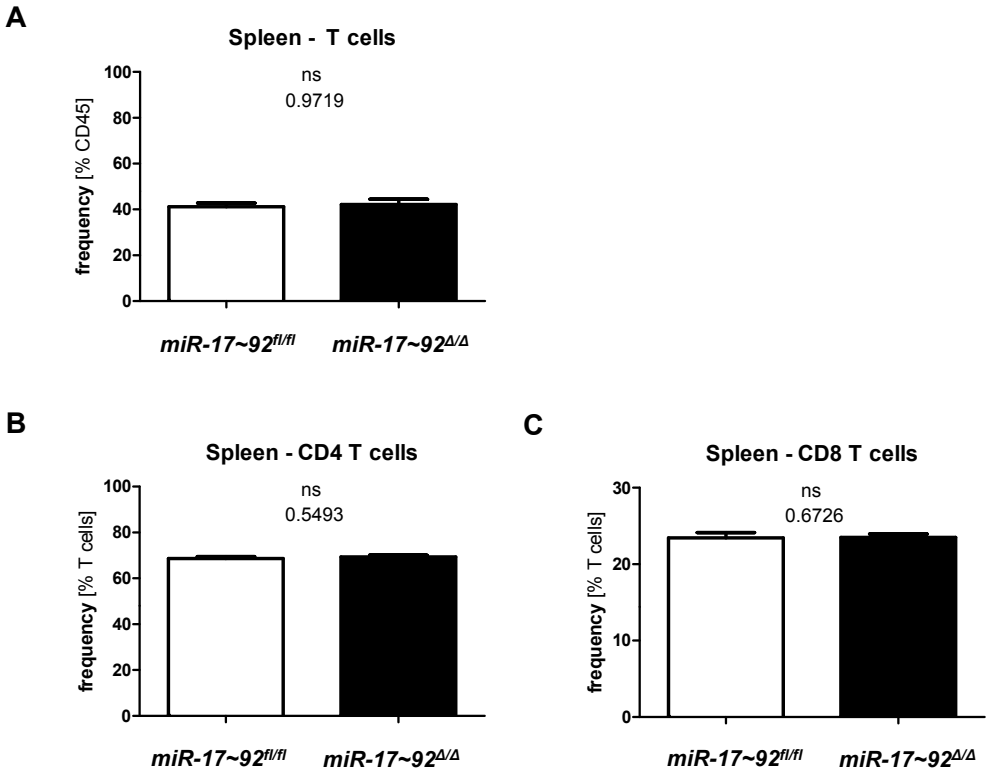

Figure 21 Splenic T cell compartment in *miR-17~92*$^{\Delta/\Delta}$ and control mice. Total T cell frequencies (A) and the fraction of CD4 (B) and CD8 (C) T cells are shown. Bars represent mean ± SEM (n=10-11).

Similar to peripheral lymph nodes the spleen also displayed an increase in naïve T cells, accompanied by a decrease in memory T cells in *miR-17~92*$^{\Delta/\Delta}$ mice (Figure 22). However, these findings were not significant. As for the peripheral lymph nodes, the fraction of regulatory T cells was not changed under steady-state conditions.

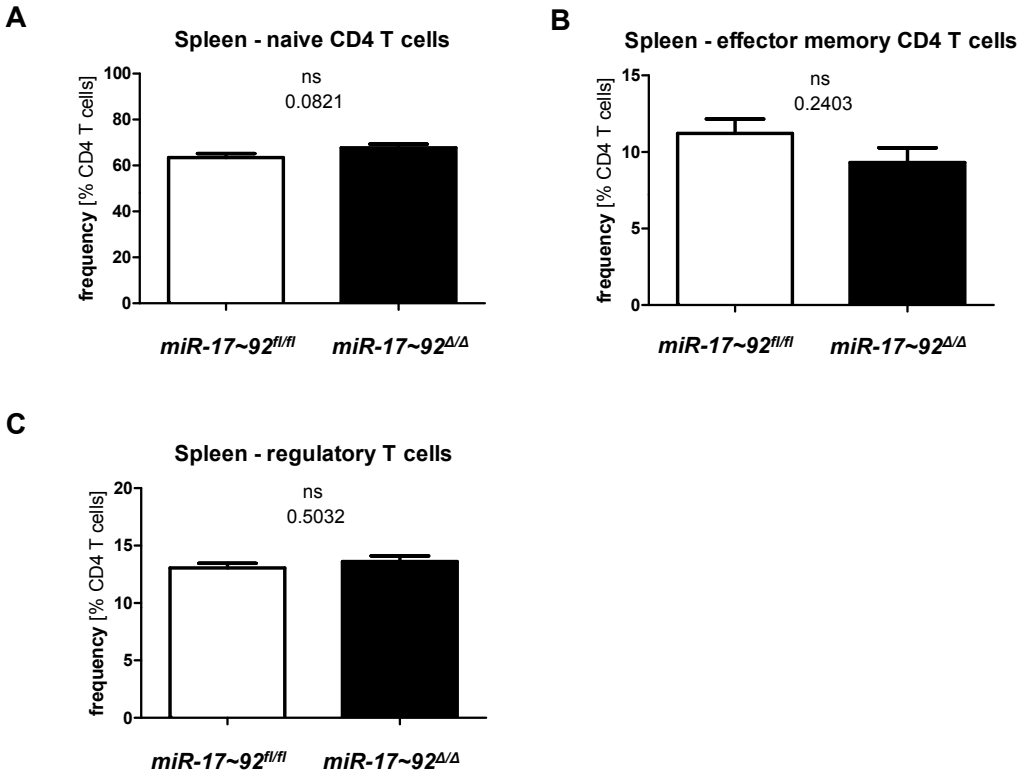

Figure 22 FACS analysis of the T cell compartment in the spleen of of *miR-17~92*$^{\Delta/\Delta}$ or *miR-17~92*$^{fl/fl}$ control mice. Naïve CD4 T cells (A) were CD62L^{+} and effector memory CD4 T cells (B) stained positive for CD44 while regulatory T cells (C) were identified with intracellular staining for FOXP3. Bars represent mean ± SEM (n=10-11).

Furthermore, T cell analysis was performed for circulating T cells in the blood. The overall T cell fraction in the blood was not changed (Figure 23). However, detailed analysis revealed changes at least in part contrary to those in spleen and peripheral lymph nodes.

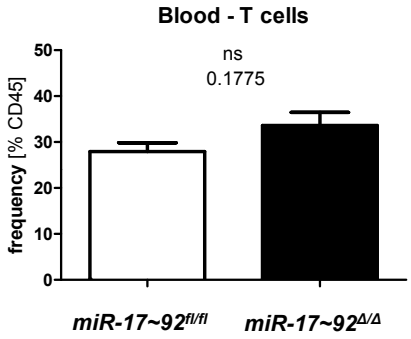

Figure 23 Circulating T cell frequencies in peripheral blood of *miR-17~92*$^{\Delta/\Delta}$ or *miR-17~92*$^{fl/fl}$ control mice. Bars represent mean ± SEM (n=5).

While memory CD4 T cell frequencies were decreased in peripheral lymph nodes, they were unchanged in the blood (Figure 24). In contrast to both spleen and peripheral lymph nodes, naïve CD4 T cell fractions were not increased but diminished while effector memory CD4 T cells were not affected significantly.

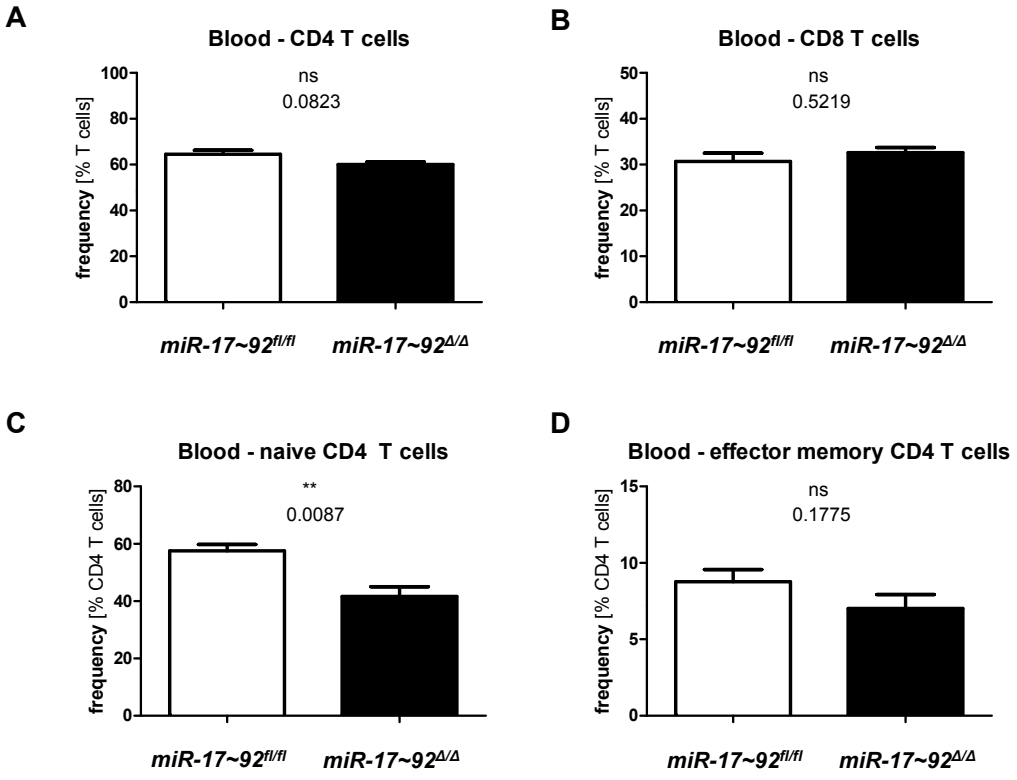

Figure 24 Detailed analysis of the T cell distribution in peripheral blood of *miR-17~92*$^{\Delta/\Delta}$ or *miR-17~92*$^{fl/fl}$ control mice. Upper panels show CD4 (A) and CD8 (B) T cell fractions, lower panels show the fraction of naïve (C) and effector memory (D) T cells. Bars represent mean ± SEM (n=5; **p≤0.01).

4.2.2 Inflammatory Conditions

4.2.2.1 General Characterization

Ldlr$^{-/-}$ *miR-17~92*$^{\Delta/\Delta}$ mice and *Ldlr*$^{-/-}$ *miR-17~92*$^{fl/fl}$ control animals were placed on high-fat diet for 5 weeks to investigate the impact of *miR-17~92* deficiency in pro-atherogenic inflammatory conditions. Figure 25 to Figure 41 illustrate the findings from this experimental setting. *Ldlr*$^{-/-}$ *miR-17~92*$^{\Delta/\Delta}$ mice displayed a minor but significant reduction in body weight while the spleen and peripheral lymph nodes were not altered in size (Figure 25).

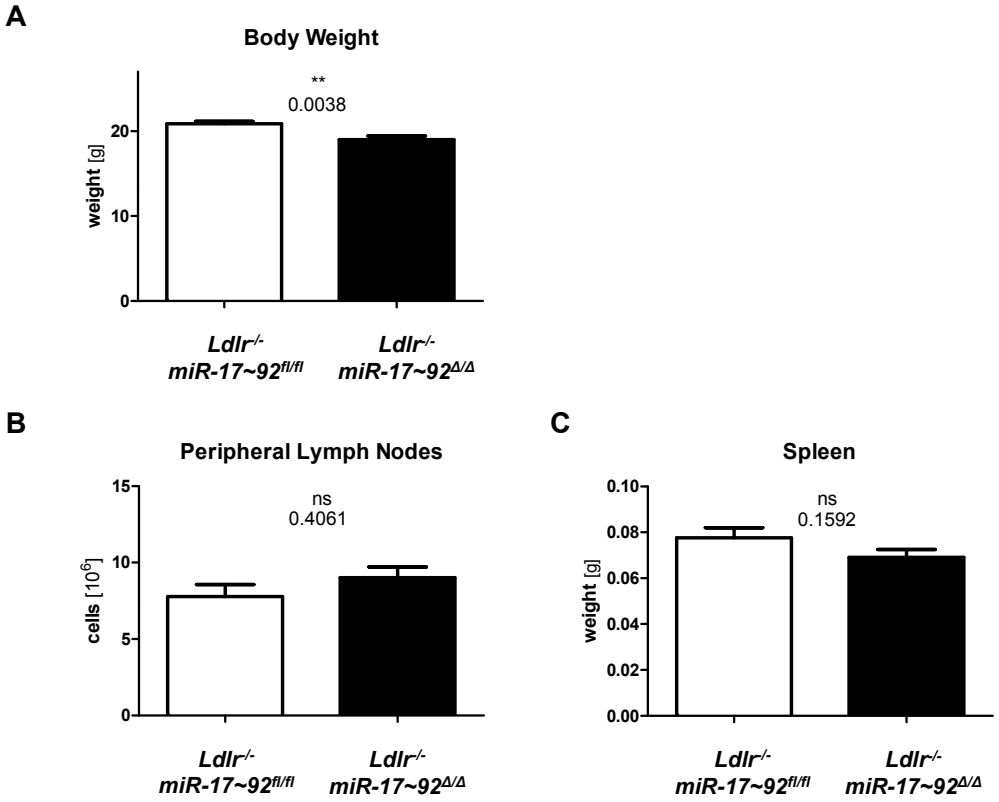

Figure 25 Body weight (A) and secondary lymphatic organ size of peripheral lymph nodes (B) and spleen (C) in *Ldlr*$^{-/-}$ *miR-17~92*$^{\Delta/\Delta}$ and control mice after 5 weeks of high-fat diet feeding. Bars represent mean ± SEM (n=18; **p≤0.01).

Since atherosclerosis in the *Ldlr*-mouse model is caused by severe hyperlipidemia, the blood cholesterol and triglyceride levels were analyzed (Figure 26). Both cholesterol and triglycerides were significantly elevated in *Ldlr*$^{-/-}$ *miR-17~92*$^{\Delta/\Delta}$ mice compared to controls .

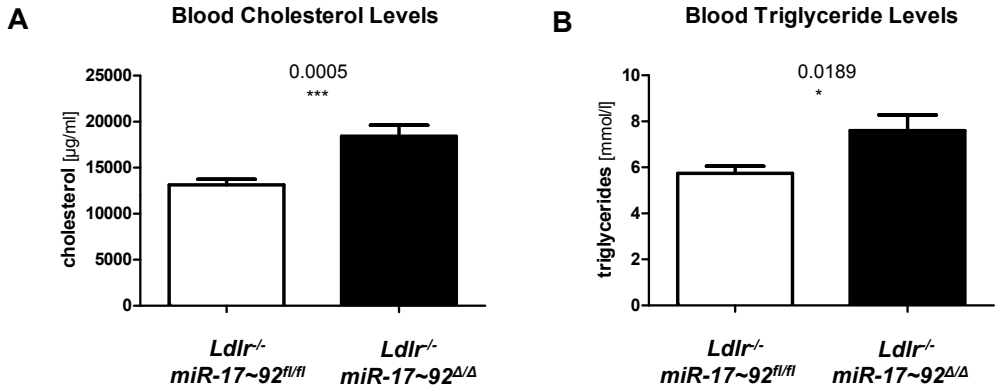

Figure 26 Cholesterol (A) and triglyceride (B) levels in peripheral blood of *Ldlr*$^{-/-}$ *miR-17~92*$^{\Delta/\Delta}$ and control mice that had been on high-fat diet for 5 weeks. Bars represent mean ± SEM (n=11-12; *p≤0.05; ; ***p≤0.001).

4.2.2.2 Immunological Characterization

The extent of plaque formation was evaluated in aortic root sections and *en face* plaque staining was performed for the aorta (Figure 27). *Ldlr*$^{-/-}$ *miR-17~92*$^{\Delta/\Delta}$ mice displayed significantly increased plaque size for both aorta and aortic root.

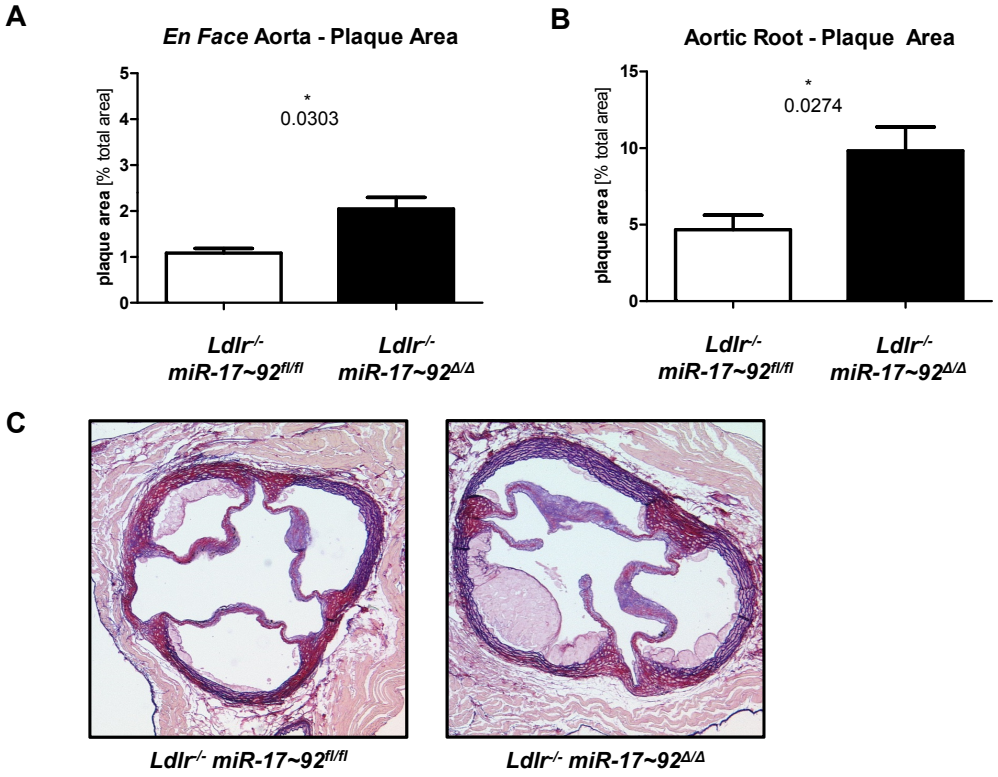

Figure 27 Oil-Red-O staining for histological evaluation of plaque size in the aorta (A) and collagen/elastin staining for plaque analysis in aortic root sections (B) with representative sections (C). *Ldlr*$^{-/-}$ *miR-17~92*$^{\Delta/\Delta}$ and *Ldlr*$^{-/-}$ *miR-17~92*$^{fl/fl}$ mice were fed a high-fat diet for 5 weeks. Bars represent mean ± SEM (n=5-7; *p≤0.05).

Plaque characterization T cell content was carried out (Figure 28). Aortic root sections stained for CD3 showed that the T cell content in aortic root sections was not altered. Considering the increased plaque size these data support an atheroprotective function of the *miR-17~92* cluster in DCs.

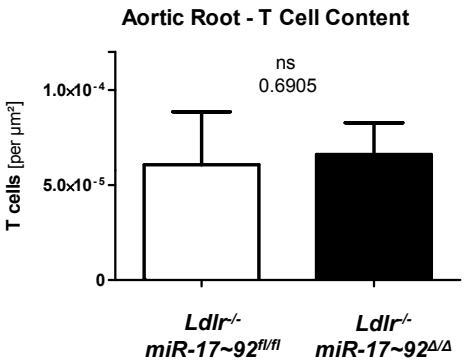

Figure 28 T cell analysis of aortic root sections of *Ldlr*$^{-/-}$ *miR-17~92*$^{\Delta/\Delta}$ and *Ldlr*$^{-/-}$ *miR-17~92*$^{fl/fl}$ mice fed a high-fat diet for 5 weeks. Immunohistochemistry with CD3 staining was performed for evaluation of the T cell content in aortic root sections. Bars represent mean ± SEM (n=4-6; *p≤0.05)

Analysis of the plaque phenotype was extended by flow cytometry using the newly developed gating scheme for identification of DC subsets. Aortae including aortic roots were isolated and enzymatically digested before staining the resulting cell suspension for flow cytometry. Analysis revealed that the DC content in aorta and aortic root was slightly but non-significantly increased in *Ldlr*$^{-/-}$ *miR-17~92*$^{\Delta/\Delta}$ mice (Figure 29).

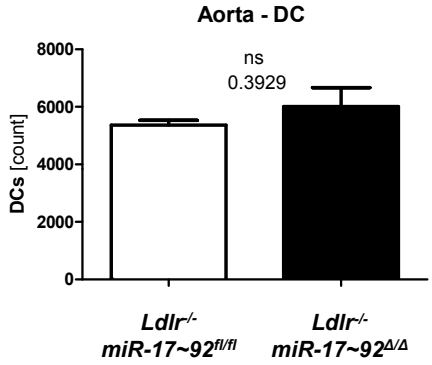

Figure 29 Absolute counts for DCs in atherosclerotic aortic vessel walls of *Ldlr*$^{-/-}$ *miR-17~92*$^{\Delta/\Delta}$ and *Ldlr*$^{-/-}$ *miR-17~92*$^{fl/fl}$ mice were fed a high-fat diet for 5 weeks. Measruements were performed by flow cytometry of enzymatically digested cell suspensions. Bars represent mean ± SEM (n=3-5).

Aortic DCs were subdivided into with the new gating strategy subsets (not shown). The slight increase in total DC numbers resulted from the expansion of a single subset in *Ldlr*$^{-/-}$ *miR-17~92*$^{\Delta/\Delta}$ mice. While the CD11b^{+}F4/80^{+}, CD11b^{-}F4/80^{-} and CD103^{+} DC subsets remained unchanged, the

$CD11b^{+}F4/80^{-}$ DC subset was significantly increased. Furthermore it was possible to identify and analyze regulatory CD4 T cells in enzymatically digested cell suspensions of the aorta (Figure 30). In line with immunohistochemical data (Figure 28) the overall CD4 T cell content was not altered. However, within the distribution of CD4 T cell fractions was altered. The number of regulatory T cells was reduced, although this finding was not significant.

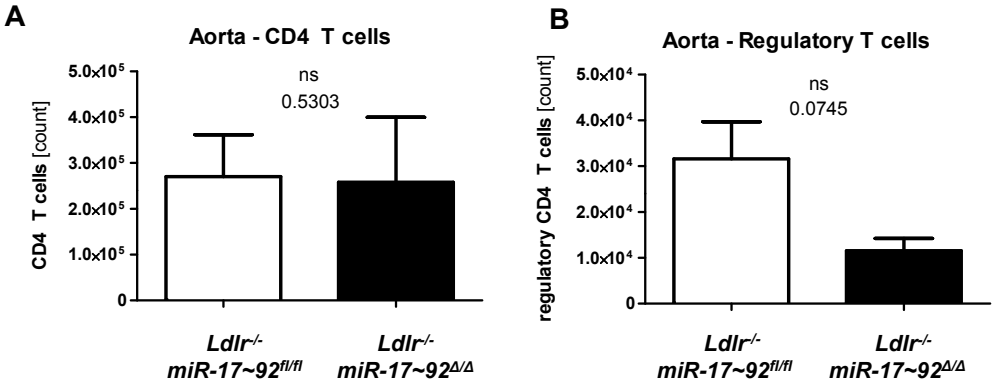

Figure 30 FACS analysis of digested aortic cell suspensions to analyze the T cell fraction in *Ldlr$^{-/-}$ miR-17~92$^{\Delta/\Delta}$* and *Ldlr$^{-/-}$ miR-17~92$^{fl/fl}$* mice fed a high-fat diet for 5 weeks. Overall CD4 T cell content (A) regulatory CD4 T cell numbers (B) are depicted. Bars represent mean ± SEM (n=8-9).

To gain better insight into the immunological status of the *Ldlr$^{-/-}$ miR-17~92$^{\Delta/\Delta}$* mice, the peripheral lymph nodes, spleen, bone marrow and blood were analyzed for the DC and T cell phenotype. In line with results from non-inflammatory mice, preDC frequencies are not altered in atherosclerotic *Ldlr$^{-/-}$ miR-17~92$^{\Delta/\Delta}$* mice compared to *Ldlr$^{-/-}$ miR-17~92$^{fl/fl}$ controls*.

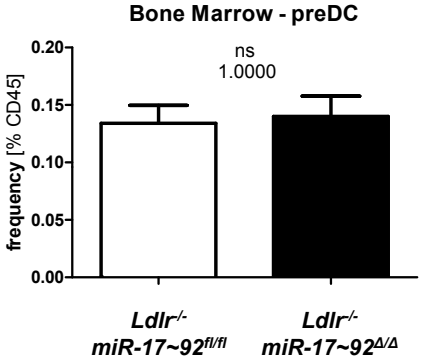

Figure 31 FACS analysis for preDCs within the bone marrow of *Ldlr*$^{-/-}$ *miR-17~92*$^{\Delta/\Delta}$ and *Ldlr*$^{-/-}$ *miR-17~92*$^{fl/fl}$ mice after 5 weeks of high-fat diet. Bars represent mean ± SEM (n=5).

Within peripheral lymph nodes a small but non-significant reduction in cDCs was observed (Figure 32). Interestingly, the DC compartment showed an increased fraction of migDC. In contrast, the proportion of resDCs was decreased. This observation seems to be caused by the inflammatory status of the mice, since migratory and resident DCs did not display any alterations in steady-state conditions.

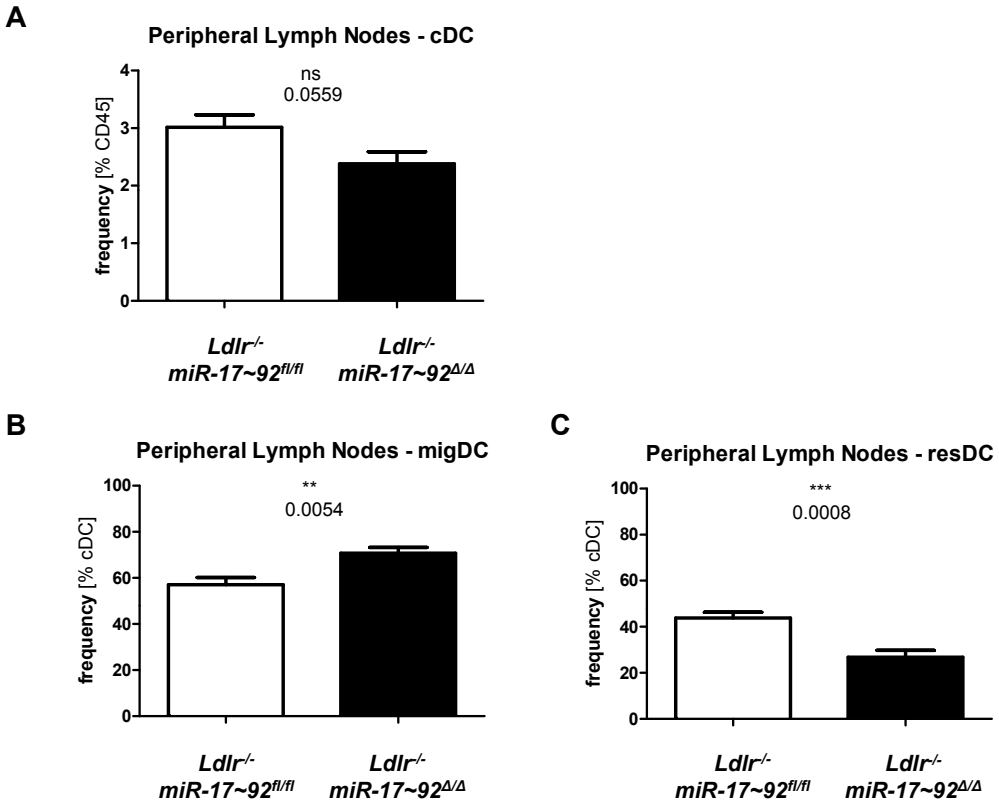

Figure 32 FACS analysis of cDCs (A), migratory (B) and resident (C) DCs in peripheral lymph nodes of *Ldlr*$^{-/-}$ *miR-17~92*$^{\Delta/\Delta}$ and control mice after they were placed on high-fat diet for 5 weeks. Bars represent mean ± SEM (n=11-13; **p≤0.01; ***p≤0.001).

Although there was a difference for migratory and resident DCs, no difference was observed when DCs were analyzed with respect to the expression of CD4 or CD8 (Figure 33). These findings further support that differentiation within the DC lineage does not seem to be affected by the loss of the *miR-17~92* cluster.

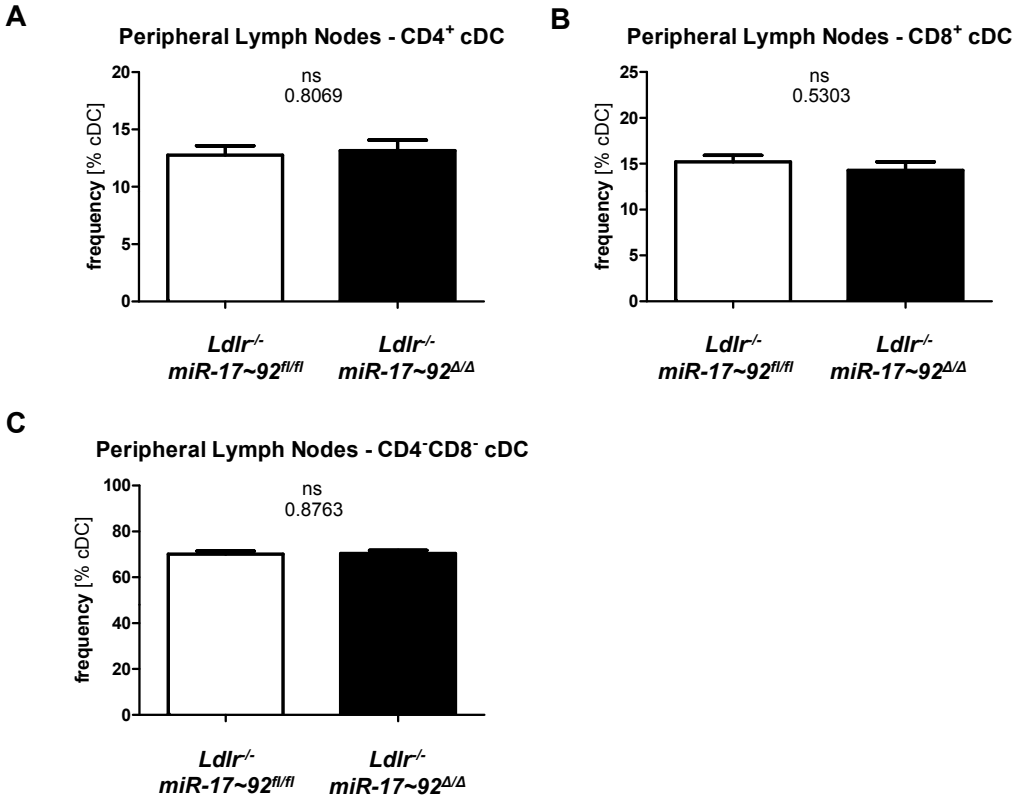

Figure 33 DC subsets in peripheral lymph nodes distinguished by the expression of CD4 and CD8. The distribution of $CD4^+$ cDC (A), $CD8^+$ cDC (B) or $CD4^-$ $CD8^-$ cDC (C) subsets was measured by flow cytometry. *Ldlr$^{-/-}$ miR-17~92$^{\Delta/\Delta}$* and *Ldlr$^{-/-}$ miR-17~92$^{fl/fl}$* mice were fed a high-fat diet for 5 weeks. Bars represent mean ± SEM (n=5-7).

Similar to non-inflammatory conditions there were no differences in the frequencies of splenic cDCs or pDCs (Figure 34) and in line with steady-state conditions there were no changes in the subset distribution of DCs with regard to CD4 and CD8 (Figure 35).

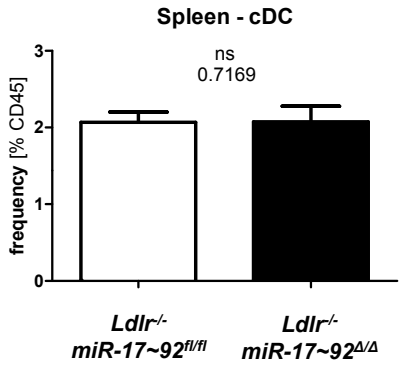

Figure 34 Splenic cDC frequencies in *Ldlr*$^{-/-}$ *miR-17~92*$^{\Delta/\Delta}$ mice compared to *Ldlr*$^{-/-}$ *miR-17~92*$^{fl/fl}$ control animals. Single cell suspensions were measured by flow cytometry. Bars represent mean ± SEM (n=11-12).

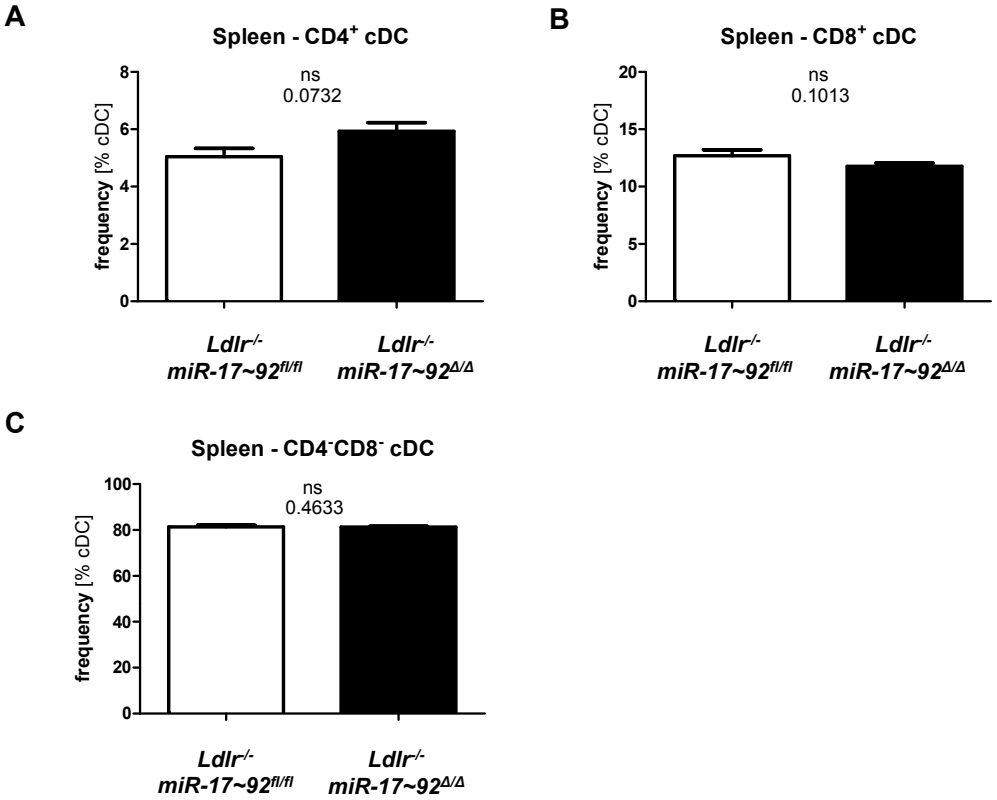

Figure 35 DC subsets within spleen based on the expression of CD4 and CD8. *Ldlr*$^{-/-}$ *miR-17~92*$^{\Delta/\Delta}$ and *Ldlr*$^{-/-}$ *miR-17~92*$^{fl/fl}$ mice were fed a high-fat diet for 5 weeks. The distribution of CD4^{+} cDC (A), CD8^{+} cDC (B) or CD4^{-} CD8^{-} cDC (C) subsets was measured by flow cytometry. Bars represent mean ± SEM (n=5-7).

T cells of peripheral lymph nodes, spleen and blood were analyzed using flow cytometry. In peripheral lymph nodes, small but significant increments in overall T cell and CD8 T cell frequencies were observed, while the fraction of CD4 T cells remained unchanged (Figure 36).

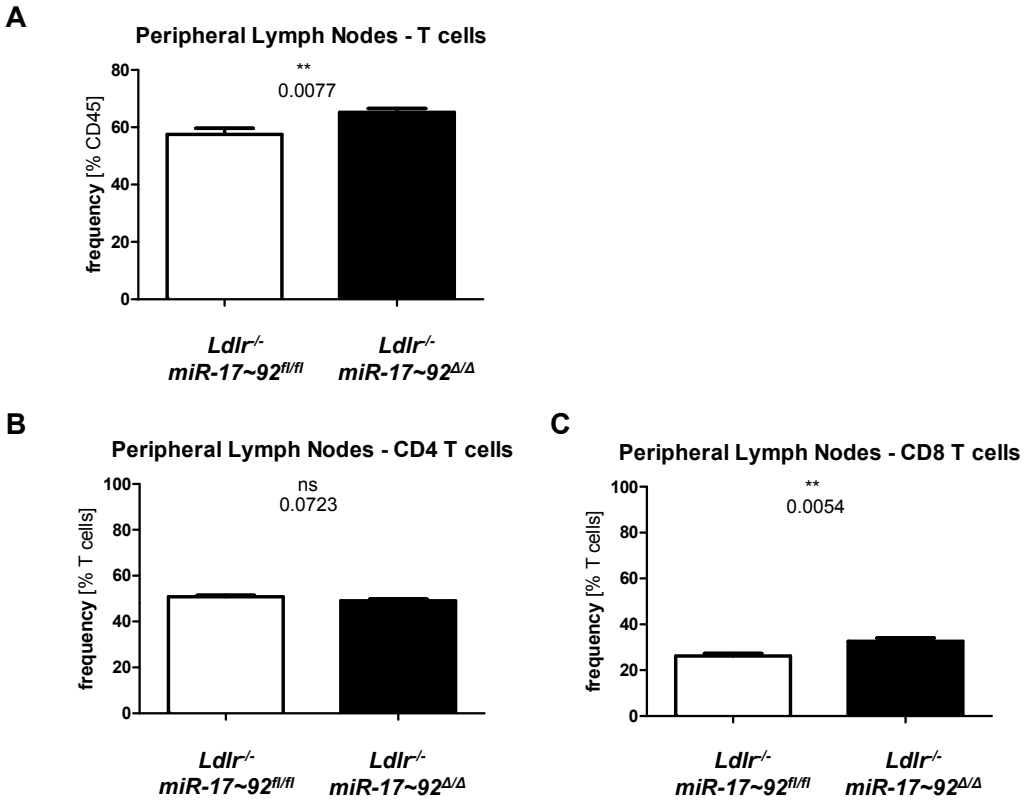

Figure 36 Flow cytometry for T cell analysis of peripheral lymph nodes in *Ldlr*$^{-/-}$ *miR-17~92*$^{\Delta/\Delta}$ and control mice after 5 weeks of high-fat diet. Total T cell frequency (A), CD4 T cells (B) and the CD8 T cells subset (C) are shown. Bars represent mean ± SEM (n=11-13; **p≤0.01).

Analogous to the results from mice in non-inflammatory conditions (Figure 19), a significant increase in naïve CD4 T cells was accompanied by a significant decrease in memory CD4 T cells (Figure 37). However, the most interesting finding was a dramatically reduced fraction of regulatory CD4 T cells that had not been observed in non-atherogenic conditions.

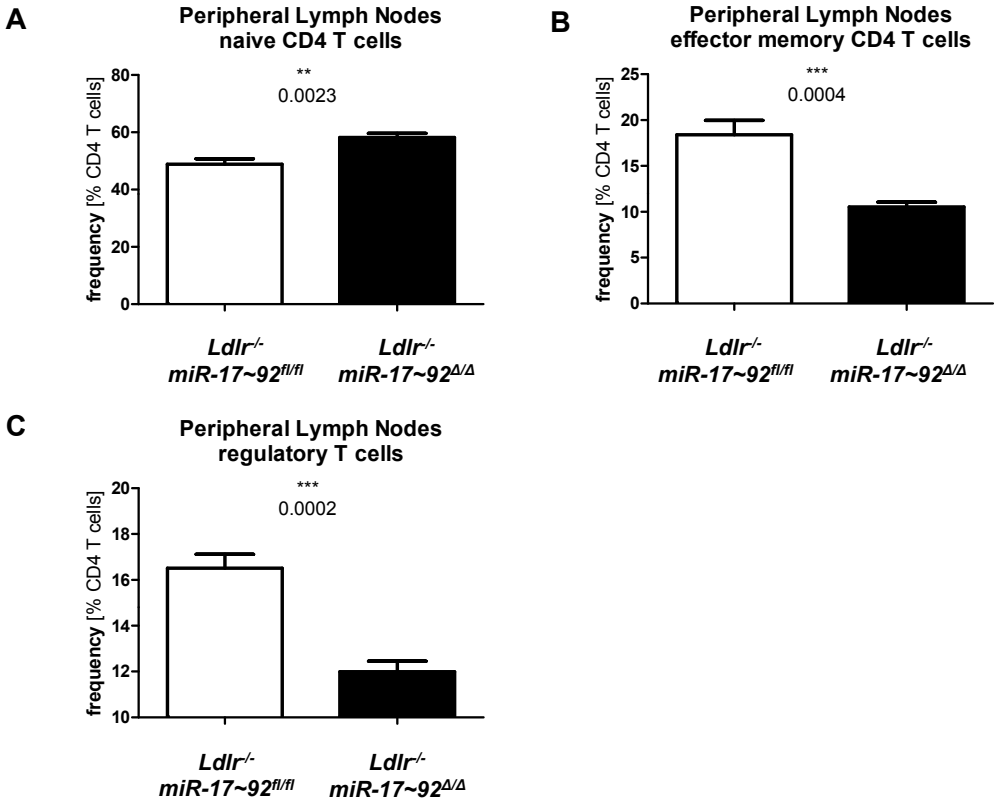

Figure 37 Analysis of the CD4 T cell fraction within peripheral lymph nodes of atherosclerotic *Ldlr*$^{-/-}$ *miR-17~92*$^{\Delta/\Delta}$ and control mice using flow cytometry. CD62L and CD44 surface staining for discrimination of naïve (A) and memory (B) CD4 T cells. Regulatory CD4 T cells were positive for CD25 and intracellular transcription factor FOXP3 (C). Bars represent mean ± SEM (n=11-13; **p≤0.01; ***p≤0.001).

Data obtained from the spleen represented a similar picture. Overall T cell frequency was not altered while CD4 and CD8 T cells were slightly shifted towards a CD8 phenotype (Figure 38).

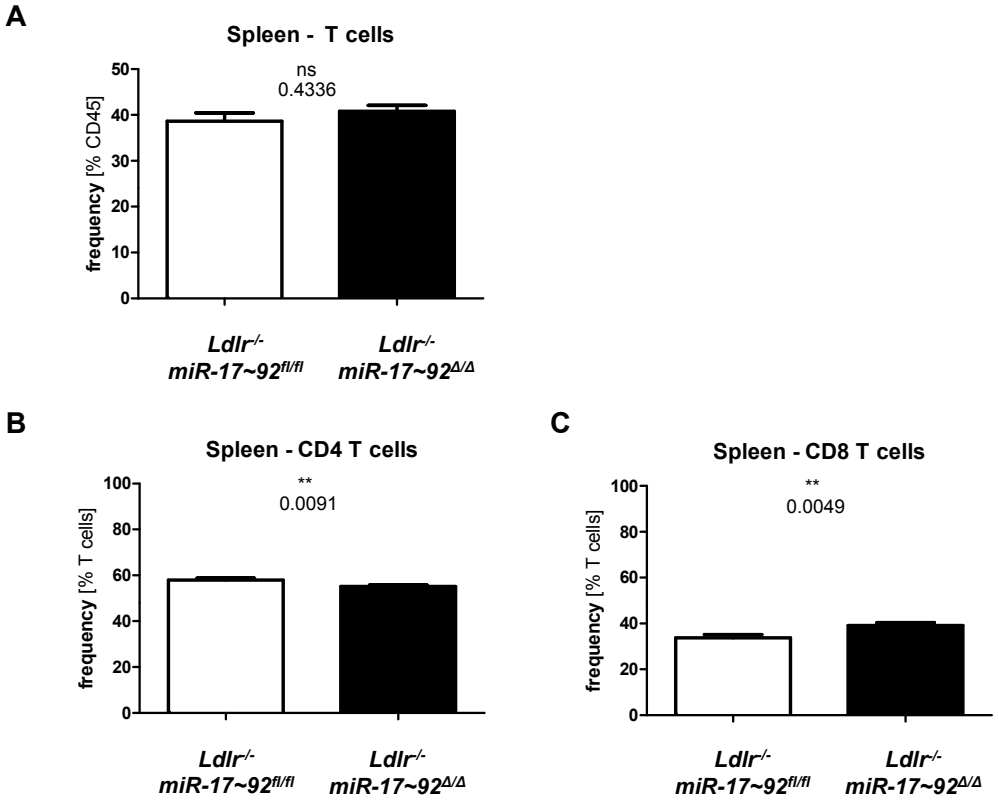

Figure 38 FACS analysis of splenic T cell fraction in atherosclerotic *Ldlr*$^{-/-}$ *miR-17~92*$^{\Delta/\Delta}$ and control mice that were fed a high-fat diet for 5 weeks. Total T cell frequency (A) and fraction CD4 (B) and CD8 (C) T cells are shown. Bars represent mean ± SEM (n=11-13; **p≤0.01).

The increase in naïve CD4 T cells and lack of memory CD4 T cells was also observed for the spleen, however, less pronounced and therefore not significant (Figure 39). Regulatory CD4 T cells were diminished in the spleen as well. This clear reduction in both lymph node and spleen was not observed in non-inflammatory *miR-17~92*$^{\Delta/\Delta}$ mice and points towards a functional defect of DCs with regard to T cell polarization under inflammatory conditions.

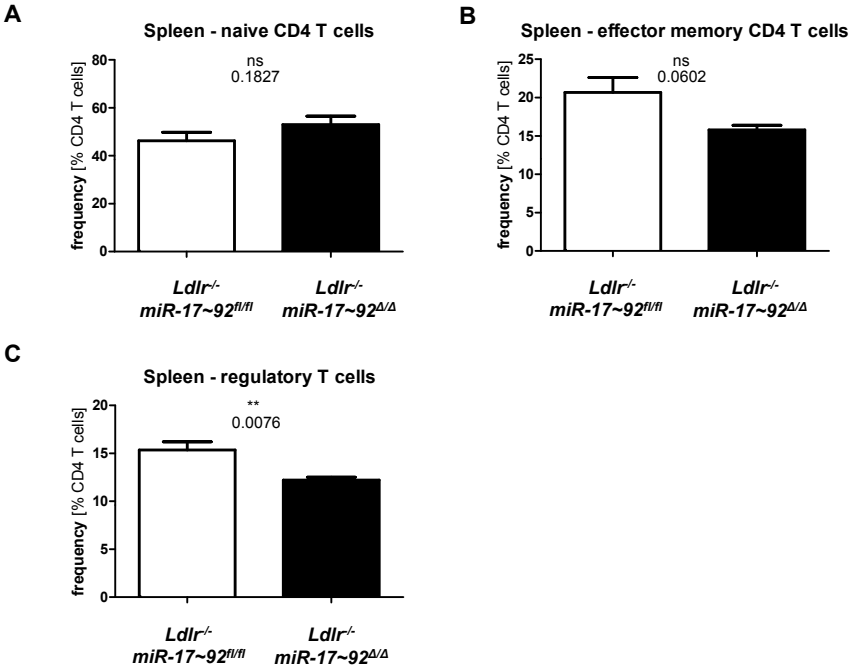

Figure 39 FACS analysis of the splenic CD4 T cell fraction in atherosclerotic *Ldlr*$^{-/-}$ *miR-17~92*$^{\Delta/\Delta}$ and control mice. CD62L and CD44 surface staining for discrimination of naïve (A) and memory (B) CD4 T cells. Regulatory CD4 T cells were positive for CD25 and intracellular transcription factor FOXP3 (C). Bars represent mean ± SEM (n=11-13; **p≤0.01).

T cells of the blood were included into analysis. Total T cell frequency was not significantly altered by *Cd11c*-specific deletion of the *miR-17~92* cluster (Figure 40).

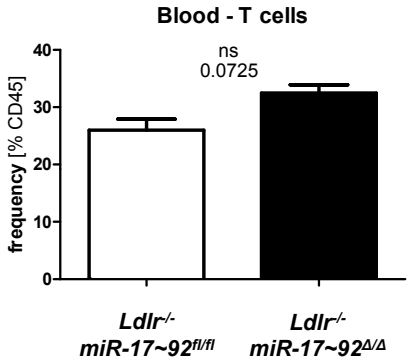

Figure 40 FACS analysis for the frequency of circulating T cells in peripheral blood of *Ldlr*$^{-/-}$ *miR-17~92*$^{\Delta/\Delta}$ mice feed a high-fat diet for 5 weeks. Bars represent mean ± SEM (n=11-13).

In line with the findings from spleen and peripheral lymph nodes the circulating T cells in the blood also demonstrated a shift towards CD8 T cells (Figure 41).

However, in contrast to peripheral lymph nodes and spleen the naïve T cells in the blood were not significantly elevated. Effector memory CD4 T cells showed a notable reduction, although this was not significant.

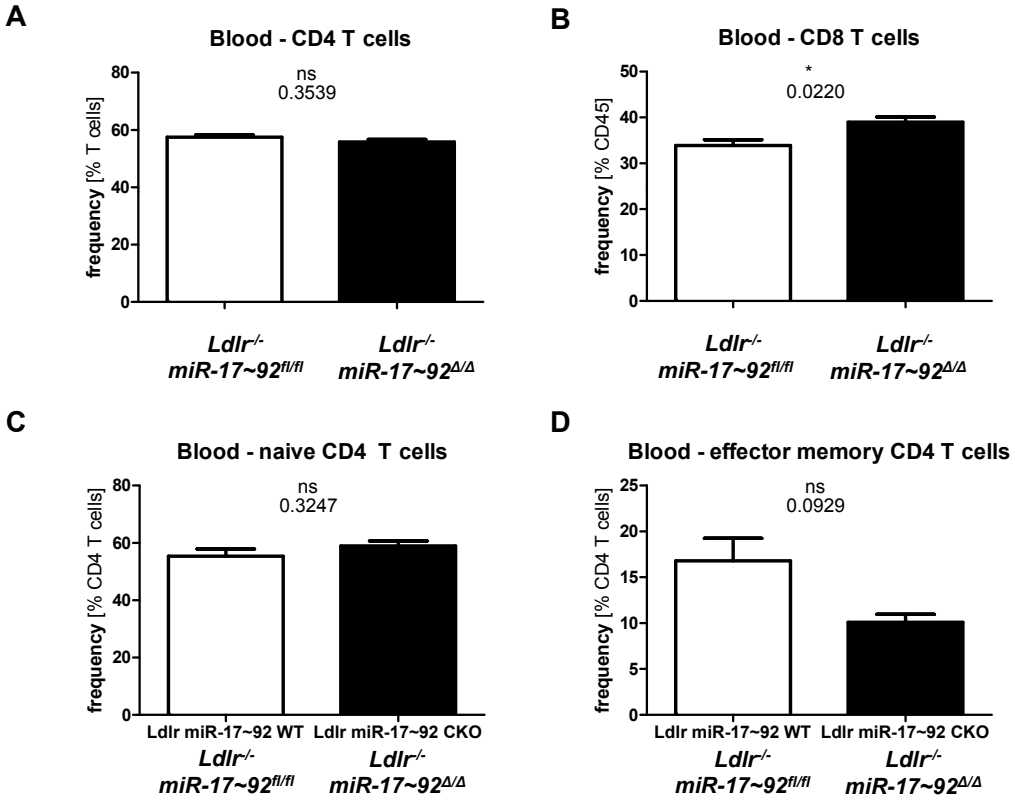

Figure 41 FACS analysis of the circulating T cell fraction in the blood. The two major T cell subsets, CD4 (A) and CD8 (B) are shown. CD4 T cells were further subdivided into naïve (C) and effector memory CD4 T cells (D). Bars represent mean ± SEM (n=11-13; *p≤0.05).

The two most interesting findings were the increased plaque formation in line with a reduction in Tregs within spleen, peripheral lymph nodes and the aorta. Notably, this reduction only occurs in inflammatory conditions. To underline that the induction of regulatory T cells is impaired in inflammatory pro-atherogenic conditions, naïve CD4 T cells of healthy *Cd45.1* donor mice were injected into *miR-17~92*$^{\Delta/\Delta}$ and *miR-17~92*$^{fl/fl}$ mice, as well as *Ldlr*$^{-/-}$ *miR-17~92*$^{\Delta/\Delta}$ and *Ldlr*$^{-/-}$ *miR-17~92*$^{fl/fl}$ mice fed a high-fat diet for 5 weeks. The fate of these transferred naïve donor T cells was analyzed for naïve CD4 T cells and regulatory T cell induction 10 days post injection. For *Ldlr*$^{-/-}$ *miR-17~92*$^{\Delta/\Delta}$ and control mice, cells were injected 25 days after they were put on high-fat diet so that T cells were analyzed after 5 weeks of high-fat diet. Resembling the findings from *miR-*

17~92$^{\Delta/\Delta}$ mice in non-inflammatory conditions, there was no difference in regulatory or naïve donor T cells within the spleen of both *Ldlr$^{-/-}$ miR-17~92$^{fl/fl}$* or control recipient mice (Figure 42). The fraction of regulatory donor T cells was slightly decreased in peripheral lymph nodes, however, this finding was not significant. In line with the data obtained from the *Ldlr$^{-/-}$ miR-17~92$^{\Delta/\Delta}$* and control mice, there was no difference in the T cell phenotype in steady-state non-atherogenic conditions.

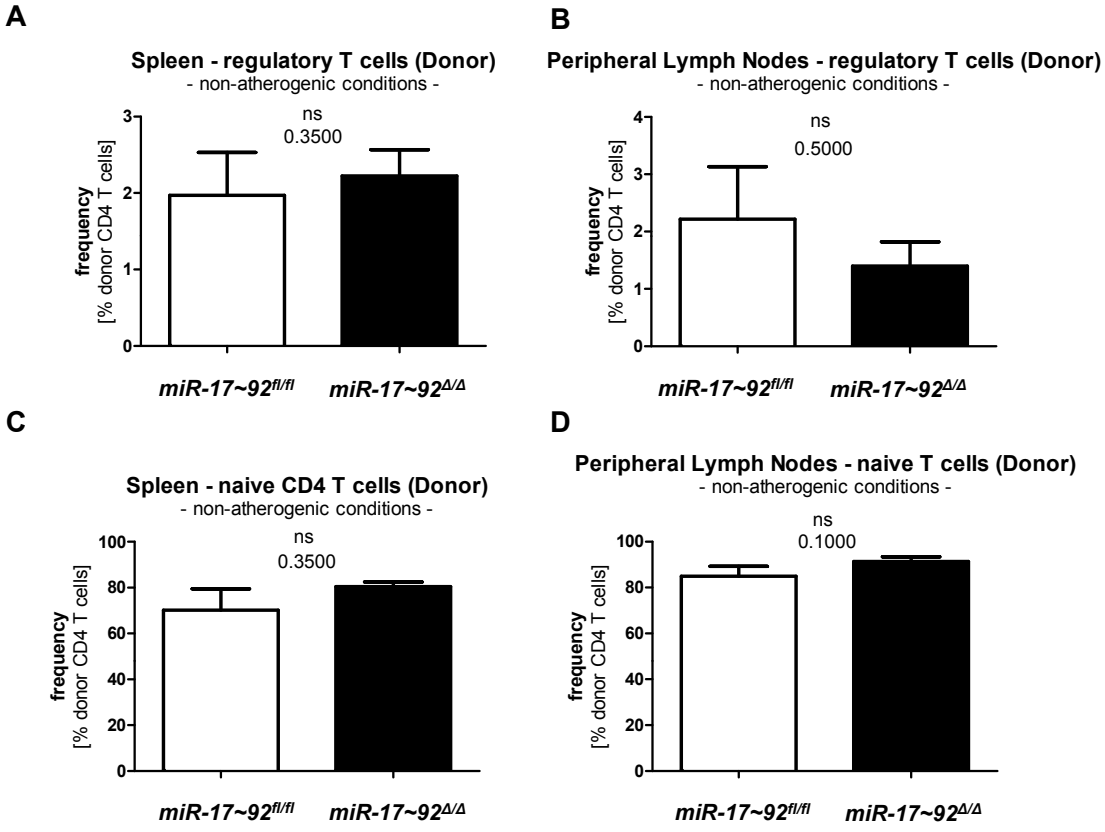

Figure 42 Adoptive transfer of naïve CD4 T cells from healthy CD45.1 donor mice into *miR-17~92$^{\Delta/\Delta}$* and *miR-17~92$^{fl/fl}$* mice in non-inflammatory conditions. Donor T cells were identified based on the expression of CD45.1 and the fraction of regulatory T cells (A,B) and naïve T cells (C,D) was analyzed within the spleen (A, C) and peripheral lymph nodes (B,D). X axis indicates recipient mice and Y axis indicates fraction of analyzed donor T cells relative to total donor CD4 T cells. Bars represent mean ± SEM (n=3-4).

The experiment was also conducted with *Ldlr$^{-/-}$ miR-17~92$^{\Delta/\Delta}$* and *Ldlr$^{-/-}$ miR-17~92$^{fl/fl}$* mice on pro-atherogenic high-fat diet (Figure 43). Interestingly, CD45.1 donor T cells now showed a reduction of regulatory T cells accompanied by an increase of naive T cells in *Ldlr$^{-/-}$ miR-17~92$^{\Delta/\Delta}$* mice, resembling the findings

from *Ldlr$^{-/-}$ miR-17~92$^{Δ/Δ}$* mice on high-fat diet. Cell numbers in both peripheral lymph nodes and spleen were not altered (Table 13).

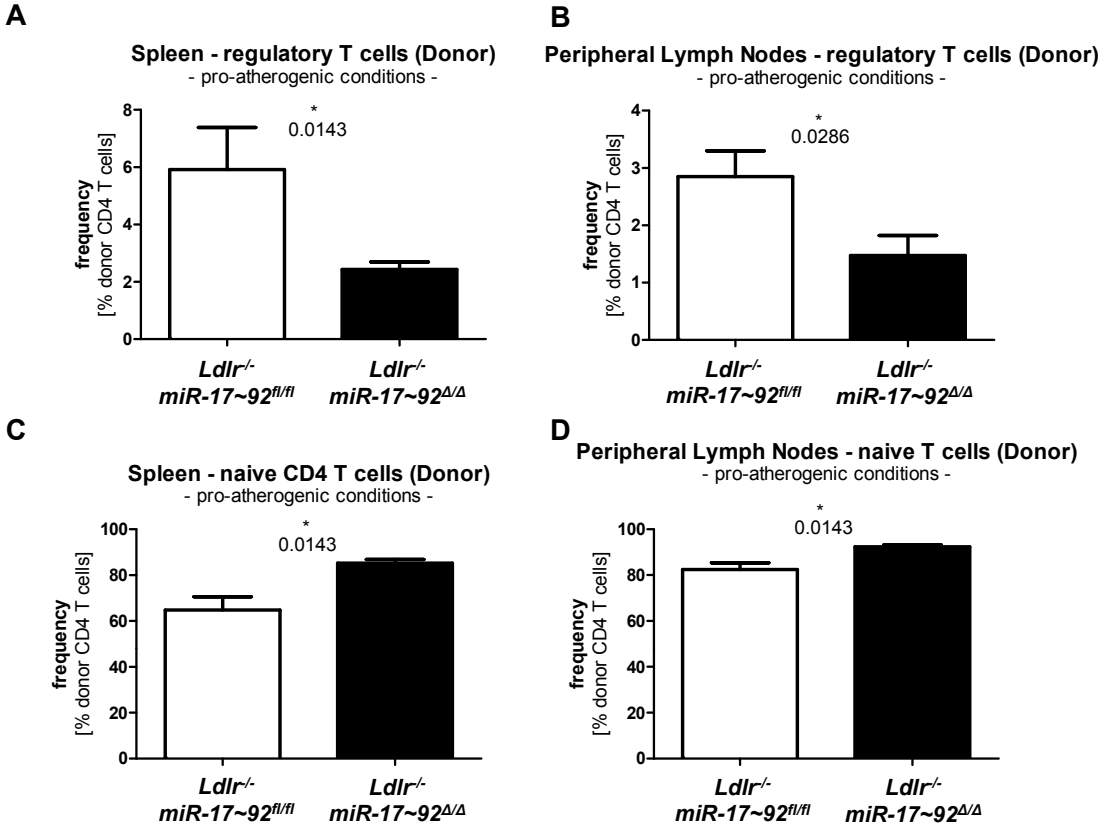

Figure 43 Adoptive transfer of naïve CD4 T cells from healthy CD45.1 donor mice into *Ldlr$^{-/-}$ miR-17~92$^{Δ/Δ}$* and *Ldlr$^{-/-}$ miR-17~92$^{fl/fl}$* control mice in pro-atherogenic conditions. Donor T cells were identified based on the expression of CD45.1 and the fraction of regulatory T cells (A,B) and naïve T cells (C,D) was analyzed within the spleen (A, C) and peripheral lymph nodes (B,D). X axis indicates recipient mice and Y axis indicates fraction of analyzed donor T cells relative to total donor CD4 T cells. Bars represent mean ± SEM (n=3-4; *p≤0.05).

Table 12 Cell counts for peripheral lymph nodes and spleen of *Ldlr$^{-/-}$ miR-17~92$^{Δ/Δ}$* and *Ldlr$^{-/-}$ miR-17~92$^{fl/fl}$* control recipient mice for naïve CD45.1 CD4 T cells after 5 weeks on high-fat diet. Cell counts were not altered significantly.

Organ	*Ldlr$^{-/-}$ miR-17~92$^{fl/fl}$*	*Ldlr$^{-/-}$ miR-17~92$^{Δ/Δ}$*
peripheral lymph nodes	$3.95 \cdot 10^7 \pm 3.83 \cdot 10^6$	$5.55 \cdot 10^7 \pm 1.24 \cdot 10^6$
spleen	$8.25 \cdot 10^6 \pm 3.39 \cdot 10^6$	$3.40 \cdot 10^6 \pm 0.76 \cdot 10^6$

These results underscore that the decrease of regulatory T cells and elevation of naïve T cells is truly dependent on inflammation. Furthermore it also demonstrates that peripheral regulatory T cell induction is affected, rather than thymic T cell differentiation.

4.2.3 *In vitro* Data

Since DC numbers and frequencies were not affected by *Cd11c*-specific deletion of *miR-17~92*, the reduction in regulatory T cells must result from a functional defect. To gain insights into the mechanisms that are altered in *miR-17~92*-deficient DCs, *in vitro* cultures of bone marrow-derived DCs were used. The notion that *miR-17~95* deletion rather causes functional defects than alterations in differentiation and development is also reflected in the results from these cultured DCs. Both *miR-17~92*$^{\Delta/\Delta}$ and *miR-17~92*$^{fl/fl}$ cultures showed comparable cell counts and yielded equal fractions and numbers of maturet CD11c^{+}MHCII^{+} DCs (Figure 44).

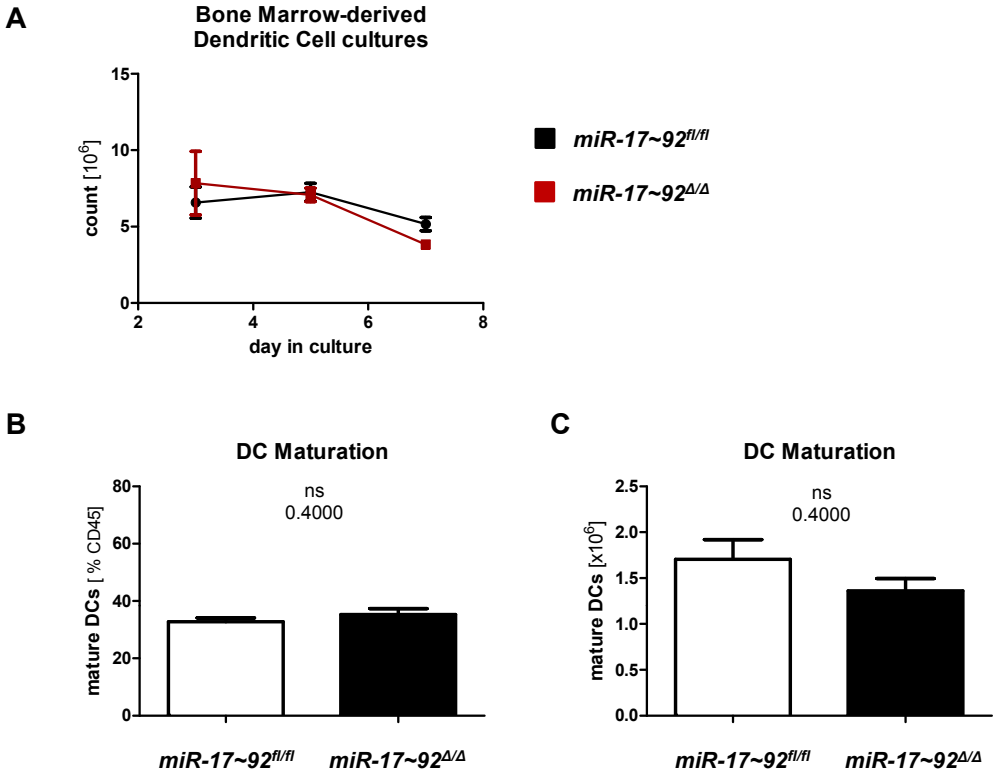

Figure 44 Baseline characterization of bone marrow-derived DC cultures from *miR-17~92*$^{\Delta/\Delta}$ and *miR-17~92*$^{fl/fl}$ DCs. Cell counts in cultures were measured during the course of the culture (A) and maturation of CD11c^{+}MHCII^{+} cDCs was measured in flow cytometry (B+C). Bars represent mean ± SEM (n=3).

DCs obtained from *miR-17~92*$^{\Delta/\Delta}$ and control cultures were measured for surface CD80 expression using flow cytometry to gain insight into DC activation. To assess the phagocytic capacity of DCs from both cultures, DCs were co-incubated with fluorescent latex beads. Bead uptake was measured using flow cytometry. Neither activation level, nor phagocytic capacity was altered in DC cultures from *miR-17~92*$^{\Delta/\Delta}$ mice (Figure 45).

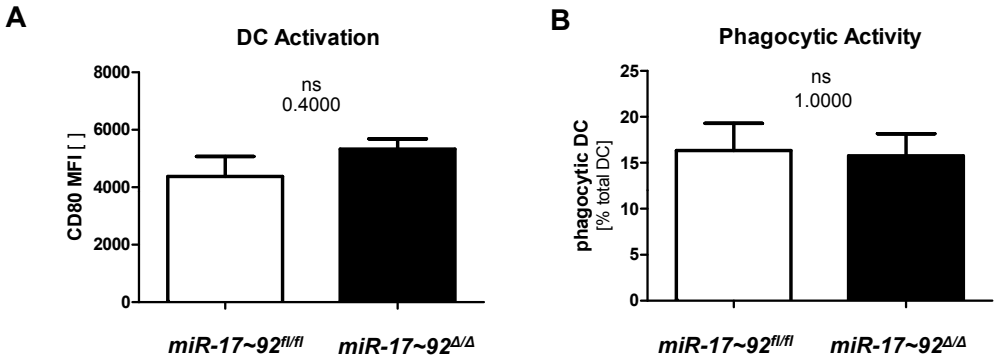

Figure 45 Activation level and phagocytic capacity on bone marrow-derived DCs from *miR-17~92*$^{\Delta/\Delta}$ and *miR-17~92*$^{fl/fl}$ mice. DC activation was assessed by FACS analysis of CD80 expression (A). Uptake of fluorescent latex beads was measured by flow cytometry to analyze the phagocytic capacity of DCs (B). Bars represent mean ± SEM (n=3).

To demonstrate the functional defect of *miR-17~92*$^{\Delta/\Delta}$ DCs in the induction of regulatory T cells, bone marrow derived DCs were used for antigen-specific T cell proliferation and T cell polarization *in vitro*. *OTII* T cells harboring the transgenic T cell receptor for amino acids 323 – 339 of chicken ovalbumin as antigen were isolated and co-incubated with DCs for 48 hours before co-cultures were applied to FACS analysis. While antigen-specific T cell proliferation was not affected, the polarization of regulatory T cells was decreased in cultures of *miR-17~92*-deficient DCs (Figure 46), similar to the obtained *in vivo* data.

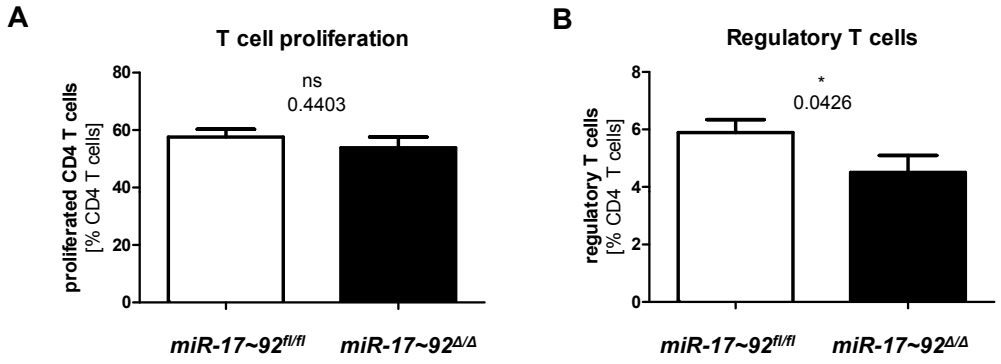

Figure 46 Antigen-specific proliferation and polarization of naïve CD4 T cells *in vitro*. CFSE stained naïve CD4 T cells isolated from OT-II mice were co-incubated with bone marrow-derived *miR-17~92*$^{\Delta/\Delta}$ or *miR-17~92*$^{fl/fl}$ in the presence of OVA and dilution of CFSE was measured by flow cytometry to assess T cell proliferation (A). The same setup was used for FACS analysis of Tregs (B), utilizing intracellular staining for Treg transcription factor FOXP3. Bars represent mean ± SEM (n=9).

These results further underline that *miR-17~92*-deficient DCs were deficient in the induction of regulatory T cells.

To reveal the mechanism of this defect it was necessary to identify *miR-17~92* targets that play a role in the interaction of DCs with T cells and in the induction of regulatory T cells. A list with putative targets of the *miR-17~92* cluster was obtained from microRNA.org (see methods for further details). Since one mRNA can be targeted by several miRNAs and some members of the *miR-17~92* cluster show highly similar binding motifs, a list of 36 332 putative targets was obtained (Table 13).

Table 13 Overview of the *miR-17~92* cluster members and the number of putative targets as predicted by the miRSVR algorithm (Betel et al., 2010).

miRNA	Number of predicted targets
miR-17	7283
miR-18a	6530
miR-19a	5225
miR-19b	5166
miR-20a	7330
miR-92a	4798
TOTAL	**36 332**

After removal of duplicates, 7466 unique targets remained. Since mRNAs can be targeted by several miRNAs, the list was ordered by the number of cluster members that are predicted to bind. The main interest focused on putative targets that were known to be associated with the capacity of DCs induce Tregs. Amongst these putative targets of interest, *Socs3* was identified. SOCS3 has been demonstrated to regulate IDO activity (Orabona et al., 2008). IDO-mediated conversion of tryptophan is involved in the peripheral induction of regulatory T cells. Therefore, SOCS3 harbors the potential to regulate the induction of regulatory T cells by DCs. *Socs3* mRNA (accession number NT_096135.6) contains two predicted binding sites for *miR-17~92* cluster members. *MiR-17* and *miR-20a* are predicted to bind within positions 3081 to 3101 and *miR-19a* and *miR-19b* from positions 3185 to 3207. To investigate whether *Socs3* is regulated by *miR-17~92* cluster members, bone marrow-derived DCs from *miR-17~92*$^{\Delta/\Delta}$ and *miR-17~92*$^{fl/fl}$ DCs were analyzed for *Socs3* mRNA levels by RT-qPCR (Figure 47).

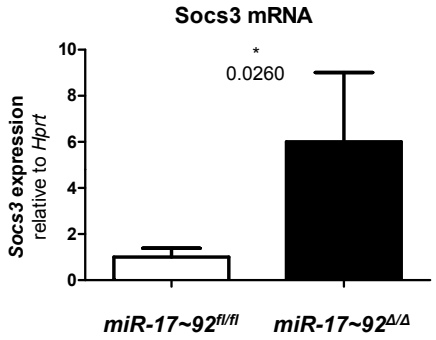

Figure 47 RT-qPCR analysis of *Socs3* mRNA levels in bone marrow-derived DCs from *miR-17~92*$^{\Delta/\Delta}$ and *miR-17~92*$^{fl/fl}$ DCs. Total RNA was isolated from cultures on day 7 and *Socs3* levels were normalized to *Hprt* mRNA levels. Bars represent mean ± SEM (n=6; *p≤0.05).

As expected, *Socs3* mRNA levels were elevated in *miR-17~92*-deficient DCs. To demonstrate that *Socs3* is a direct target of *miR-17~92* cluster members, the predicted target site and a control target site of the *Socs3* mRNA 3'-untranslated region (UTR) were cloned into the psiCHECK-2 dual luciferase reporter system (Figure 48). A 196 bp fragment of the *Socs3* mRNA 3'-UTR without any predicted target sites for *miR-17~92* cluster members was cloned from position 2645 to 2841. The resulting construct served as a control and was termed psiCHECK-2-Socs3-ctrl. A construct termed psiCHECK-2-Socs3-17~92 was cloned from positions 3049 to 3241 and contained the binding sites for *miR-17~92* members *miR-17*, *miR-20a*, *miR-19a* and *miR-19b*.

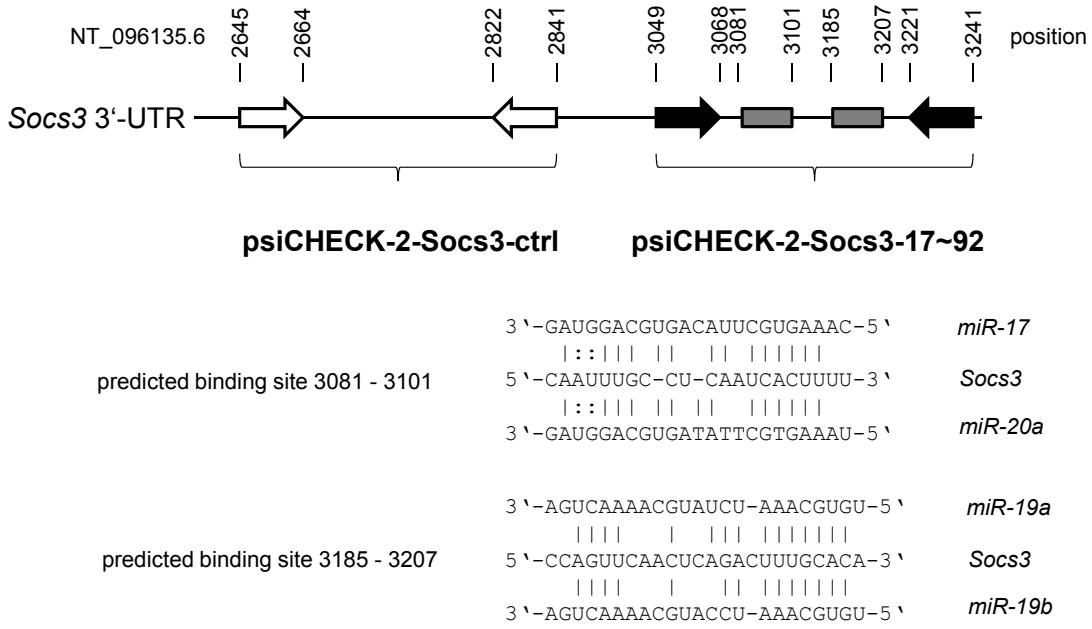

Figure 48 Cloning strategy for psiCHECK-2 dual luciferase reporter constructs carrying the two predicted binding sites of *miR-17~92* cluster members. Arrows indicate primer positions. The control construct termed psiCHECK-2-Socs3-ctrl contained a 196 bp long fragment of the *Socs3* 3'-UTR that had no predicted binding sites for *miR-17~92* cluster members. The construct containing the binding sites of the *miR-17~92* cluster members *miR-17*, *miR-20a*, *miR-19a* *miR-19b* was termed psiCHECK-2-Socs3-17~92. The amplified fragment was 192 bp long. Pairing of the predicted binding sites (lower panel) was obtained from the miRSVR algorithm at microRNA.org (Betel et al., 2010).

Constructs were co-transfected with miRNA precursors (Pre-miR) in HEK293F cells to measure luciferase activity. Expression of both renilla and firefly luciferase allowed for data normalization to exclude bias from varying transfection efficiencies. The co-transfection of Pre-miRs allowed to overexpress distinct miRNAs. A random Pre-miR sequence served as a negative control miRNA precursor (Pre-miR-ctrl) with no designated mRNA target and was used to normalize luciferase activity. Initially, the HEK293F cells transfected with psiCHECK-2-Socs3-17~92 or psiCHECK-2-Socs3-ctrl were co-transfected with the Pre-miR control or a Pre-miR mix for overexpression of *miR-17*, *miR-19a*, *miR-19b* and *miR-20a* in equimolar amounts. This mixture was termed Pre-miR-17~92. As expected, Pre-miR-17~92 was able to

downregulate relative luciferase activity for the psiCHECK-2-Socs3-17~92 construct, while it was not able to do so for the control construct without binding sites (Figure 49). This clearly indicates a direct interaction between *miR-17~92* cluster members and the 3'-UTR of *Socs3* mRNA.

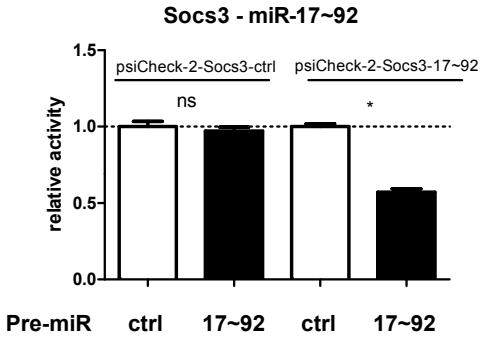

Figure 49 Luciferase assay for assessing the ability of *miR-17~92* cluster members to bind predicted target sites within the 3'-UTR of *Socs3* mRNA. PsiCHECK-2-Socs3-17~92 and control construct psiCHECK-2-Socs3-ctrl were co-transfected with Pre-miRs of *miR-17~92* cluster members *miR-17*, *miR-19a*, *miR-19b* and *miR-20a* or controls. Relative luciferase activity in HEK293F cells was measured 24 hours after transfection. Bars represent mean ± SEM (n=3; *p≤0.05).

To identify the cluster member responsible for the downregulation of luciferase activity, the experiment was repeated using single Pre-miRs for co-transfection (Figure 50). Luciferase data revealed that *miR-19a* and *miR-20a* directly targeted *Socs3* while *miR-17* and *miR-19b* did not bind to the predicted target sites.

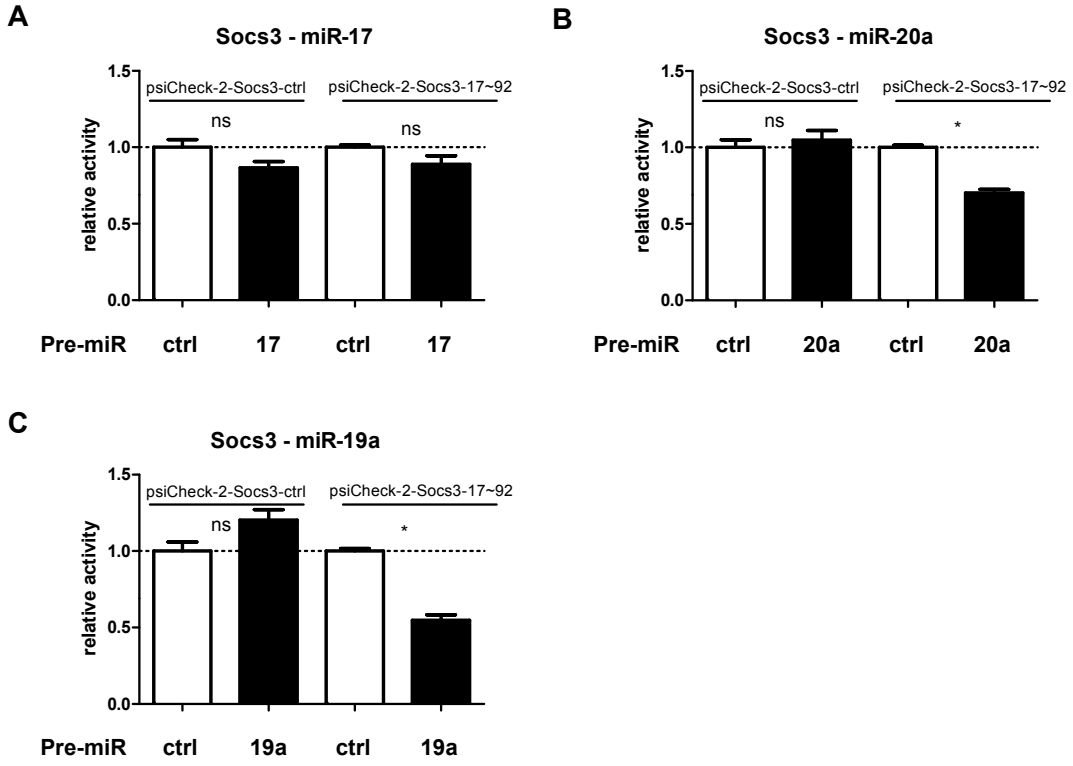

Figure 50 Luciferase assays demonstrating the ability of *miR-17~92* cluster members to bind 3'-UTR of *Socs3* mRNA. HEK293F cells were co-transfected with psiCHECK-2-Socs3-17~92 or control construct psiCHECK-2-Socs3-ctrl and with single Pre-miRs for *miR-17* (A), *miR-20a* (B), *miR-19a* (C) or control. Bars represent mean ± SEM (n=3; *p≤0.05).

In summary, these results show that *Socs3* is a direct target of *miR-17~92* cluster members *miR-20a* and *miR-19a*. Interestingly, both miRNAs use different binding sites. While *miR-20a* targets site one at positions 3081 to 3101, *miR-19a* targets the second site at positions 3185 to 3207.

Since *Socs3* is a direct target of *miR-17~92* cluster members, it was tested whether the tryptophan metabolism is involved in the impaired induction of Tregs by *miR-17~92*-deficient DCs. Splenic $CD11c^+$ DC were isolated from *Ldlr*$^{-/-}$ *miR-17~92*$^{\Delta/\Delta}$ and *Ldlr*$^{-/-}$ *miR-17~92*$^{fl/fl}$ control animals that had been on high-fat died for 5 weeks. They were co-cultivated with naïve CD4 T cells from transgenic *OTII* in presence of OVA and with or without additional L-tryptophan. After 5 days, the fraction of induced regulatory T cells was investigated (Figure 51).

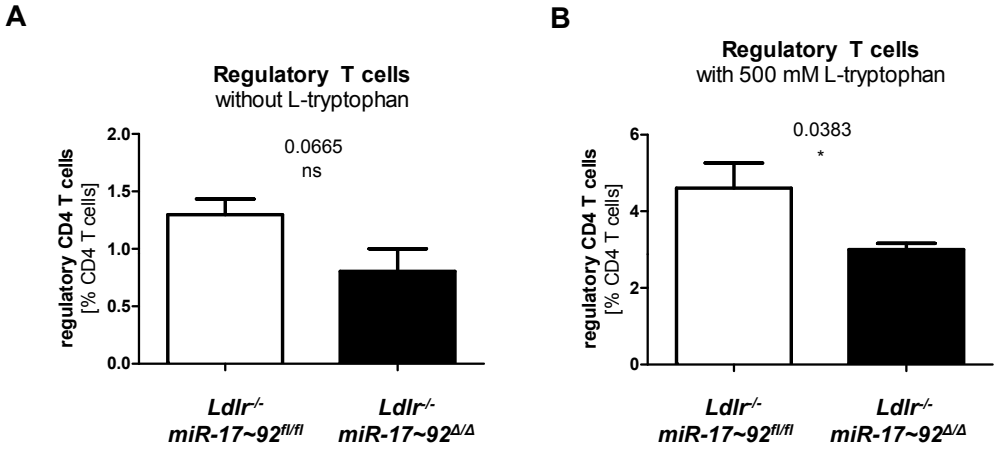

Figure 51 Regulatory T cell conversion of naïve CD4 T cells. Naïve T cells were co-cultured with isolated splenic DCs from *Ldlr*$^{-/-}$ *miR-17~92*$^{\Delta/\Delta}$ and *Ldlr*$^{-/-}$ *miR-17~92*$^{fl/fl}$ mice that had been on diet for 5 weeks. Cells were incubated in absence (A) or presence (B) L-tryptophan for five days. Bars represent mean ± SEM (n=3; *p≤0.05).

Less Tregs were induced by DCs from *Ldlr*$^{-/-}$ *miR-17~92*$^{\Delta/\Delta}$ mice compared to DCs from control mice. However, this difference was not significant. Interestingly, adjusting L Tryptophan concentration to 500 mM, the difference became more pronounced and DCs from *Ldlr*$^{-/-}$ *miR-17~92*$^{\Delta/\Delta}$ mice induced significantly less regulatory T cells. These findings indicate a function of the *miR-17~92* cluster in the L-tryptophan metabolism and its role in regulatory T cell induction.

5 Discussion

The aortic DC compartment of healthy and atherosclerotic mice was explored and a systemic analysis was performed. Primary work by Choi et al. regarding the characterization of aortic DCs was further refined and extended. A new gating strategy for aortic DCs is presented and a previously unrecognized DC subset was discovered.

Furthermore, an atheroprotective role for miRNA cluster *miR-17~92* was defined. While Treg levels in *miR-17~92*$^{\Delta/\Delta}$ mice were not altered when compared to *miR-17~92*$^{fl/fl}$ control mice, *Ldlr*$^{-/-}$ *miR-17~92*$^{\Delta/\Delta}$ mice displayed a significant reduction in spleen and peripheral lymph nodes, accompanied by a significant increase in plaque size. *Socs3* was identified to be targeted by *miR-17~92* cluster members *miR-20a* and *miR-19a* and an integrative model is suggested.

5.1 Aortic Dendritic Cell Subsets in Healthy and Atherosclerotic Mice

Single cell suspensions from enzymatically digested aortae including the aortic root were analyzed in flow cytometry. After segregation of CD11c^{-}MHCII^{+} cells that were postulated to be macrophages (Choi et al., 2011), CD11c^{+}MHCII^{+} DCs were distinguished into a discrete CD103^{+} population, and CD103^{-} DC subset. The latter could be further subdivided into CD11b^{-}F4/80^{+} and CD11b^{+}F4/80^{+} DCs, in line with previous findings (Choi et al., 2011). Furthermore, a previously unrecognized CD11b^{-}F4/80^{-} DC subset was described. This aortic DC subset was independent of atherosclerotic lesion formation and present in healthy and diseased aortae of B6 and *Ldlr*$^{-/-}$ mice. The subset of CD11b^{-}F4/80^{-} DC stained negative for CD3, CD19, CD103, NK1.1, F4/80, CD11b and CD64, however, it was partially SIRPα^{+} and requires further characterization in future studies.

The role of SIRPα in DCs is poorly understood; however, a function in autoimmunity, migration and the interaction with T cells has been reported

(Matozaki et al., 2009b). Binding of SIRPα to its ligand CD47 on T cells has been demonstrated to induce T cell proliferation and activate cytotoxic T cells (Seiffert et al., 2001). Therefore, SIRPα$^+$ DCs could contribute to disease aggravation. This notion is underlined by the fact that SIRPα has been demonstrated to contribute to autoimmune diseases like experimental autoimmune encephalomyelitis (EAE), collagen induced arthritis and 2,4-dinitro-1-fluorobenzene (DNFB)-induced contact hypersensitivity (Motegi et al., 2008; Okuzawa et al., 2008; Tomizawa et al., 2007). However, further studies are required to investigate a subset specific role of SIRPα$^+$ DCs.

Less DCs than macrophages could be detected in healthy vessels. Previous reports suggested vascular DCs to originate from circulating monocytes (Jongstra-Bilen et al., 2006), however, subset-specific analysis of the origin of aortic DCs has not been attempted. One of the first studies addressing this question was provided by Choi et al. They demonstrated that the subset of CD11b$^+$F4/80$^+$ DCs, similar to macrophages, strongly depends on M-CSF and expresses CX3CR1 and CD14 in healthy mice. This is consistent with a potential monocytic origin. In their study, only CD103$^+$ DCs were identified as true DCs fully depending on FLT3-signaling for their accumulation in the aorta (Choi et al., 2011). In line with these findings, macrophages and the subset of CD11b$^+$F4/80$^+$ DCs were not affected in *Flt3l*$^{-/-}$ mice in the presented work.

Nevertheless it was possible to demonstrate for the first time that both CD103$^+$ and CD11b$^+$F4/80$^-$ DCs were FLT3L-dependent and lacked expression of CD64 under non-inflammatory conditions. CD64 is a marker associated with monocyte-derived DCs (Langlet et al., 2012). Therefore, aortic CD103$^+$ and CD11b$^+$F4/80$^-$ DC subsets belong to conventional rather than monocyte-derived DCs. This indicates that they arise from a designated DC precursor in the aorta under physiological conditions and is further supported by the reduction of both CD103$^+$ and CD11b$^+$ DCs in Flt3 and Flt3l-deficient mice in other non-lymphoid tissues (Bogunovic et al., 2009; Ginhoux et al., 2009). CDPs and preDCs, both FLT3 dependent, have been demonstrated to differentiate into both CD103$^+$ and CD11b$^+$ cDCs in the liver and kidney (Ginhoux et al., 2009) and FLT3L is well

known to drive the differentiation of DC progenitors (Belz and Nutt, 2012; Hashimoto et al., 2011).

In contrast to physiological conditions, $CD64^+$ $CD11b^+F4/80^-$ and $CD64^+$ $CD11b^+F4/80^+$ DCs emerge under inflammatory pro-atherogenic conditions, indicating that these subsets may at least in part be derived from immigrating monocytes. However, monocytes can lose expression of typical monocyte markers such as CD14 and CD64 and acquire a DC-like phenotype by expression of typical DC markers like CD80, CD86 or HLA-DR (Randolph et al., 1998). Therefore, CD64 might still not be an unambiguous marker to discriminate between monocyte-derived and conventional DCs.
All DC subsets increased with atherosclerosis and continued diet, except for the $CD11b^-F4/80^-$ DC subset, finally yielding higher numbers of $CD11c^+$ DCs than macrophages. Given that $CD11c^+MHCII^+CD11b^+F4/80^+$ DCs represent the largest DC subpopulation, and that macrophages can express CD11c under inflammatory conditions (Ley et al., 2011), it remains to be defined whether a discrimination between DCs and macrophages is valid.

Because of these overlapping and ambiguous markers, further functional characterizations of the capacity of aortic $CD11c^+$ and $CD11c^-$ cells and of distinct DC subsets (with regard to migration, phagocytosis and immune priming) are required. These studies, in combination with studies on transcriptional programing in myeloid cells, will help answering the arising questions concerning the overlapping phenotype and functions of conventional DCs, monocyte-derived DCs and macrophages. Recently, studies have been published trying to establish the transcriptional network in myeloid cells (Elpek et al., 2011; Gautier et al., 2012; Heng et al., 2008; Miller et al., 2012). Furthermore, a new transcription factor has been proposed to clearly distinguish monocytes from DCs. Transcription factor *Zbtb64* seems to be expressed only in cDCs but not in monocytes, macrophages, B or T cells (Meredith et al., 2012; Satpathy et al., 2012a). However, in all these studies classical markers like CD11c, CD11b or F4/80 are used to discriminate between the different DC subsets that are investigated. Although there is some consensus on markers associated with them, the use of markers varies from study to study and

complicates the integration into a unifying model. Nonetheless, these studies will help to understand the origin of DCs in the long run, but in order to gain a complete picture, different organs have to be described thoroughly in the first place. A first step to describe the aortic DC compartment in healthy and atherosclerotic conditions is provided with the data of this thesis. The data presented in this study enhances the knowledge about the presence of distinct DC subsets and their accumulation in atherosclerosis. With this description of the aortic DC subsets and their phenotype, a subsequent characterization with respect to functions and transcriptional programming is possible. This systematic survey of their phenotype and FLT3L requirements is one step to shed light on this complex cellular network.

5.2 The Role of the miR-17~92 Cluster in Dendritic Cells

Mice harboring the *Cd11c*-specific *miR-17~92* deficiency were investigated in physiological as well as in pro-atherogenic conditions. As expected, these mice did not show any gross abnormalities. Interestingly, they displayed only few differences to control mice when characterizing the immunological status of DCs and T cells in peripheral lymph nodes, spleen and blood under physiological conditions. Lymphatic organs did not display significant alterations in size and DC development did not seem to be impaired. PreDC frequencies in the bone marrow were not altered and DC frequencies in spleen and peripheral lymph nodes remained unchanged, as well. The subset distribution was normal and expression of co-stimulatory molecules CD40 and CD86 was not altered under physiological conditions either. Furthermore the aorta demonstrated a normal compartment of vascular DCs. Thus, there was no evidence for a role of the microRNA cluster *miR-17~92* in the context of DC differentiation from preDCs.

DCs are characterized by their ability to stimulate T cells, hence, T cells were also included into analysis. The DC phenotype did not show any alterations under physiological conditions. In line, there was no indication for an altered T

cell phenotype as an indirect result of the DC-specific deletion or *miR-17~92,* except for the increase in naïve CD4 T cells in peripheral lymph nodes. While experiments with blood showed the opposite result, T cells in the spleen remained unchanged. Notably, there was no difference in Treg frequencies. A lack of a T cell phenotype indicates that the interaction with T cells is not affected under physiological conditions.

Although the role of *miR-17~92* in DCs has not been characterized, it is known that GM-CSF-derived DCs express only low levels of *miR-17~92* in steady-state (Kuipers et al., 2010) and that *miR-17~92* levels increase under the influence of inflammatory stimuli, such as IL-6 (Brock et al., 2009). Therefore, lack of significant changes in *miR-17~92*-deficient mice under physiological conditions is not surprising. In line with this notion, *Ldlr*$^{-/-}$ mice with *Cd11c*-specific deletion of the miRNA cluster *miR-17~92* displayed changes in their immunological status when they were fed a high fat diet, resulting in the induction of pro-inflammatory conditions. While lymphatic tissues where not altered in size, *Ldlr*$^{-/-}$ *miR-17~92*$^{\Delta/\Delta}$ mice suffered from increased plaque size compared to controls after five weeks of high fat diet feeding. Both lesion burden in the aortic root as wells as the aorta were increased. The *miR-17~92* cluster has not been characterized in DCs and leaving the question unanswered, whether it can be considered pro- or anti-inflammatory. However, the findings presented in this thesis demonstrate for the first time, that the loss of miRNA cluster *miR-17~92* in DCs results in a pro-inflammatory response and that the cluster therefore can be considered to confer anti-inflammatory properties.

Interestingly, the lymphatic DC compartment and bone marrow-borne preDCs did not display any significant alterations in DC or preDC frequency or subset distribution. This indicates that *miR-17~92* deletion does not result in impaired DC development of differentiation. It rather seems to cause functional alterations. Since T cell priming is a key characteristic feature of DCs, it is not surprising to see alterations in the T cell compartment. The frequency of naïve CD4 T cells is increased and more importantly, the fraction of regulatory T cells is dramatically diminished in lymphatic tissues. Although effector cells are less abundant, the loss in Tregs clearly explains the increased plaque size. Other

studies have demonstrated that a reduction in Tregs is associated with an increase in plaque burden (Ait-Oufella et al., 2006). In line with these findings adoptive transfer of Tregs can reduce lesion size (Mor et al., 2007). Furthermore, the number of aortic Tregs trends towards a reduction in *Ldlr*$^{-/-}$ *miR-17~92*$^{\Delta/\Delta}$ mice, although not significantly. This finding is also in line with the literature as Choi et al. found that a reduction of Treg frequencies in lymphatic tissue and within the aorta results in increased lesion size (Choi et al., 2011). These studies corroborate the increase in lesion area to be a direct result of the impaired induction of Tregs.

Importantly, *miR-17~92* seems to exert its functions only under inflammatory conditions. The transfer of naïve CD45.1^{+} CD4 T cells did not result in different ratios of Treg conversion within the transferred cells when healthy *miR-17~92*$^{\Delta/\Delta}$ and *miR-17~92*$^{fl/fl}$ mice where compared. Only under pro-atherogenic conditions *Ldlr*$^{-/-}$ *miR-17~92*$^{\Delta/\Delta}$ where impaired in inducing Tregs. This clearly supports the assumption that the cluster is predominantly relevant in inflammation. In conjunction with its anti-inflammatory role it is conceivable that the microRNA cluster *miR-17~92* is part of a negative regulation loop to limit inflammatory responses. Furthermore, the adoptive transfer experiment demonstrates that peripheral Treg induction instead of thymic Treg formation is impaired in mice deficient in the *miR-17~92* cluster. The inability of *miR-17~92*-deficient DCs to induce Tregs is also supported by *in vitro* data from Treg conversion assays: In line with the unaltered total T cell frequencies in *Ldlr*$^{-/-}$ *miR-17~92*$^{\Delta/\Delta}$ mice, bone marrow-derived *miR-17~92*$^{\Delta/\Delta}$ DCs were capable to induce T cell proliferation *in vitro* to the same extent as controls and only the polarization towards Tregs was impaired (Figure 46).

This thesis defines an anti-inflammatory role of the microRNA cluster *miR-17~92* for the first time. It was shown that this effect is mediated by the impairment in peripheral induction of Tregs. However, the detailed mechanism behind remains in part elusive. Amongst the putative targets of *miR17~92* cluster members, *Socs3* was identified and shown to be directly targeted by *miR-20a* and *miR-19a* in luciferase assays. Despite the lack of a *miR-17~92*-mediated phenotype in non-inflammatory conditions, *miR-17~92*$^{\Delta/\Delta}$ DCs

displayed increased levels of *Socs3* mRNA in steady state. Therefore, this thesis identifies *Socs3* as a confirmed *miR-17~92* targets. Notably, the cluster is predicted to target several mRNAs of the IL-6/STAT3 pathway, for example *Il6*, *Il6r* or *gp130*. *Stat3* has also been confirmed to be regulated by members of the cluster *miR-17~92* (Brock et al., 2011; Carraro et al., 2009; Wu et al., 2013).

In DCs, the induction of Tregs can be linked to *Socs3* and a hypothesis for the mechanism behind *miR-17~92*-mediated regulation of Treg induction can be derived from the findings in this thesis. L-Tryptophan is required for the induction of naïve T cells into Tregs and its conversion into the metabolite L-Kynurenine is mediated by the enzyme indoleamine 2,3-dioxygenase. Importantly, IDO activity is regulated by SOCS3. SOCS3 possesses a SOCS box domain which participates in the formation of an E3 ubiquitin ligase complex and targets apart from several other signaling proteins also IDO for proteasomal degradation (Orabona et al., 2008). It has been shown that SOCS3-mediated IDO degradation results in decreased peripheral Treg induction (Catani et al., 2013; Munn and Mellor, 2013; Orabona et al., 2008). By combining the data from the literature with the findings from this thesis, a model is suggested (Figure 52). *MiR-17~92* cluster members *miR-20a* and *miR-19a* target *Socs3* and thus indirectly control Treg polarization by regulating IDO activity.

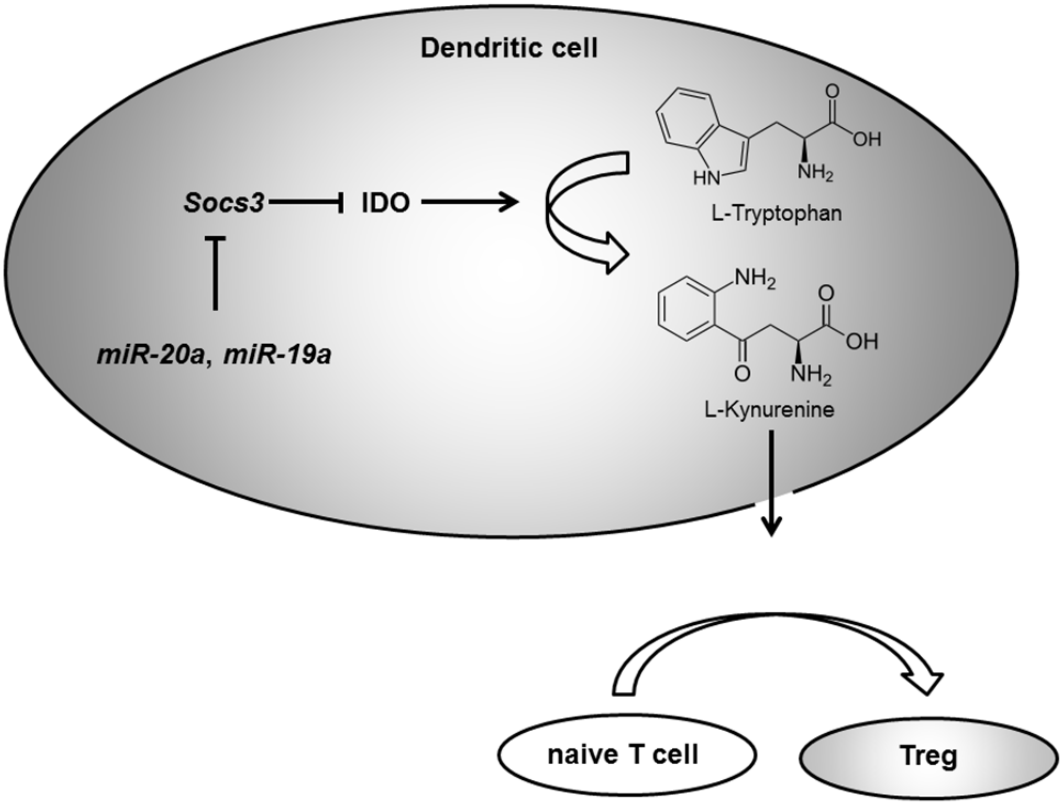

Figure 52 Model for the *miR-17~92*-mediated regulation of Treg polarization in DCs. Cluster members *miR-20a* and *miR-19a* target *Socs3* and thus indirectly control IDO activity. As result, IDO-mediated Treg polarization is under indirect control of the microRNA cluster *miR-17~92*. In *mir-17~92*-deficient DCs, increased SOCS3 levels lead to enhanced proteasomal degradation of IDO, reducing TRP conversion to KYN and therefore resulting in diminished peripheral Treg induction.

Increased SOCS3 levels in *miR-17~92*-deficient mice lead to enhanced proteasomal degradation of IDO, resulting in reduced TRP conversion and subsequently in impaired Treg conversion.

This model is supported by *in vitro* Treg conversion assays with TRP (Figure 51). In line with the literature, Treg conversion in normal culture medium results only in a modest conversion of naïve CD4 T cells to Tregs, while the frequency of Tregs in TRP-supplemented medium is increased almost fourfold. As expected from the model, inability of *miR-17~92*-deficient DCs to convert naïve T cells into Tregs is more pronounced in TRP-supplemented medium and *miR-17~92*-deficient DCs are significantly less capable of polarizing Tregs in TRP-supplemented conditions. However, this data needs further confirmation *in vivo*. Furthermore, the regulation of TRP or KYN levels, as well as the

degradation of IDO in *miR-17~92*-deficient DCs remain to be investigated to corroborate this hypothesis.

In this thesis *miR-17~92*-deficient DCs with increased *Socs3* levels are impaired to induce Tregs. However, Li et al. reported that forced expression of SOCS3 results in a tolerogenic DC phenotype (Li et al., 2006). This opposing result might be at least in part explained by the nature of microRNAs. Single miRNAs can target several mRNAs (Bushati and Cohen, 2007). Consequently, the deletion of a complete cluster of six microRNAs will affect more than one particular target. Considering that other members of the IL-6/STAT3 pathway have been predicted and confirmed to be regulated by *miR-17~92* cluster members, the result of *miR-17~92*-deficiency can be expected to be far more complex than the upregulation of a single target, namely *Socs3*. However, the net outcome of *miR-17~92*-deficiency in DCs is a reduction of Tregs.

In contrast to the proposed hypothesis that MHCII^{lo} DCs contribute to peripheral tolerance (Thomson et al., 2009), Idoyaga et al. have recently shown that MHCII^{hi} migatory DCs rather than MHCII^{lo} resident DCs are responsible for the induction of Tregs and peripheral tolerance (Idoyaga et al., 2013). Interestingly, the inability of *Ldlr*$^{-/-}$ *miR-17~92*$^{\Delta/\Delta}$ mice to induce peripheral Tregs is accompanied by an increase in migDCs. This seems to be contradictory; however, it supports the hypothesis that *miR-17~92*-deficient DCs are functionally impaired DCs and that the observed phenotype is not a result of altered differentiation or altered DC frequencies.

To obtain a DC specific deletion of the cluster, the Cre-Lox system was used and *miR-17~92*$^{fl/fl}$ mice were crossed with *Cd11c-cre* deleter mice. Although the *Cd11c*-specific deletion is accepted in the field and has been successfully used in various studies (Caton et al., 2007; Chow et al., 2011), this system is confined by the lack of specificity. Since CD11c expression, or at least *Cd11c* promoter activity, is not restricted to DCs, other studies that relied on the *Cd11c* promoter have shown that not only DCs might be targeted with this system. Using the *Cd11c-DTR* system for example, not only DCs, but also tissue-resident, marginal-zone and metallophilic macrophages, as well as NK cells,

NKT cells and some CD11c^{+} B and T cells were targeted (Satpathy et al., 2012b). To exclude off target effects, the specificity of *miR-17~92*-deletion using *Cd11c*-cre mice needs to be evaluated in cells other than DCs. There is evidence that CD8 T cells are sensitive to diphtheria toxin in *Cd11c-DTR* mice (Bennett and Clausen, 2007) and since *Cd11c-cre miR-17~92*$^{\Delta/\Delta}$ mice show a shift in the T cell compartment towards CD8 T cells, an off target effect can be inferred. This notion is further underlined by the fact that overexpression of the cluster leads to increased effector activity in CD8 T cells (Wu et al., 2012). Furthermore, *Ldlr*$^{-/-}$ *miR-17~92*$^{\Delta/\Delta}$ mice displayed a significant reduction in effector CD8 T cells of the peripheral lymph nodes (14.69±1.88 *vs.* 6.29±0.72 % CD8 T cells in *Ldlr*$^{-/-}$ *miR-17~92*$^{fl/fl}$ *vs. Ldlr*$^{-/-}$ *miR-17~92*$^{\Delta/\Delta}$ mice, P=0.0021, data not shown). However, this was not true for the spleen. To this extend, the deletion specificity has not successfully been evaluated in *Cd11c-cre miR-17~92*$^{\Delta/\Delta}$ mice. Although attempted repeatedly, the analysis was hindered by the genomic organization surrounding the cluster, complicating appropriate probe design.

Although this thesis provides data that demonstrates the impairment of *miR-17~92*-deficient DCs in the induction of Treg-mediated peripheral tolerance, the conclusion that CD11c-specific deletion of the cluster aggravates atherosclerosis has to be drawn carefully. Both blood triglyceride and cholesterol levels are significantly elevated in *Ldlr*$^{-/-}$ *miR-17~92*$^{\Delta/\Delta}$ mice and could also substantially contribute to the phenotype. The uptake of lipoproteins or cholesterol from the blood is a hallmark of aortic DCs. Accordingly, depletion of CD11c^{+} DCs two weeks after the onset of high fat diet feeding leads to increased levels of cholesterol. Conversely, an increase in DC life-span results in decreased cholesterol levels and reduced plaque burden (Gautier et al., 2009). Although *miR-17~92*$^{\Delta/\Delta}$ DCs did not show altered phagocytosis *in vitro*, *miR-17~92*-deficient DCs could be impaired in the uptake of cholesterol. This mechanism could result in elevated cholesterol levels, subsequently leading to enhanced lesion formation. Therefore, further experiments are needed to evaluate the contribution of this observation to lesion development. Both alterations in cholesterol hemostasis and impairment in the induction of peripheral tolerance could play a role in *Ldlr*$^{-/-}$ *miR-17~92*$^{\Delta/\Delta}$ mice.

In summary, the data on *miR-17~92*-deficient DCs in atherosclerosis supports an anti-inflammatory role of the cluster in DCs. For the first time, *miR-17~92*-deficient DCs are demonstrated to be impaired in the induction of peripheral tolerance and *Socs3* is demonstrated to be a target of *miR-20a* and *miR-19a*. Although some findings await further validation, this work provides new insights into the regulation of immunological tolerance and thus this new knowledge can also be applied to other (auto-inflammatory) diseases such as systemic lupus erythematosus, EAE, graft rejection or colitis.

6 References

Adams, S., Braidy, N., Bessesde, A., Brew, B.J., Grant, R., Teo, C., and Guillemin, G.J. (2012). The kynurenine pathway in brain tumor pathogenesis. Cancer research *72*, 5649-5657.

Ait-Oufella, H., Salomon, B.L., Potteaux, S., Robertson, A.K., Gourdy, P., Zoll, J., Merval, R., Esposito, B., Cohen, J.L., Fisson, S*., et al.* (2006). Natural regulatory T cells control the development of atherosclerosis in mice. Nature medicine *12*, 178-180.

Andres, V., Pello, O.M., and Silvestre-Roig, C. (2012). Macrophage proliferation and apoptosis in atherosclerosis. Current opinion in lipidology *23*, 429-438.

Angeli, V., Llodra, J., Rong, J.X., Satoh, K., Ishii, S., Shimizu, T., Fisher, E.A., and Randolph, G.J. (2004). Dyslipidemia associated with atherosclerotic disease systemically alters dendritic cell mobilization. Immunity *21*, 561-574.

Ardavin, C. (2003). Origin, precursors and differentiation of mouse dendritic cells. Nature reviews Immunology *3*, 582-590.

Azukizawa, H., Dohler, A., Kanazawa, N., Nayak, A., Lipp, M., Malissen, B., Autenrieth, I., Katayama, I., Riemann, M., Weih, F*., et al.* (2011). Steady state migratory RelB+ langerin+ dermal dendritic cells mediate peripheral induction of antigen-specific CD4+ CD25+ Foxp3+ regulatory T cells. European journal of immunology *41*, 1420-1434.

Baek, D., Villen, J., Shin, C., Camargo, F.D., Gygi, S.P., and Bartel, D.P. (2008). The impact of microRNAs on protein output. Nature *455*, 64-71.

Behm-Ansmant, I., Rehwinkel, J., Doerks, T., Stark, A., Bork, P., and Izaurralde, E. (2006). mRNA degradation by miRNAs and GW182 requires both CCR4:NOT deadenylase and DCP1:DCP2 decapping complexes. Genes & development *20*, 1885-1898.

Belkaid, Y. (2007). Regulatory T cells and infection: a dangerous necessity. Nature reviews Immunology *7*, 875-888.

Belz, G.T., and Nutt, S.L. (2012). Transcriptional programming of the dendritic cell network. Nature reviews Immunology *12*, 101-113.

Benagiano, M., Azzurri, A., Ciervo, A., Amedei, A., Tamburini, C., Ferrari, M., Telford, J.L., Baldari, C.T., Romagnani, S., Cassone, A*., et al.* (2003). T helper type 1 lymphocytes drive inflammation in human atherosclerotic lesions. Proceedings of the National Academy of Sciences of the United States of America *100*, 6658-6663.

Bennett, C.L., and Clausen, B.E. (2007). DC ablation in mice: promises, pitfalls, and challenges. Trends in immunology *28*, 525-531.

Bentzon, J.F., and Falk, E. (2010). Atherosclerotic lesions in mouse and man: is it the same disease? Current opinion in lipidology *21*, 434-440.

Betel, D., Koppal, A., Agius, P., Sander, C., and Leslie, C. (2010). Comprehensive modeling of microRNA targets predicts functional non-conserved and non-canonical sites. Genome biology *11*, R90.

Bobryshev, Y.V. (2010). Dendritic cells and their role in atherogenesis. Laboratory investigation; a journal of technical methods and pathology *90*, 970-984.

Bogunovic, M., Ginhoux, F., Helft, J., Shang, L., Hashimoto, D., Greter, M., Liu, K., Jakubzick, C., Ingersoll, M.A., Leboeuf, M.*, et al.* (2009). Origin of the lamina propria dendritic cell network. Immunity *31*, 513-525.

Boldin, M.P., Taganov, K.D., Rao, D.S., Yang, L., Zhao, J.L., Kalwani, M., Garcia-Flores, Y., Luong, M., Devrekanli, A., Xu, J.*, et al.* (2011). miR-146a is a significant brake on autoimmunity, myeloproliferation, and cancer in mice. The Journal of experimental medicine *208*, 1189-1201.

Brasel, K., De Smedt, T., Smith, J.L., and Maliszewski, C.R. (2000). Generation of murine dendritic cells from flt3-ligand-supplemented bone marrow cultures. Blood *96*, 3029-3039.

Brock, M., Trenkmann, M., Gay, R.E., Gay, S., Speich, R., and Huber, L.C. (2011). MicroRNA-18a enhances the interleukin-6-mediated production of the acute-phase proteins fibrinogen and haptoglobin in human hepatocytes. The Journal of biological chemistry *286*, 40142-40150.

Brock, M., Trenkmann, M., Gay, R.E., Michel, B.A., Gay, S., Fischler, M., Ulrich, S., Speich, R., and Huber, L.C. (2009). Interleukin-6 modulates the expression of the bone morphogenic protein receptor type II through a novel STAT3-microRNA cluster 17/92 pathway. Circulation research *104*, 1184-1191.

Buono, C., Binder, C.J., Stavrakis, G., Witztum, J.L., Glimcher, L.H., and Lichtman, A.H. (2005). T-bet deficiency reduces atherosclerosis and alters plaque antigen-specific immune responses. Proceedings of the National Academy of Sciences of the United States of America *102*, 1596-1601.

Buono, C., Come, C.E., Stavrakis, G., Maguire, G.F., Connelly, P.W., and Lichtman, A.H. (2003). Influence of interferon-gamma on the extent and phenotype of diet-induced atherosclerosis in the LDLR-deficient mouse. Arteriosclerosis, thrombosis, and vascular biology *23*, 454-460.

Busch, M., and Zernecke, A. (2012). microRNAs in the regulation of dendritic cell functions in inflammation and atherosclerosis. Journal of molecular medicine *90*, 877-885.

Bushati, N., and Cohen, S.M. (2007). microRNA functions. Annual review of cell and developmental biology *23*, 175-205.

Carraro, G., El-Hashash, A., Guidolin, D., Tiozzo, C., Turcatel, G., Young, B.M., De Langhe, S.P., Bellusci, S., Shi, W., Parnigotto, P.P.*, et al.* (2009). miR-17 family of microRNAs controls FGF10-mediated embryonic lung epithelial branching morphogenesis through MAPK14 and STAT3 regulation of E-Cadherin distribution. Developmental biology *333*, 238-250.

Catani, L., Sollazzo, D., Trabanelli, S., Curti, A., Evangelisti, C., Polverelli, N., Palandri, F., Baccarani, M., Vianelli, N., and Lemoli, R.M. (2013). Decreased expression of indoleamine 2,3-dioxygenase 1 in dendritic cells contributes to impaired regulatory T cell development in immune thrombocytopenia. Annals of hematology *92*, 67-78.

Caton, M.L., Smith-Raska, M.R., and Reizis, B. (2007). Notch-RBP-J signaling controls the homeostasis of CD8- dendritic cells in the spleen. The Journal of experimental medicine *204*, 1653-1664.

Cederbom, L., Hall, H., and Ivars, F. (2000). CD4+CD25+ regulatory T cells down-regulate co-stimulatory molecules on antigen-presenting cells. European journal of immunology *30*, 1538-1543.

Ceppi, M., Pereira, P.M., Dunand-Sauthier, I., Barras, E., Reith, W., Santos, M.A., and Pierre, P. (2009). MicroRNA-155 modulates the interleukin-1 signaling pathway in activated human monocyte-derived dendritic cells. Proceedings of the National Academy of Sciences of the United States of America *106*, 2735-2740.

Chang, T.Y., Chang, C.C., and Cheng, D. (1997). Acyl-coenzyme A:cholesterol acyltransferase. Annual review of biochemistry *66*, 613-638.

Choi, J.H., Cheong, C., Dandamudi, D.B., Park, C.G., Rodriguez, A., Mehandru, S., Velinzon, K., Jung, I.H., Yoo, J.Y., Oh, G.T.*, et al.* (2011). Flt3 signaling-dependent dendritic cells protect against atherosclerosis. Immunity *35*, 819-831.

Choi, J.H., Do, Y., Cheong, C., Koh, H., Boscardin, S.B., Oh, Y.S., Bozzacco, L., Trumpfheller, C., Park, C.G., and Steinman, R.M. (2009). Identification of antigen-presenting dendritic cells in mouse aorta and cardiac valves. The Journal of experimental medicine *206*, 497-505.

Chow, A., Brown, B.D., and Merad, M. (2011). Studying the mononuclear phagocyte system in the molecular age. Nature reviews Immunology *11*, 788-798.

D'Amico, A., and Wu, L. (2003). The early progenitors of mouse dendritic cells and plasmacytoid predendritic cells are within the bone marrow hemopoietic precursors expressing Flt3. The Journal of experimental medicine *198*, 293-303.

Dahlof, B. (2010). Cardiovascular disease risk factors: epidemiology and risk assessment. The American journal of cardiology *105*, 3A-9A.

Daro, E., Pulendran, B., Brasel, K., Teepe, M., Pettit, D., Lynch, D.H., Vremec, D., Robb, L., Shortman, K., McKenna, H.J.*, et al.* (2000). Polyethylene glycol-modified GM-CSF expands CD11b(high)CD11c(high) but notCD11b(low)CD11c(high) murine dendritic cells in vivo: a comparative analysis with Flt3 ligand. Journal of immunology *165*, 49-58.

Davenport, P., and Tipping, P.G. (2003). The role of interleukin-4 and interleukin-12 in the progression of atherosclerosis in apolipoprotein E-deficient mice. The American journal of pathology *163*, 1117-1125.

Ditiatkovski, M., Toh, B.H., and Bobik, A. (2006). GM-CSF deficiency reduces macrophage PPAR-gamma expression and aggravates atherosclerosis in ApoE-deficient mice. Arteriosclerosis, thrombosis, and vascular biology *26*, 2337-2344.

Djuranovic, S., Nahvi, A., and Green, R. (2011). A parsimonious model for gene regulation by miRNAs. Science *331*, 550-553.

Dong, C., Juedes, A.E., Temann, U.A., Shresta, S., Allison, J.P., Ruddle, N.H., and Flavell, R.A. (2001). ICOS co-stimulatory receptor is essential for T-cell activation and function. Nature *409*, 97-101.

Doring, Y., Manthey, H.D., Drechsler, M., Lievens, D., Megens, R.T., Soehnlein, O., Busch, M., Manca, M., Koenen, R.R., Pelisek, J.*, et al.* (2012). Auto-antigenic protein-DNA complexes stimulate plasmacytoid dendritic cells to promote atherosclerosis. Circulation *125*, 1673-1683.

Doring, Y., and Zernecke, A. (2012). Plasmacytoid dendritic cells in atherosclerosis. Frontiers in physiology *3*, 230.

Du, T., and Zamore, P.D. (2005). microPrimer: the biogenesis and function of microRNA. Development *132*, 4645-4652.

Dunand-Sauthier, I., Santiago-Raber, M.L., Capponi, L., Vejnar, C.E., Schaad, O., Irla, M., Seguin-Estevez, Q., Descombes, P., Zdobnov, E.M., Acha-Orbea, H.*, et al.* (2011). Silencing of c-Fos expression by microRNA-155 is critical for dendritic cell maturation and function. Blood *117*, 4490-4500.

El Gazzar, M., Church, A., Liu, T., and McCall, C.E. (2011). MicroRNA-146a regulates both transcription silencing and translation disruption of TNF-alpha during TLR4-induced gene reprogramming. Journal of leukocyte biology *90*, 509-519.

El Gazzar, M., and McCall, C.E. (2012). MicroRNAs regulatory networks in myeloid lineage development and differentiation: regulators of the regulators. Immunology and cell biology *90*, 587-593.

Elhage, R., Jawien, J., Rudling, M., Ljunggren, H.G., Takeda, K., Akira, S., Bayard, F., and Hansson, G.K. (2003). Reduced atherosclerosis in interleukin-18 deficient apolipoprotein E-knockout mice. Cardiovascular research *59*, 234-240.

Elpek, K.G., Bellemare-Pelletier, A., Malhotra, D., Reynoso, E.D., Lukacs-Kornek, V., DeKruyff, R.H., and Turley, S.J. (2011). Lymphoid organ-resident dendritic cells exhibit unique transcriptional fingerprints based on subset and site. PloS one *6*, e23921.

Fallarino, F., Grohmann, U., Hwang, K.W., Orabona, C., Vacca, C., Bianchi, R., Belladonna, M.L., Fioretti, M.C., Alegre, M.L., and Puccetti, P. (2003). Modulation of tryptophan catabolism by regulatory T cells. Nature immunology *4*, 1206-1212.

Filipowicz, W., Bhattacharyya, S.N., and Sonenberg, N. (2008). Mechanisms of post-transcriptional regulation by microRNAs: are the answers in sight? Nature reviews Genetics *9*, 102-114.

Galkina, E., Kadl, A., Sanders, J., Varughese, D., Sarembock, I.J., and Ley, K. (2006). Lymphocyte recruitment into the aortic wall before and during development of atherosclerosis is partially L-selectin dependent. The Journal of experimental medicine *203*, 1273-1282.

Gautier, E.L., Huby, T., Saint-Charles, F., Ouzilleau, B., Pirault, J., Deswaerte, V., Ginhoux, F., Miller, E.R., Witztum, J.L., Chapman, M.J.*, et al.* (2009). Conventional dendritic cells at the crossroads between immunity and cholesterol homeostasis in atherosclerosis. Circulation *119*, 2367-2375.

Gautier, E.L., Shay, T., Miller, J., Greter, M., Jakubzick, C., Ivanov, S., Helft, J., Chow, A., Elpek, K.G., Gordonov, S.*, et al.* (2012). Gene-expression profiles and transcriptional regulatory pathways that underlie the identity and diversity of mouse tissue macrophages. Nature immunology *13*, 1118-1128.

Geissmann, F., Jung, S., and Littman, D.R. (2003). Blood monocytes consist of two principal subsets with distinct migratory properties. Immunity *19*, 71-82.

Getz, G.S., and Reardon, C.A. (2012). Animal models of atherosclerosis. Arteriosclerosis, thrombosis, and vascular biology *32*, 1104-1115.

Ghani, S., Riemke, P., Schonheit, J., Lenze, D., Stumm, J., Hoogenkamp, M., Lagendijk, A., Heinz, S., Bonifer, C., Bakkers, J.*, et al.* (2011). Macrophage development from HSCs requires PU.1-coordinated microRNA expression. Blood *118*, 2275-2284.

Ginhoux, F., Liu, K., Helft, J., Bogunovic, M., Greter, M., Hashimoto, D., Price, J., Yin, N., Bromberg, J., Lira, S.A.*, et al.* (2009). The origin and development of nonlymphoid tissue CD103+ DCs. The Journal of experimental medicine *206*, 3115-3130.

Giraldez, A.J., Mishima, Y., Rihel, J., Grocock, R.J., Van Dongen, S., Inoue, K., Enright, A.J., and Schier, A.F. (2006). Zebrafish MiR-430 promotes deadenylation and clearance of maternal mRNAs. Science *312*, 75-79.

Gostner, P., Pernter, P., Bonatti, G., Graefen, A., and Zink, A.R. (2011). New radiological insights into the life and death of the Tyrolean Iceman. J Archaeol Sci *38*, 3425-3431.

Gotsman, I., Grabie, N., Gupta, R., Dacosta, R., MacConmara, M., Lederer, J., Sukhova, G., Witztum, J.L., Sharpe, A.H., and Lichtman, A.H. (2006). Impaired regulatory T-cell response and enhanced atherosclerosis in the absence of inducible costimulatory molecule. Circulation *114*, 2047-2055.

Greenwald, R.J., Freeman, G.J., and Sharpe, A.H. (2005). The B7 family revisited. Annual review of immunology *23*, 515-548.

Grohmann, U., Bianchi, R., Belladonna, M.L., Silla, S., Fallarino, F., Fioretti, M.C., and Puccetti, P. (2000). IFN-gamma inhibits presentation of a tumor/self peptide by CD8 alpha- dendritic cells via potentiation of the CD8 alpha+ subset. Journal of immunology *165*, 1357-1363.

Grohmann, U., Orabona, C., Fallarino, F., Vacca, C., Calcinaro, F., Falorni, A., Candeloro, P., Belladonna, M.L., Bianchi, R., Fioretti, M.C.*, et al.* (2002). CTLA-4-Ig regulates tryptophan catabolism in vivo. Nature immunology *3*, 1097-1101.

Gupta, S., Pablo, A.M., Jiang, X., Wang, N., Tall, A.R., and Schindler, C. (1997). IFN-gamma potentiates atherosclerosis in ApoE knock-out mice. The Journal of clinical investigation *99*, 2752-2761.

Gurtner, G.J., Newberry, R.D., Schloemann, S.R., McDonald, K.G., and Stenson, W.F. (2003). Inhibition of indoleamine 2,3-dioxygenase augments trinitrobenzene sulfonic acid colitis in mice. Gastroenterology *125*, 1762-1773.

Hamilton, J.A. (2008). Colony-stimulating factors in inflammation and autoimmunity. Nature reviews Immunology *8*, 533-544.

Hansson, G.K. (2005). Inflammation, atherosclerosis, and coronary artery disease. The New England journal of medicine *352*, 1685-1695.

Hansson, G.K., and Hermansson, A. (2011). The immune system in atherosclerosis. Nature immunology *12*, 204-212.

Hansson, G.K., Robertson, A.K., and Soderberg-Naucler, C. (2006). Inflammation and atherosclerosis. Annual review of pathology *1*, 297-329.

Hashimi, S.T., Fulcher, J.A., Chang, M.H., Gov, L., Wang, S., and Lee, B. (2009). MicroRNA profiling identifies miR-34a and miR-21 and their target genes JAG1 and WNT1 in the coordinate regulation of dendritic cell differentiation. Blood *114*, 404-414.

Hashimoto, D., Miller, J., and Merad, M. (2011). Dendritic cell and macrophage heterogeneity in vivo. Immunity *35*, 323-335.

He, X., Yan, Y.L., Eberhart, J.K., Herpin, A., Wagner, T.U., Schartl, M., and Postlethwait, J.H. (2011). miR-196 regulates axial patterning and pectoral appendage initiation. Developmental biology *357*, 463-477.

Heng, T.S., Painter, M.W., and Immunological Genome Project, C. (2008). The Immunological Genome Project: networks of gene expression in immune cells. Nature immunology *9*, 1091-1094.

Herman, A.E., Freeman, G.J., Mathis, D., and Benoist, C. (2004). CD4+CD25+ T regulatory cells dependent on ICOS promote regulation of effector cells in the prediabetic lesion. The Journal of experimental medicine *199*, 1479-1489.

Huntzinger, E., and Izaurralde, E. (2011). Gene silencing by microRNAs: contributions of translational repression and mRNA decay. Nature reviews Genetics *12*, 99-110.

Idoyaga, J., Fiorese, C., Zbytnuik, L., Lubkin, A., Miller, J., Malissen, B., Mucida, D., Merad, M., and Steinman, R.M. (2013). Specialized role of migratory dendritic cells in peripheral tolerance induction. The Journal of clinical investigation.

James, V., Zhang, Y., Foxler, D.E., de Moor, C.H., Kong, Y.W., Webb, T.M., Self, T.J., Feng, Y., Lagos, D., Chu, C.Y.*, et al.* (2010). LIM-domain proteins, LIMD1, Ajuba, and WTIP are required for microRNA-mediated gene silencing. Proceedings of the National Academy of Sciences of the United States of America *107*, 12499-12504.

Jiang, L., Huang, Q., Chang, J., Wang, E., and Qiu, X. (2011a). MicroRNA HSA-miR-125a-5p induces apoptosis by activating p53 in lung cancer cells. Experimental lung research *37*, 387-398.

Jiang, S., Li, C., Olive, V., Lykken, E., Feng, F., Sevilla, J., Wan, Y., He, L., and Li, Q.J. (2011b). Molecular dissection of the miR-17-92 cluster's critical dual roles in promoting Th1 responses and preventing inducible Treg differentiation. Blood *118*, 5487-5497.

Jongstra-Bilen, J., Haidari, M., Zhu, S.N., Chen, M., Guha, D., and Cybulsky, M.I. (2006). Low-grade chronic inflammation in regions of the normal mouse arterial intima predisposed to atherosclerosis. The Journal of experimental medicine *203*, 2073-2083.

Jurkin, J., Schichl, Y.M., Koeffel, R., Bauer, T., Richter, S., Konradi, S., Gesslbauer, B., and Strobl, H. (2010). miR-146a is differentially expressed by myeloid dendritic cell subsets and desensitizes cells to TLR2-dependent activation. Journal of immunology *184*, 4955-4965.

Karsunky, H., Merad, M., Cozzio, A., Weissman, I.L., and Manz, M.G. (2003). Flt3 ligand regulates dendritic cell development from Flt3+ lymphoid and myeloid-committed progenitors to Flt3+ dendritic cells in vivo. The Journal of experimental medicine *198*, 305-313.

Katz, J.B., Muller, A.J., and Prendergast, G.C. (2008). Indoleamine 2,3-dioxygenase in T-cell tolerance and tumoral immune escape. Immunological reviews *222*, 206-221.

Kawahara, I., Kitagawa, N., Tsutsumi, K., Nagata, I., Hayashi, T., and Koji, T. (2007). The expression of vascular dendritic cells in human atherosclerotic carotid plaques. Human pathology *38*, 1378-1385.

Kingston, D., Schmid, M.A., Onai, N., Obata-Onai, A., Baumjohann, D., and Manz, M.G. (2009). The concerted action of GM-CSF and Flt3-ligand on in vivo dendritic cell homeostasis. Blood *114*, 835-843.

Kohyama, M., Sugahara, D., Sugiyama, S., Yagita, H., Okumura, K., and Hozumi, N. (2004). Inducible costimulator-dependent IL-10 production by regulatory T cells specific for self-antigen. Proceedings of the National Academy of Sciences of the United States of America *101*, 4192-4197.

Kruth, H.S., Jones, N.L., Huang, W., Zhao, B., Ishii, I., Chang, J., Combs, C.A., Malide, D., and Zhang, W.Y. (2005). Macropinocytosis is the endocytic pathway that mediates macrophage foam cell formation with native low density lipoprotein. The Journal of biological chemistry *280*, 2352-2360.

Kuipers, H., Schnorfeil, F.M., and Brocker, T. (2010). Differentially expressed microRNAs regulate plasmacytoid vs. conventional dendritic cell development. Molecular immunology *48*, 333-340.

Langlet, C., Tamoutounour, S., Henri, S., Luche, H., Ardouin, L., Gregoire, C., Malissen, B., and Guilliams, M. (2012). CD64 expression distinguishes monocyte-derived and conventional dendritic cells and reveals their distinct role during intramuscular immunization. Journal of immunology *188*, 1751-1760.

Lanzavecchia, A., and Sallusto, F. (2011). Ralph M. Steinman 1943-2011. Cell *147*, 1216-1217.

Laurat, E., Poirier, B., Tupin, E., Caligiuri, G., Hansson, G.K., Bariety, J., and Nicoletti, A. (2001). In vivo downregulation of T helper cell 1 immune responses reduces atherogenesis in apolipoprotein E-knockout mice. Circulation *104*, 197-202.

Ley, K., Miller, Y.I., and Hedrick, C.C. (2011). Monocyte and macrophage dynamics during atherogenesis. Arteriosclerosis, thrombosis, and vascular biology *31*, 1506-1516.

Li, Y., Chu, N., Rostami, A., and Zhang, G.X. (2006). Dendritic cells transduced with SOCS-3 exhibit a tolerogenic/DC2 phenotype that directs type 2 Th cell differentiation in vitro and in vivo. Journal of immunology *177*, 1679-1688.

Libby, P. (2002). Inflammation in atherosclerosis. Nature *420*, 868-874.

Liu, K., and Nussenzweig, M.C. (2010). Origin and development of dendritic cells. Immunological reviews *234*, 45-54.

Liu, K., Victora, G.D., Schwickert, T.A., Guermonprez, P., Meredith, M.M., Yao, K., Chu, F.F., Randolph, G.J., Rudensky, A.Y., and Nussenzweig, M. (2009). In vivo analysis of dendritic cell development and homeostasis. Science *324*, 392-397.

Liu, P., Yu, Y.R., Spencer, J.A., Johnson, A.E., Vallanat, C.T., Fong, A.M., Patterson, C., and Patel, D.D. (2008). CX3CR1 deficiency impairs dendritic cell accumulation in arterial intima and reduces atherosclerotic burden. Arteriosclerosis, thrombosis, and vascular biology *28*, 243-250.

Livak, K.J., and Schmittgen, T.D. (2001). Analysis of relative gene expression data using real-time quantitative PCR and the 2(-Delta Delta C(T)) Method. Methods *25*, 402-408.

Lloyd-Jones, D.M. (2010). Cardiovascular risk prediction: basic concepts, current status, and future directions. Circulation *121*, 1768-1777.

Lu, C., Huang, X., Zhang, X., Roensch, K., Cao, Q., Nakayama, K.I., Blazar, B.R., Zeng, Y., and Zhou, X. (2011). miR-221 and miR-155 regulate human dendritic cell development, apoptosis, and IL-12 production through targeting of p27kip1, KPC1, and SOCS-1. Blood *117*, 4293-4303.

Lykken, E.A., and Li, Q.J. (2011). microRNAs at the regulatory frontier: an investigation into how microRNAs impact the development and effector functions of CD4 T cells. Immunologic research *49*, 87-96.

Maganto-Garcia, E., Tarrio, M., and Lichtman, A.H. (2012). Mouse models of atherosclerosis. Current protocols in immunology / edited by John E Coligan [et al] *Chapter 15*, Unit 15 24 11-23.

Mallat, Z., Ait-Oufella, H., and Tedgui, A. (2007). Regulatory T-cell immunity in atherosclerosis. Trends in cardiovascular medicine *17*, 113-118.

Manthey, H.D., and Zernecke, A. (2011). Dendritic cells in atherosclerosis: functions in immune regulation and beyond. Thrombosis and haemostasis *106*, 772-778.

Martinez-Nunez, R.T., Louafi, F., Friedmann, P.S., and Sanchez-Elsner, T. (2009). MicroRNA-155 modulates the pathogen binding ability of dendritic cells (DCs) by down-regulation of DC-specific intercellular adhesion molecule-3 grabbing non-integrin (DC-SIGN). The Journal of biological chemistry *284*, 16334-16342.

Masaki, S., Ohtsuka, R., Abe, Y., Muta, K., and Umemura, T. (2007). Expression patterns of microRNAs 155 and 451 during normal human erythropoiesis. Biochemical and biophysical research communications *364*, 509-514.

Matozaki, T., Murata, Y., Okazawa, H., and Ohnishi, H. (2009a). Functions and molecular mechanisms of the CD47-SIRPalpha signalling pathway. Trends in cell biology *19*, 72-80.

Matozaki, T., Murata, Y., Okazawa, H., and Ohnishi, H. (2009b). Functions and molecular mechanisms of the CD47-SIRPalpha signalling pathway. Trends Cell Biol *19*, 72-80.

McKenna, H.J., Stocking, K.L., Miller, R.E., Brasel, K., De Smedt, T., Maraskovsky, E., Maliszewski, C.R., Lynch, D.H., Smith, J., Pulendran, B*., et al.* (2000). Mice lacking flt3 ligand have deficient hematopoiesis affecting hematopoietic progenitor cells, dendritic cells, and natural killer cells. Blood *95*, 3489-3497.

Meenhuis, A., van Veelen, P.A., de Looper, H., van Boxtel, N., van den Berge, I.J., Sun, S.M., Taskesen, E., Stern, P., de Ru, A.H., van Adrichem, A.J*., et al.* (2011). MiR-17/20/93/106 promote hematopoietic cell expansion by targeting sequestosome 1-regulated pathways in mice. Blood *118*, 916-925.

Mellor, A.L., and Munn, D.H. (2004). IDO expression by dendritic cells: tolerance and tryptophan catabolism. Nature reviews Immunology *4*, 762-774.

Meredith, M.M., Liu, K., Darrasse-Jeze, G., Kamphorst, A.O., Schreiber, H.A., Guermonprez, P., Idoyaga, J., Cheong, C., Yao, K.H., Niec, R.E*., et al.* (2012). Expression of the zinc finger transcription factor zDC (Zbtb46, Btbd4) defines the classical dendritic cell lineage. The Journal of experimental medicine *209*, 1153-1165.

Mestas, J., and Ley, K. (2008). Monocyte-endothelial cell interactions in the development of atherosclerosis. Trends in cardiovascular medicine *18*, 228-232.

Miki, T., Sun, H., Lee, Y., Tandin, A., Kovscek, A.M., Subbotin, V., Fung, J.J., and Valdivia, L.A. (2001). Blockade of tryptophan catabolism prevents spontaneous tolerogenicity of liver allografts. Transplantation proceedings *33*, 129-130.

Miller, J.C., Brown, B.D., Shay, T., Gautier, E.L., Jojic, V., Cohain, A., Pandey, G., Leboeuf, M., Elpek, K.G., Helft, J*., et al.* (2012). Deciphering the transcriptional network of the dendritic cell lineage. Nature immunology *13*, 888-899.

Millonig, G., Niederegger, H., Rabl, W., Hochleitner, B.W., Hoefer, D., Romani, N., and Wick, G. (2001). Network of vascular-associated dendritic cells in intima of healthy young individuals. Arteriosclerosis, thrombosis, and vascular biology *21*, 503-508.

Mittelbrunn, M., Gutierrez-Vazquez, C., Villarroya-Beltri, C., Gonzalez, S., Sanchez-Cabo, F., Gonzalez, M.A., Bernad, A., and Sanchez-Madrid, F. (2011). Unidirectional transfer of microRNA-loaded exosomes from T cells to antigen-presenting cells. Nature communications *2*, 282.

Montecalvo, A., Larregina, A.T., Shufesky, W.J., Stolz, D.B., Sullivan, M.L., Karlsson, J.M., Baty, C.J., Gibson, G.A., Erdos, G., Wang, Z*., et al.* (2012). Mechanism of transfer of functional microRNAs between mouse dendritic cells via exosomes. Blood *119*, 756-766.

Moore, K.J., Kunjathoor, V.V., Koehn, S.L., Manning, J.J., Tseng, A.A., Silver, J.M., McKee, M., and Freeman, M.W. (2005). Loss of receptor-mediated lipid uptake via scavenger receptor A or CD36 pathways does not ameliorate atherosclerosis in hyperlipidemic mice. The Journal of clinical investigation *115*, 2192-2201.

Moore, K.J., and Tabas, I. (2011). Macrophages in the pathogenesis of atherosclerosis. Cell *145*, 341-355.

Mor, A., Planer, D., Luboshits, G., Afek, A., Metzger, S., Chajek-Shaul, T., Keren, G., and George, J. (2007). Role of naturally occurring CD4+ CD25+ regulatory T cells in experimental atherosclerosis. Arteriosclerosis, thrombosis, and vascular biology *27*, 893-900.

Motegi, S., Okazawa, H., Murata, Y., Kanazawa, Y., Saito, Y., Kobayashi, H., Ohnishi, H., Oldenborg, P.A., Ishikawa, O., and Matozaki, T. (2008). Essential roles of SHPS-1 in induction of contact hypersensitivity of skin. Immunol Lett *121*, 52-60.

Munn, D.H., and Mellor, A.L. (2013). Indoleamine 2,3 dioxygenase and metabolic control of immune responses. Trends in immunology *34*, 137-143.

Murphy, W.A., Jr., Nedden Dz, D., Gostner, P., Knapp, R., Recheis, W., and Seidler, H. (2003). The iceman: discovery and imaging. Radiology *226*, 614-629.

Nahid, M.A., Satoh, M., and Chan, E.K. (2011). Mechanistic role of microRNA-146a in endotoxin-induced differential cross-regulation of TLR signaling. Journal of immunology *186*, 1723-1734.

Naik, S.H. (2008). Demystifying the development of dendritic cell subtypes, a little. Immunology and cell biology *86*, 439-452.

Naik, S.H., Proietto, A.I., Wilson, N.S., Dakic, A., Schnorrer, P., Fuchsberger, M., Lahoud, M.H., O'Keeffe, M., Shao, Q.X., Chen, W.F.*, et al.* (2005). Cutting edge: generation of splenic CD8+ and CD8- dendritic cell equivalents in Fms-like tyrosine kinase 3 ligand bone marrow cultures. Journal of immunology *174*, 6592-6597.

Napoli, C., D'Armiento, F.P., Mancini, F.P., Postiglione, A., Witztum, J.L., Palumbo, G., and Palinski, W. (1997). Fatty streak formation occurs in human fetal aortas and is greatly enhanced by maternal hypercholesterolemia. Intimal accumulation of low density lipoprotein and its oxidation precede monocyte recruitment into early atherosclerotic lesions. The Journal of clinical investigation *100*, 2680-2690.

Nielsen, C.B., Shomron, N., Sandberg, R., Hornstein, E., Kitzman, J., and Burge, C.B. (2007). Determinants of targeting by endogenous and exogenous microRNAs and siRNAs. Rna *13*, 1894-1910.

Niessner, A., and Weyand, C.M. (2010). Dendritic cells in atherosclerotic disease. Clinical immunology *134*, 25-32.

O'Connell, R.M., Chaudhuri, A.A., Rao, D.S., and Baltimore, D. (2009). Inositol phosphatase SHIP1 is a primary target of miR-155. Proceedings of the National Academy of Sciences of the United States of America *106*, 7113-7118.

O'Connell, R.M., Kahn, D., Gibson, W.S., Round, J.L., Scholz, R.L., Chaudhuri, A.A., Kahn, M.E., Rao, D.S., and Baltimore, D. (2010). MicroRNA-155 promotes autoimmune inflammation by enhancing inflammatory T cell development. Immunity *33*, 607-619.

Okuzawa, C., Kaneko, Y., Murata, Y., Miyake, A., Saito, Y., Okajo, J., Tomizawa, T., Okazawa, H., Ohnishi, H., Matozaki, T.*, et al.* (2008). Resistance to collagen-induced arthritis in SHPS-1 mutant mice. Biochem Biophys Res Commun *371*, 561-566.

Olive, V., Jiang, I., and He, L. (2010). mir-17-92, a cluster of miRNAs in the midst of the cancer network. The international journal of biochemistry & cell biology *42*, 1348-1354.

Onai, N., Obata-Onai, A., Schmid, M.A., Ohteki, T., Jarrossay, D., and Manz, M.G. (2007). Identification of clonogenic common Flt3+M-CSFR+ plasmacytoid and conventional dendritic cell progenitors in mouse bone marrow. Nature immunology *8*, 1207-1216.

Orabona, C., Pallotta, M.T., Volpi, C., Fallarino, F., Vacca, C., Bianchi, R., Belladonna, M.L., Fioretti, M.C., Grohmann, U., and Puccetti, P. (2008). SOCS3 drives proteasomal degradation of indoleamine 2,3-dioxygenase (IDO) and antagonizes IDO-dependent tolerogenesis. Proceedings of the National Academy of Sciences of the United States of America *105*, 20828-20833.

Packard, R.R., Maganto-Garcia, E., Gotsman, I., Tabas, I., Libby, P., and Lichtman, A.H. (2008). CD11c(+) dendritic cells maintain antigen processing, presentation capabilities, and CD4(+) T-

cell priming efficacy under hypercholesterolemic conditions associated with atherosclerosis. Circulation research *103*, 965-973.

Paul, W.E. (2011). Bridging innate and adaptive immunity. Cell *147*, 1212-1215.

Paulson, K.E., Zhu, S.N., Chen, M., Nurmohamed, S., Jongstra-Bilen, J., and Cybulsky, M.I. (2010). Resident intimal dendritic cells accumulate lipid and contribute to the initiation of atherosclerosis. Circulation research *106*, 383-390.

Paulsson, G., Zhou, X., Tornquist, E., and Hansson, G.K. (2000). Oligoclonal T cell expansions in atherosclerotic lesions of apolipoprotein E-deficient mice. Arteriosclerosis, thrombosis, and vascular biology *20*, 10-17.

Persson, E.K., Jaensson, E., and Agace, W.W. (2010). The diverse ontogeny and function of murine small intestinal dendritic cell/macrophage subsets. Immunobiology *215*, 692-697.

Rana, T.M. (2007). Illuminating the silence: understanding the structure and function of small RNAs. Nature reviews Molecular cell biology *8*, 23-36.

Randolph, G.J., Beaulieu, S., Lebecque, S., Steinman, R.M., and Muller, W.A. (1998). Differentiation of monocytes into dendritic cells in a model of transendothelial trafficking. Science *282*, 480-483.

Rodriguez, A., Vigorito, E., Clare, S., Warren, M.V., Couttet, P., Soond, D.R., van Dongen, S., Grocock, R.J., Das, P.P., Miska, E.A*., et al.* (2007). Requirement of bic/microRNA-155 for normal immune function. Science *316*, 608-611.

Ross, R. (1999). Atherosclerosis--an inflammatory disease. The New England journal of medicine *340*, 115-126.

Ross, R., and Harker, L. (1976). Hyperlipidemia and atherosclerosis. Science *193*, 1094-1100.

Sakurai, K., Zou, J.P., Tschetter, J.R., Ward, J.M., and Shearer, G.M. (2002). Effect of indoleamine 2,3-dioxygenase on induction of experimental autoimmune encephalomyelitis. Journal of neuroimmunology *129*, 186-196.

Salaun, B., Yamamoto, T., Badran, B., Tsunetsugu-Yokota, Y., Roux, A., Baitsch, L., Rouas, R., Fayyad-Kazan, H., Baumgaertner, P., Devevre, E*., et al.* (2011). Differentiation associated regulation of microRNA expression in vivo in human CD8+ T cell subsets. Journal of translational medicine *9*, 44.

Sasaki, N., Yamashita, T., Takeda, M., and Hirata, K. (2012). Regulatory T cells in atherogenesis. Journal of atherosclerosis and thrombosis *19*, 503-515.

Sato, K., Tateishi, S., Kubo, K., Mimura, T., Yamamoto, K., and Kanda, H. (2005). Downregulation of IL-12 and a novel negative feedback system mediated by CD25+CD4+ T cells. Biochemical and biophysical research communications *330*, 226-232.

Sato, K., Yamashita, N., Baba, M., and Matsuyama, T. (2003). Modified myeloid dendritic cells act as regulatory dendritic cells to induce anergic and regulatory T cells. Blood *101*, 3581-3589.

Satpathy, A.T., Kc, W., Albring, J.C., Edelson, B.T., Kretzer, N.M., Bhattacharya, D., Murphy, T.L., and Murphy, K.M. (2012a). Zbtb46 expression distinguishes classical dendritic cells and their

committed progenitors from other immune lineages. The Journal of experimental medicine *209*, 1135-1152.

Satpathy, A.T., Wu, X., Albring, J.C., and Murphy, K.M. (2012b). Re(de)fining the dendritic cell lineage. Nature immunology *13*, 1145-1154.

Schiller, N.K., Kubo, N., Boisvert, W.A., and Curtiss, L.K. (2001). Effect of gamma-irradiation and bone marrow transplantation on atherosclerosis in LDL receptor-deficient mice. Arteriosclerosis, thrombosis, and vascular biology *21*, 1674-1680.

Seiffert, M., Brossart, P., Cant, C., Cella, M., Colonna, M., Brugger, W., Kanz, L., Ullrich, A., and Buhring, H.J. (2001). Signal-regulatory protein alpha (SIRPalpha) but not SIRPbeta is involved in T-cell activation, binds to CD47 with high affinity, and is expressed on immature CD34(+)CD38(-) hematopoietic cells. Blood *97*, 2741-2749.

Serbina, N.V., Salazar-Mather, T.P., Biron, C.A., Kuziel, W.A., and Pamer, E.G. (2003). TNF/iNOS-producing dendritic cells mediate innate immune defense against bacterial infection. Immunity *19*, 59-70.

Shamshiev, A.T., Ampenberger, F., Ernst, B., Rohrer, L., Marsland, B.J., and Kopf, M. (2007). Dyslipidemia inhibits Toll-like receptor-induced activation of CD8alpha-negative dendritic cells and protective Th1 type immunity. The Journal of experimental medicine *204*, 441-452.

Shaposhnik, Z., Wang, X., Weinstein, M., Bennett, B.J., and Lusis, A.J. (2007). Granulocyte macrophage colony-stimulating factor regulates dendritic cell content of atherosclerotic lesions. Arteriosclerosis, thrombosis, and vascular biology *27*, 621-627.

Shortman, K., and Naik, S.H. (2007). Steady-state and inflammatory dendritic-cell development. Nature reviews Immunology *7*, 19-30.

Skalen, K., Gustafsson, M., Rydberg, E.K., Hulten, L.M., Wiklund, O., Innerarity, T.L., and Boren, J. (2002). Subendothelial retention of atherogenic lipoproteins in early atherosclerosis. Nature *417*, 750-754.

Smith, J.D., Trogan, E., Ginsberg, M., Grigaux, C., Tian, J., and Miyata, M. (1995). Decreased atherosclerosis in mice deficient in both macrophage colony-stimulating factor (op) and apolipoprotein E. Proceedings of the National Academy of Sciences of the United States of America *92*, 8264-8268.

Steinman, R.M., and Cohn, Z.A. (1973). Identification of a novel cell type in peripheral lymphoid organs of mice. I. Morphology, quantitation, tissue distribution. The Journal of experimental medicine *137*, 1142-1162.

Steinman, R.M., and Cohn, Z.A. (1974). Identification of a novel cell type in peripheral lymphoid organs of mice. II. Functional properties in vitro. The Journal of experimental medicine *139*, 380-397.

Steinman, R.M., Kaplan, G., Witmer, M.D., and Cohn, Z.A. (1979). Identification of a novel cell type in peripheral lymphoid organs of mice. V. Purification of spleen dendritic cells, new surface markers, and maintenance in vitro. The Journal of experimental medicine *149*, 1-16.

Steinman, R.M., Lustig, D.S., and Cohn, Z.A. (1974). Identification of a novel cell type in peripheral lymphoid organs of mice. 3. Functional properties in vivo. The Journal of experimental medicine *139*, 1431-1445.

Stemme, S., Faber, B., Holm, J., Wiklund, O., Witztum, J.L., and Hansson, G.K. (1995). T lymphocytes from human atherosclerotic plaques recognize oxidized low density lipoprotein. Proceedings of the National Academy of Sciences of the United States of America *92*, 3893-3897.

Sun, Y., Varambally, S., Maher, C.A., Cao, Q., Chockley, P., Toubai, T., Malter, C., Nieves, E., Tawara, I., Wang, Y.*, et al.* (2011). Targeting of microRNA-142-3p in dendritic cells regulates endotoxin-induced mortality. Blood *117*, 6172-6183.

Swanson, K.A., Zheng, Y., Heidler, K.M., Mizobuchi, T., and Wilkes, D.S. (2004). CDllc+ cells modulate pulmonary immune responses by production of indoleamine 2,3-dioxygenase. American journal of respiratory cell and molecular biology *30*, 311-318.

Swirski, F.K., Libby, P., Aikawa, E., Alcaide, P., Luscinskas, F.W., Weissleder, R., and Pittet, M.J. (2007). Ly-6Chi monocytes dominate hypercholesterolemia-associated monocytosis and give rise to macrophages in atheromata. The Journal of clinical investigation *117*, 195-205.

Swirski, F.K., Nahrendorf, M., Etzrodt, M., Wildgruber, M., Cortez-Retamozo, V., Panizzi, P., Figueiredo, J.L., Kohler, R.H., Chudnovskiy, A., Waterman, P.*, et al.* (2009). Identification of splenic reservoir monocytes and their deployment to inflammatory sites. Science *325*, 612-616.

Tabas, I., Williams, K.J., and Boren, J. (2007). Subendothelial lipoprotein retention as the initiating process in atherosclerosis: update and therapeutic implications. Circulation *116*, 1832-1844.

Tacke, F., Alvarez, D., Kaplan, T.J., Jakubzick, C., Spanbroek, R., Llodra, J., Garin, A., Liu, J., Mack, M., van Rooijen, N.*, et al.* (2007). Monocyte subsets differentially employ CCR2, CCR5, and CX3CR1 to accumulate within atherosclerotic plaques. The Journal of clinical investigation *117*, 185-194.

Taganov, K.D., Boldin, M.P., Chang, K.J., and Baltimore, D. (2006). NF-kappaB-dependent induction of microRNA miR-146, an inhibitor targeted to signaling proteins of innate immune responses. Proceedings of the National Academy of Sciences of the United States of America *103*, 12481-12486.

Tang, Q., Adams, J.Y., Tooley, A.J., Bi, M., Fife, B.T., Serra, P., Santamaria, P., Locksley, R.M., Krummel, M.F., and Bluestone, J.A. (2006). Visualizing regulatory T cell control of autoimmune responses in nonobese diabetic mice. Nature immunology *7*, 83-92.

Tanzer, A., and Stadler, P.F. (2004). Molecular evolution of a microRNA cluster. Journal of molecular biology *339*, 327-335.

Tedgui, A., and Mallat, Z. (2006). Cytokines in atherosclerosis: pathogenic and regulatory pathways. Physiological reviews *86*, 515-581.

Thery, C., Ostrowski, M., and Segura, E. (2009). Membrane vesicles as conveyors of immune responses. Nature reviews Immunology *9*, 581-593.

Thomas, M., Lange-Grunweller, K., Weirauch, U., Gutsch, D., Aigner, A., Grunweller, A., and Hartmann, R.K. (2012). The proto-oncogene Pim-1 is a target of miR-33a. Oncogene *31*, 918-928.

Thomson, A.W., Turnquist, H.R., Zahorchak, A.F., and Raimondi, G. (2009). Tolerogenic dendritic cell-regulatory T-cell interaction and the promotion of transplant tolerance. Transplantation *87*, S86-90.

Tili, E., Michaille, J.J., Cimino, A., Costinean, S., Dumitru, C.D., Adair, B., Fabbri, M., Alder, H., Liu, C.G., Calin, G.A.*, et al.* (2007). Modulation of miR-155 and miR-125b levels following lipopolysaccharide/TNF-alpha stimulation and their possible roles in regulating the response to endotoxin shock. Journal of immunology *179*, 5082-5089.

Tomizawa, T., Kaneko, Y., Saito, Y., Ohnishi, H., Okajo, J., Okuzawa, C., Ishikawa-Sekigami, T., Murata, Y., Okazawa, H., Okamoto, K.*, et al.* (2007). Resistance to experimental autoimmune encephalomyelitis and impaired T cell priming by dendritic cells in Src homology 2 domain-containing protein tyrosine phosphatase substrate-1 mutant mice. J Immunol *179*, 869-877.

Turner, M.L., Schnorfeil, F.M., and Brocker, T. (2011). MicroRNAs regulate dendritic cell differentiation and function. Journal of immunology *187*, 3911-3917.

Uyemura, K., Demer, L.L., Castle, S.C., Jullien, D., Berliner, J.A., Gately, M.K., Warrier, R.R., Pham, N., Fogelman, A.M., and Modlin, R.L. (1996). Cross-regulatory roles of interleukin (IL)-12 and IL-10 in atherosclerosis. The Journal of clinical investigation *97*, 2130-2138.

van de Laar, L., Coffer, P.J., and Woltman, A.M. (2012). Regulation of dendritic cell development by GM-CSF: molecular control and implications for immune homeostasis and therapy. Blood *119*, 3383-3393.

Vasilescu, C., Rossi, S., Shimizu, M., Tudor, S., Veronese, A., Ferracin, M., Nicoloso, M.S., Barbarotto, E., Popa, M., Stanciulea, O.*, et al.* (2009). MicroRNA fingerprints identify miR-150 as a plasma prognostic marker in patients with sepsis. PloS one *4*, e7405.

Ventura, A., Young, A.G., Winslow, M.M., Lintault, L., Meissner, A., Erkeland, S.J., Newman, J., Bronson, R.T., Crowley, D., Stone, J.R.*, et al.* (2008). Targeted deletion reveals essential and overlapping functions of the miR-17 through 92 family of miRNA clusters. Cell *132*, 875-886.

Vickers, K.C., Palmisano, B.T., Shoucri, B.M., Shamburek, R.D., and Remaley, A.T. (2011). MicroRNAs are transported in plasma and delivered to recipient cells by high-density lipoproteins. Nature cell biology *13*, 423-433.

Vremec, D., Lieschke, G.J., Dunn, A.R., Robb, L., Metcalf, D., and Shortman, K. (1997). The influence of granulocyte/macrophage colony-stimulating factor on dendritic cell levels in mouse lymphoid organs. European journal of immunology *27*, 40-44.

Wang, P., Hou, J., Lin, L., Wang, C., Liu, X., Li, D., Ma, F., Wang, Z., and Cao, X. (2010). Inducible microRNA-155 feedback promotes type I IFN signaling in antiviral innate immunity by targeting suppressor of cytokine signaling 1. Journal of immunology *185*, 6226-6233.

Waskow, C., Liu, K., Darrasse-Jeze, G., Guermonprez, P., Ginhoux, F., Merad, M., Shengelia, T., Yao, K., and Nussenzweig, M. (2008). The receptor tyrosine kinase Flt3 is required for dendritic cell development in peripheral lymphoid tissues. Nature immunology *9*, 676-683.

Weber, C., Meiler, S., Doring, Y., Koch, M., Drechsler, M., Megens, R.T., Rowinska, Z., Bidzhekov, K., Fecher, C., Ribechini, E.*, et al.* (2011). CCL17-expressing dendritic cells drive atherosclerosis by restraining regulatory T cell homeostasis in mice. The Journal of clinical investigation *121*, 2898-2910.

Weber, C., and Noels, H. (2011). Atherosclerosis: current pathogenesis and therapeutic options. Nature medicine *17*, 1410-1422.

Weber, C., Zernecke, A., and Libby, P. (2008). The multifaceted contributions of leukocyte subsets to atherosclerosis: lessons from mouse models. Nature reviews Immunology *8*, 802-815.

Weigert, A., Weichand, B., Sekar, D., Sha, W., Hahn, C., Mora, J., Ley, S., Essler, S., Dehne, N., and Brune, B. (2012). HIF-1alpha is a negative regulator of plasmacytoid DC development in vitro and in vivo. Blood *120*, 3001-3006.

Wu, T., Wieland, A., Araki, K., Davis, C.W., Ye, L., Hale, J.S., and Ahmed, R. (2012). Temporal expression of microRNA cluster miR-17-92 regulates effector and memory CD8+ T-cell differentiation. Proceedings of the National Academy of Sciences of the United States of America *109*, 9965-9970.

Wu, W., Takanashi, M., Borjigin, N., Ohno, S.I., Fujita, K., Hoshino, S., Osaka, Y., Tsuchida, A., and Kuroda, M. (2013). MicroRNA-18a modulates STAT3 activity through negative regulation of PIAS3 during gastric adenocarcinogenesis. British journal of cancer *108*, 653-661.

Wu, W.H., Hu, C.P., Chen, X.P., Zhang, W.F., Li, X.W., Xiong, X.M., and Li, Y.J. (2011). MicroRNA-130a mediates proliferation of vascular smooth muscle cells in hypertension. American journal of hypertension *24*, 1087-1093.

Xiao, C., Srinivasan, L., Calado, D.P., Patterson, H.C., Zhang, B., Wang, J., Henderson, J.M., Kutok, J.L., and Rajewsky, K. (2008). Lymphoproliferative disease and autoimmunity in mice with increased miR-17-92 expression in lymphocytes. Nature immunology *9*, 405-414.

Yamazaki, S., Iyoda, T., Tarbell, K., Olson, K., Velinzon, K., Inaba, K., and Steinman, R.M. (2003). Direct expansion of functional CD25+ CD4+ regulatory T cells by antigen-processing dendritic cells. The Journal of experimental medicine *198*, 235-247.

Yamazaki, S., Patel, M., Harper, A., Bonito, A., Fukuyama, H., Pack, M., Tarbell, K.V., Talmor, M., Ravetch, J.V., Inaba, K.*, et al.* (2006). Effective expansion of alloantigen-specific Foxp3+ CD25+ CD4+ regulatory T cells by dendritic cells during the mixed leukocyte reaction. Proceedings of the National Academy of Sciences of the United States of America *103*, 2758-2763.

Yilmaz, A., Lochno, M., Traeg, F., Cicha, I., Reiss, C., Stumpf, C., Raaz, D., Anger, T., Amann, K., Probst, T.*, et al.* (2004). Emergence of dendritic cells in rupture-prone regions of vulnerable carotid plaques. Atherosclerosis *176*, 101-110.

Zernecke, A., Bidzhekov, K., Noels, H., Shagdarsuren, E., Gan, L., Denecke, B., Hristov, M., Koppel, T., Jahantigh, M.N., Lutgens, E.*, et al.* (2009). Delivery of microRNA-126 by apoptotic bodies induces CXCL12-dependent vascular protection. Science signaling *2*, ra81.

Zhang, Y., Liu, D., Chen, X., Li, J., Li, L., Bian, Z., Sun, F., Lu, J., Yin, Y., Cai, X.*, et al.* (2010). Secreted monocytic miR-150 enhances targeted endothelial cell migration. Molecular cell *39*, 133-144.

Zhou, H., Huang, X., Cui, H., Luo, X., Tang, Y., Chen, S., Wu, L., and Shen, N. (2010). miR-155 and its star-form partner miR-155* cooperatively regulate type I interferon production by human plasmacytoid dendritic cells. Blood *116*, 5885-5894.

Zhou, X., Paulsson, G., Stemme, S., and Hansson, G.K. (1998). Hypercholesterolemia is associated with a T helper (Th) 1/Th2 switch of the autoimmune response in atherosclerotic apo E-knockout mice. The Journal of clinical investigation *101*, 1717-1725.

Zhu, S.N., Chen, M., Jongstra-Bilen, J., and Cybulsky, M.I. (2009). GM-CSF regulates intimal cell proliferation in nascent atherosclerotic lesions. The Journal of experimental medicine *206*, 2141-2149.

7 Acknowledgements

This thesis involved the help of many people and at this point I want to thank them for their support. First of all, I want to thank Alma Zernecke for giving me the opportunity to conduct this thesis. Not only she provided a challenging project, she also made sure that the lab was perfectly equipped and we were always able to conduct all necessary experiments. She also allowed me to take responsibility, for example regarding animal administration, and always trusted me.

In addition, I want to express my gratitude to Heike Hermanns for the discussions we had, her help within the project and whenever needed. Together with Manfred Lutz she agreed to supervise this thesis and therefore I thank both of them for their support.

Furthermore, I want to thank Miriam Koch, Sweena Chaudhari and Helga Manthey for their support and the great time we shared in and especially outside of the lab. All the knowledge about atherosclerosis, DCs and microRNAs I gained within this thesis will fade over the years, but the time we had I will never forget.

I want to thank Theresa Henninger, Melanie Schott, Yvonne Kerstan and Louisa Molinari for their extraordinary technical assistance and for the great time we had. You know that this thesis would not have been possible without you and I will never forget you and your help!

I want to thank Johannes Drechsler, Christine Siegl, Christine Mais, Sabine Walter, Carmen Schäfer and Daniela Krämer for the kind lab neighborhood, helping out with consumables and in particular for the time we had outside of the lab. In addition, I want to thank the members of the Nieswandt's group for the kind lab neighborhood.

A special thank you goes to Patrick Kunz, for his support and all the discussions about life sciences and life in sciences.

I also want to thank Thilo Westhofen for working together on aortic DC subsets. In addition, I want to thank Sebastian Beißler, Hendrik Beckert, Karolina Scholtyschik and Hannes Hofmann for their work during their time in the lab.

The work presented in this thesis is based on laboratory animals and at this point I want to thank Marie Blum, Sandra Umbenhauer, Wolfgang Radl, Melanie Kraiß and their colleagues for their work in the animal facility. I always trusted and relied on them and whenever needed on short notice they helped me out.

Additionally, I want to thank Christian Weinberger for the time we shared (not only at the institute). Together with Bernhard Fröhlich we fought against viruses, upgraded computers, installed network attached storage and discussed about mountaineering – thank you!

A warm word of thank you also goes to Daniel Göbel, Sebastian Hämmerling, Mario Artmann and Hilke Gehret.

Last but not least I want to thank my parents and my brother for their ongoing support throughout my whole life. I always relied on you and I always will.

8 Publications

Busch M, Westhofen TC, Lutz MB and Zernecke A "Dendritic cell subset distributions in the aorta in healthy and atherosclerotic mice." submitted

Koch M, Manthey HD, Martin Busch et al. "Coagulation factor XII promotes atherosclerosis and pro-inflammatory T cell responses in mice." submitted

Chaudhari SM, Sluimer JC, Koch M, Manthey HD, Busch M et al. "HIF1alpha in dendritic cells restrains inflammation and atherosclerosis in mice." submitted

Manthey HD, Barnsteiner S, Cochain C, Karshovska E, Koch M, Chaudhari SM, Busch M et al. "Role of the chemokine receptor Ccr6 in monocyte recruitment and atherosclerosis in mice." submitted

Kulathu Y, Garcia FJ, Mevissen TET, Busch M et al. (2013) "Regulation of A20 and other OTU DUBs by reversible oxidation." Nature Communications 4:1569

Busch M, and Zernecke A (2012). "microRNAs in the regulation of dendritic cell functions in inflammation and atherosclerosis." Journal of Molecular Medicine 90(8):877.

Doring Y, Manthey HD, Drechsler M, Lievens D, Megens RT, Soehnlein O, Busch M et al. (2012). "Auto-antigenic protein-DNA complexes stimulate plasmacytoid dendritic cells to promote atherosclerosis." Circulation 125(13): 1673.

Muench P, Probst S, Schuetz J, Leiprecht N, Busch M et al. (2010). "Cutaneous papillomavirus E6 proteins must interact with p300 and block p53-mediated apoptosis for cellular immortalization and tumorigenesis." Cancer Research 70(17): 6913.

9 Curriculum Vitae

10 Affidavit/ Eidesstattliche Erklärung

Affidavit

I hereby confirm that my thesis entitled *Aortic Dendritic Cell Subsets in Healthy and Atherosclerotic Mice and The Role of the miR-17~92 Cluster in Dendritic Cells* is the result of my own work. I did not receive any help or support from commercial consultants. All sources and / or materials applied are listed and specified in the thesis. Furthermore, I confirm that this thesis has not yet been submitted as part of another examination process neither in identical nor in similar form.

Kaisheim, _____

Eidesstattliche Erklärung

Hiermit erkläre ich an Eides statt, die Dissertation *Subsets dendritischer Zellen in der Aorta gesunder und atherosklerotischer Mäuse und Rolle des miR-17~92 Clusters in dendritischen Zellen* eigenständig, d.h. insbesondere selbständig und ohne Hilfe eines kommerziellen Promotionsberaters, angefertigt und keine anderen als die von mir angegebenen Quellen und Hilfsmittel verwendet zu haben. Ich erkläre außerdem, dass die Dissertation weder in gleicher noch in ähnlicher Form bereits in einem anderen Prüfungsverfahren vorgelegen hat.

Kaisheim, _____